

AD-A082 073

AMPEX CORP REDWOOD CITY CA ADVANCED TECHNOLOGY DIV
OPTICAL CORRELATION STUDIES. CONTINUATION OF LENS PROGRAM.(U)

F/G 20/6

OCT 79 L R WEINER

N00014-77-C-0447

UNCLASSIFIED

RR-79-23

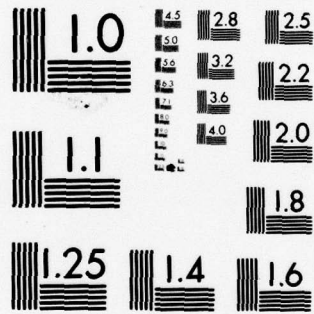
NL

1 OF 2

AD-

A082073





MICROCOPY RESOLUTION TEST CHART
NATIONAL BUREAU OF STANDARDS-1963-A

N00014-77-C-0447

RR 79-23

(13)

OPTICAL CORRELATION STUDIES

Continuation of LENS Program

**AMPEX CORPORATION
Advanced Technology Division
401 Broadway
Redwood City, CA 94063**

**DTIC
ELECTE
MAR 19 1980
S D C**

1 October 1979

Final Report for Period 1 June 1977 - 28 April 1979

Prepared for

**OFFICE OF NAVAL RESEARCH
Department of the Navy
800 North Quincy Street
Arlington, Virginia 22217**

**This document has been approved
for public release and sale; its
distribution is unlimited.**

Unclassified

SECURITY CLASSIFICATION OF THIS PAGE (When Data Entered)

REPORT DOCUMENTATION PAGE		READ INSTRUCTIONS BEFORE COMPLETING FORM
1. REPORT NUMBER N00014-77-C-0447	2. GOVT ACCESSION NO.	3. RECIPIENT'S CATALOG NUMBER
6. TITLE (and Subtitle) OPTICAL CORRELATION STUDIES. Continuation of LENS Program.		9. TYPE OF REPORT & PERIOD COVERED Final Report, 1 June 1977-28 Apr 1979
7. AUTHOR(s) 10. Lawrence R. Weiner		14. PERFORMING ORG. REPORT NUMBER RR-79-23
9. PERFORMING ORGANIZATION NAME AND ADDRESS AMPEX CORPORATION, Advanced Technology Division 401 Broadway Redwood City, California 94063		15. CONTRACT OR GRANT NUMBER(s) N00014-77-C-0447
11. CONTROLLING OFFICE NAME AND ADDRESS Office of Naval Research, Dept. of the Navy 800 N. Quincy Street 613A:CG Arlington, Virginia 22217		10. PROGRAM ELEMENT, PROJECT, TASK AREA & WORK UNIT NUMBERS NR 366-003
14. MONITORING AGENCY NAME & ADDRESS (if different from Controlling Office)		12. REPORT DATE 1 Oct 1979
		13. NUMBER OF PAGES 140 12 136
		15. SECURITY CLASS. (of this report) Unclassified
		15a. DECLASSIFICATION/DOWNGRADING SCHEDULE
16. DISTRIBUTION STATEMENT (of this Report) <div style="border: 1px solid black; padding: 5px; text-align: center;">This document has been approved for public release and sale; its distribution is unlimited.</div>		
17. DISTRIBUTION STATEMENT (of the abstract entered in Block 20, if different from Report)		
18. SUPPLEMENTARY NOTES Additional investigation performed by Ampex after the official end of contract is described in Appendix A.		
19. KEY WORDS (Continue on reverse side if necessary and identify by block number) Optical Correlation, Ambiguity Surface Generation, Coherent Optical Processing, Film Recording.		
20. ABSTRACT (Continue on reverse side if necessary and identify by block number) Passive ambiguity surface formation using a coherent optical technique was investigated. Experiments were performed using signals recorded on film. The optical outputs were digitized and analyzed to measure the effectiveness of this method.		

403899 *James*

Unclassified

SECURITY CLASSIFICATION OF THIS PAGE (When Data Entered)

INSTRUCTIONS FOR PREPARATION OF REPORT DOCUMENTATION PAGE

RESPONSIBILITY. The controlling DoD office will be responsible for completion of the Report Documentation Page, DD Form 1473, in all technical reports prepared by or for DoD organizations.

CLASSIFICATION. Since this Report Documentation Page, DD Form 1473, is used in preparing announcements, bibliographies, and data banks, it should be unclassified if possible. If a classification is required, identify the classified items on the page by the appropriate symbol.

COMPLETION GUIDE

General. Make Blocks 1, 4, 5, 6, 7, 11, 13, 15, and 16 agree with the corresponding information on the report cover. Leave Blocks 2 and 3 blank.

Block 1. Report Number. Enter the unique alphanumeric report number shown on the cover.

Block 2. Government Accession No. Leave blank. This space is for use by the Defense Documentation Center.

Block 3. Recipient's Catalog Number. Leave blank. This space is for the use of the report recipient to assist in future retrieval of the document.

Block 4. Title and Subtitle. Enter the title in all capital letters exactly as it appears on the publication. Titles should be unclassified whenever possible. Write out the English equivalent for Greek letters and mathematical symbols in the title (see "Abstracting Scientific and Technical Reports of Defense-sponsored RDT/E," AD-667 000). If the report has a subtitle, this subtitle should follow the main title, be separated by a comma or semicolon if appropriate, and be initially capitalized. If a publication has a title in a foreign language, translate the title into English and follow the English translation with the title in the original language. Make every effort to simplify the title before publication.

Block 5. Type of Report and Period Covered. Indicate here whether report is interim, final, etc., and, if applicable, inclusive dates of period covered, such as the life of a contract covered in a final contractor report.

Block 6. Performing Organization Report Number. Only numbers other than the official report number shown in Block 1, such as series numbers for in-house reports or a contractor/grantee number assigned by him, will be placed in this space. If no such numbers are used, leave this space blank.

Block 7. Author(s). Include corresponding information from the report cover. Give the name(s) of the author(s) in conventional order (for example, John R. Doe or, if author prefers, J. Robert Doe). In addition, list the affiliation of an author if it differs from that of the performing organization.

Block 8. Contract or Grant Number(s). For a contractor or grantee report, enter the complete contract or grant number(s) under which the work reported was accomplished. Leave blank in in-house reports.

Block 9. Performing Organization Name and Address. For in-house reports enter the name and address, including office symbol, of the performing activity. For contractor or grantee reports enter the name and address of the contractor or grantee who prepared the report and identify the appropriate corporate division, school, laboratory, etc., of the author. List city, state, and ZIP Code.

Block 10. Program Element, Project, Task Area, and Work Unit Numbers. Enter here the number code from the applicable Department of Defense form, such as the DD Form 1498, "Research and Technology Work Unit Summary" or the DD Form 1634, "Research and Development Planning Summary," which identifies the program element, project, task area, and work unit or equivalent under which the work was authorized.

Block 11. Controlling Office Name and Address. Enter the full, official name and address, including office symbol, of the controlling office (Equates to funding/sponsoring agency. For definition see DoD Directive 5200.20, "Distribution Statements on Technical Documents.")

Block 12. Report Date. Enter here the day, month, and year or month and year as shown on the cover.

Block 13. Number of Pages. Enter the total number of pages.

Block 14. Monitoring Agency Name and Address (if different from Controlling Office). For use when the controlling or funding office does not directly administer a project, contract, or grant, but delegates the administrative responsibility to another organization.

Blocks 15 & 15a. Security Classification of the Report: Declassification/Downgrading Schedule of the Report. Enter in 15 the highest classification of the report. If appropriate, enter in 15a the declassification/downgrading schedule of the report, using the abbreviations for declassification/downgrading schedules listed in paragraph 4-207 of DoD 5200.1-R.

Block 16. Distribution Statement of the Report. Insert here the applicable distribution statement of the report from DoD Directive 5200.20, "Distribution Statements on Technical Documents."

Block 17. Distribution Statement (of the abstract entered in Block 20, if different from the distribution statement of the report). Insert here the applicable distribution statement of the abstract from DoD Directive 5200.20, "Distribution Statements on Technical Documents."

Block 18. Supplementary Notes. Enter information not included elsewhere but useful, such as: Prepared in cooperation with Translation of (or by) Presented at conference of To be published in

Block 19. Key Words. Select terms or short phrases that identify the principal subjects covered in the report, and are sufficiently specific and precise to be used as index entries for cataloging, conforming to standard terminology. The DoD "Thesaurus of Engineering and Scientific Terms" (TEST) AD-672 000, can be helpful.

Block 20. Abstract. The abstract should be a brief (not to exceed 200 words) factual summary of the most significant information contained in the report. If possible, the abstract of a classified report should be unclassified and the abstract to an unclassified report should consist of publicly-releasable information. If the report contains a significant bibliography or literature survey, mention it here. For information on preparing abstracts see "Abstracting Scientific and Technical Reports of Defense-Sponsored RDT&E," AD-667 000.

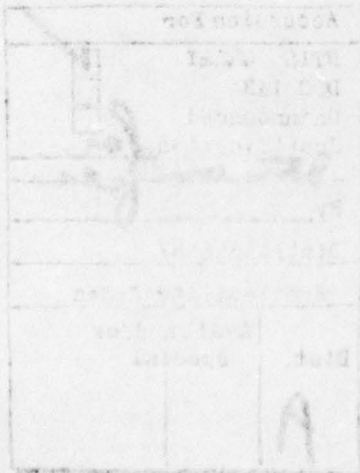
TABLE OF CONTENTS

1.0	INTRODUCTION	1
1.1	Film Based Surface Generation	2
1.2	Program Results	8
2.0	ALGORITHM FOR FORMING OPTICAL PASSIVE AMBIGUITY SURFACES	9
2.1	Image Plane Correlator Theory	9
2.2	Optical Implementation	14
2.3	Alignment Tolerance	14
3.0	RECORDING SIGNALS ON FILM	17
3.1	Temporal-Spatial Analogies	17
3.2	Film Recorder System	18
3.3	Idealized Film as a Coherent Light Modulator	32
3.4	Summary of Film Recording Characteristics	38
3.5	Raster Recording Realities	41
4.0	SYNTHETIC DATA PROCESSING	45
4.1	Data Description	45
4.2	Choice of IPC Processing Parameters	46
4.3	Film Recorder Format	47
4.4	Modulation and Traceability	47
4.5	Digital Simulation of the Optical Algorithm	50
5.0	OPTICAL SYSTEM	59
5.1	Component Alignment	59
5.2	Scaling of the Optical Output	60
5.3	Light Budget	62

Accession For	
NTIS GMAI	<input checked="" type="checkbox"/>
DDC TAB	<input type="checkbox"/>
Unannounced	<input type="checkbox"/>
Justification	<input type="checkbox"/>
By <i>for</i>	
Distribution/	
Availability Codes	
Dist.	Avail and/or special
A	

Table of Contents (Continued)

6.0	DETECTION AND DIGITIZATION	65
6.1	Camera and Video Processing	65
6.2	Analog/Digital Conversion	68
7.0	DISTRIBUTION OF DIGITIZED OPTICAL DATA	75
7.1	April 21, 1978	75
7.2	August 28, 1978	75
7.3	February 28, 1979	76
7.4	March 7, 1979	77
7.5	Additional Experiments	77
8.0	BIBLIOGRAPHY	83
	APPENDIX A	87
	Improvements of Film Recording Characteristics	
	APPENDIX B	93
	Selected Correspondence	
	APPENDIX C	
	Optical Ambiguity Surface Generation	135



1.0 INTRODUCTION

The work which is about to be described was done under ONR Contract N00014-77-C-0447 in conjunction with NOSC, ENSCO Corporation, and Carnegie-Mellon University. Figure 1.1 shows the primary division of program responsibilities. Ampex was able to fulfill the program requirements without expenditures for material (other than expendables such as film and magnetic tape) by utilizing the Government/Ampex Signal Processing (GASP) facilities located in Redwood City, California.

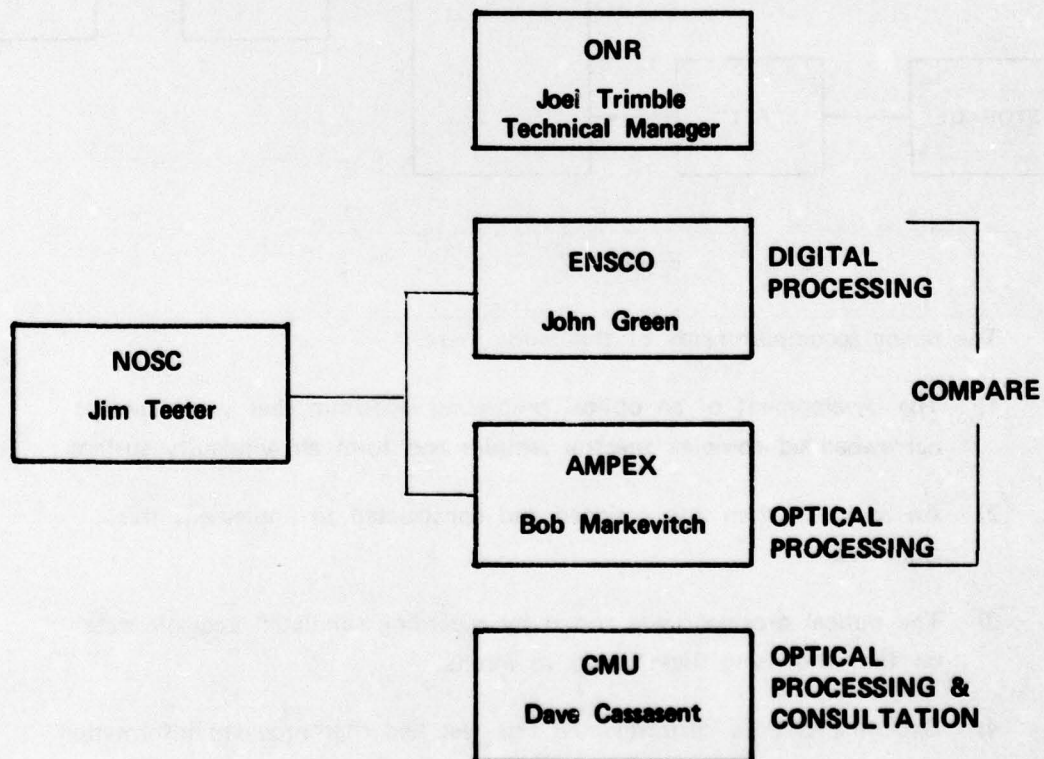


Figure 1.1 Program Organization

1.1 Film Based Surface Generation

The present program has provided information that is vital in the determination of the role that optical processing will play in acoustic data gathering systems. The program plan was designed to investigate whether a special purpose optical processor can truly interface with and augment the performance of digital processing equipment. Figure 1.2 shows the major components of such a configuration.

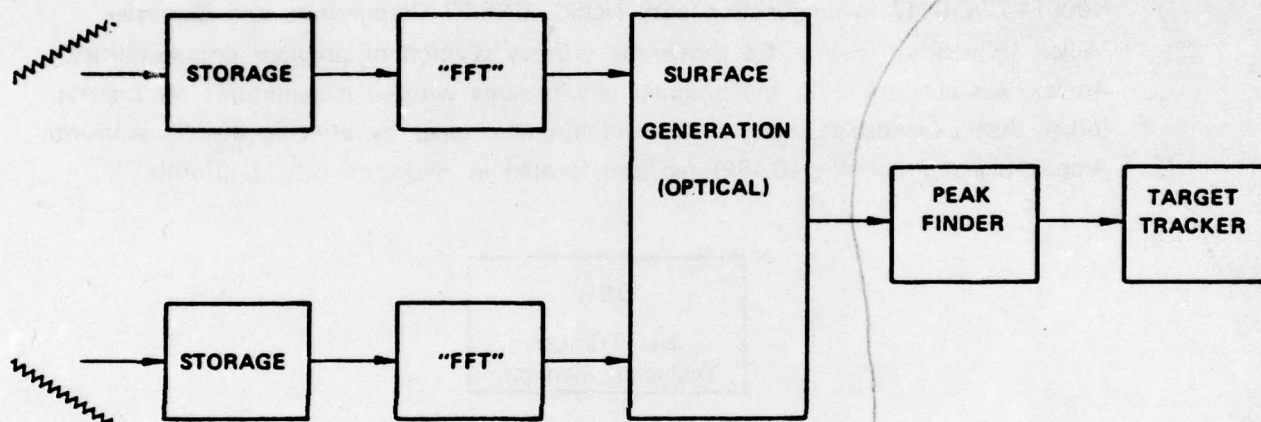


Figure 1.2

The major accomplishments of this study were:

- (1) The development of an optical processing algorithm that would accept narrowbanded complex spectral samples and form an ambiguity surface.
- (2) An optical system was designed and constructed to implement this algorithm.
- (3) The optical processor was tested by recording simulated acoustic data on film and using these masks as inputs.
- (4) Experiments were performed on this test bed that provided information on accuracy and detectability of the optical output.
- (5) Direct comparisons of the optically generated surfaces to surfaces calculated digitally with the same data were made.

- (6) It was ascertained that these optical techniques would be amenable to real-time implementation if spatial light modulators were substituted for the film media.

Details of the processing algorithm, optical design, and film formatting are contained in this report and in the supplement that has been appended to this report entitled "Optical Ambiguity Surface Generation". Of particular interest in the supplement is a process flow diagram which explains the operation of the optical components. Also included are examples of actual input films of selected test waveforms and the resultant ambiguity surfaces.

NOSC provided a data test set that consisted of 14 blocks of signal, each of which simulated two channels of 3600 narrowbanded complex samples. Each block was equivalent to one hour of signal recorded at 1 sample/second. The blocks varied in signal to noise ratio from plus infinity to minus infinity. The signal occupies a 0.1 Hz bandwidth in a processing bandwidth of .25 Hz. One channel was Dopplered by a constant .08 Hz. This data was provided to all the project participants where it was used by Ensco to prepare the digital surfaces and by Ampex to record the film inputs for optical processing at both Ampex and Carnegie-Mellon.

The optical processor was laid out on a 4 x 8 foot laboratory bench as shown in Fig. 1.3. The design contains less than a dozen lenses and is very easy to align. Since the algorithm does not require any interferometric techniques, the output will not decorrelate for slight misalignments or vibration. Instead, translation of most components will cause offsets in either range or Doppler, however, this is not likely to occur since all components are firmly anchored to the bench. Real-time devices could easily be accommodated in this rather straight forward optical design.

The two-dimensional range-Doppler output of the optical system was detected by a vidicon camera and then displayed on a variety of monitoring devices including standard black and white TV monitors, an analog isometric display, and a color contour monitor. The video was also sampled and stored in a frame buffer. The processing hardware is shown in Fig. 1.4.

As a result of experiments run on this system, over a hundred films were recorded and approximately 40 surfaces were digitized and distributed to NOSc and Ensco for further analysis. The tests included correlating channels of different S/N, using both 256 second and 512 second integration times, imbedding calibration markers in the signal, formation of multiple surfaces in one optical frame, and the processing of sine

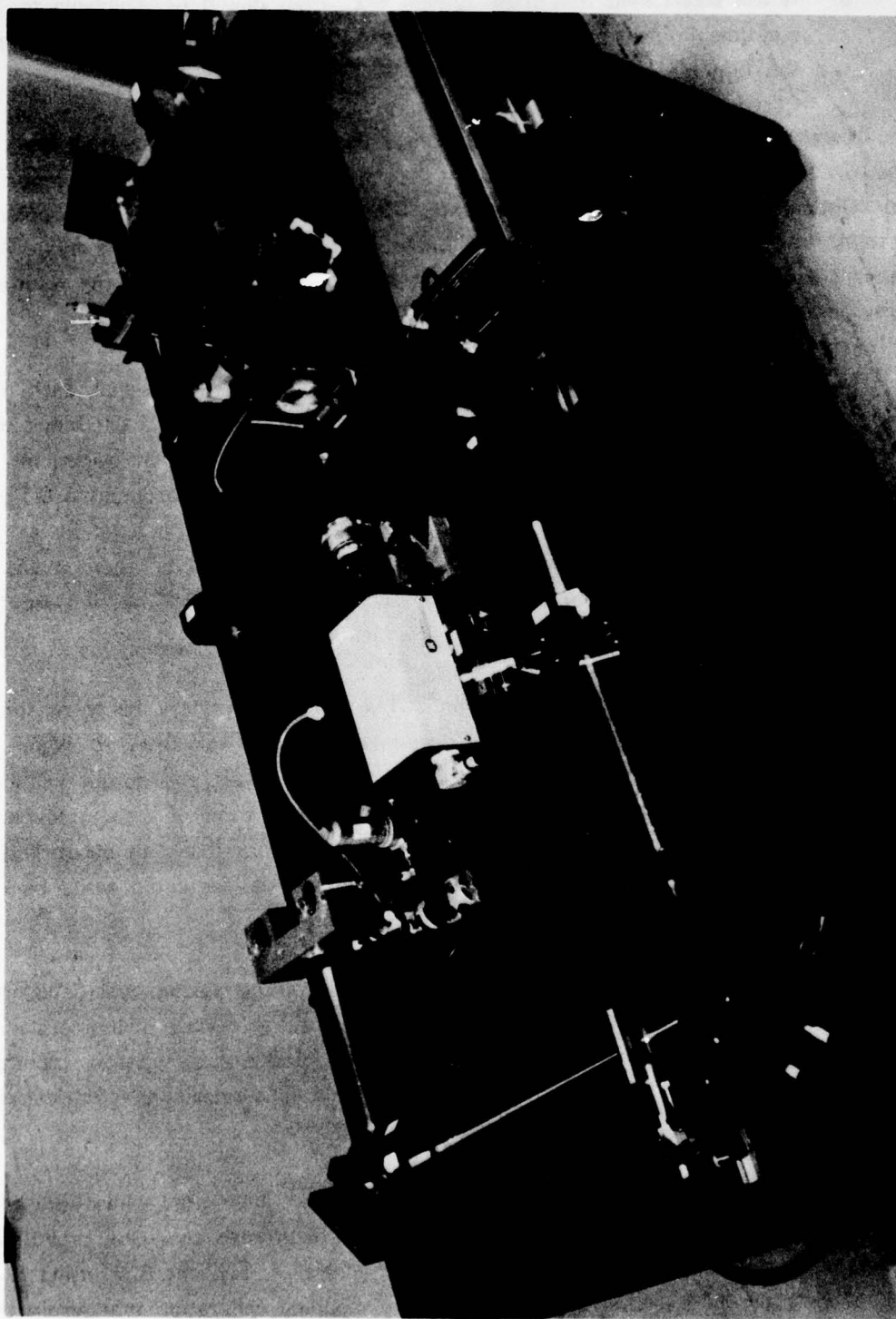


Figure 1.3 LENS Optical Bench

wave and impulse data. We believe this represents one of the most thorough characterizations of an optical signal processing concept that has ever been done!

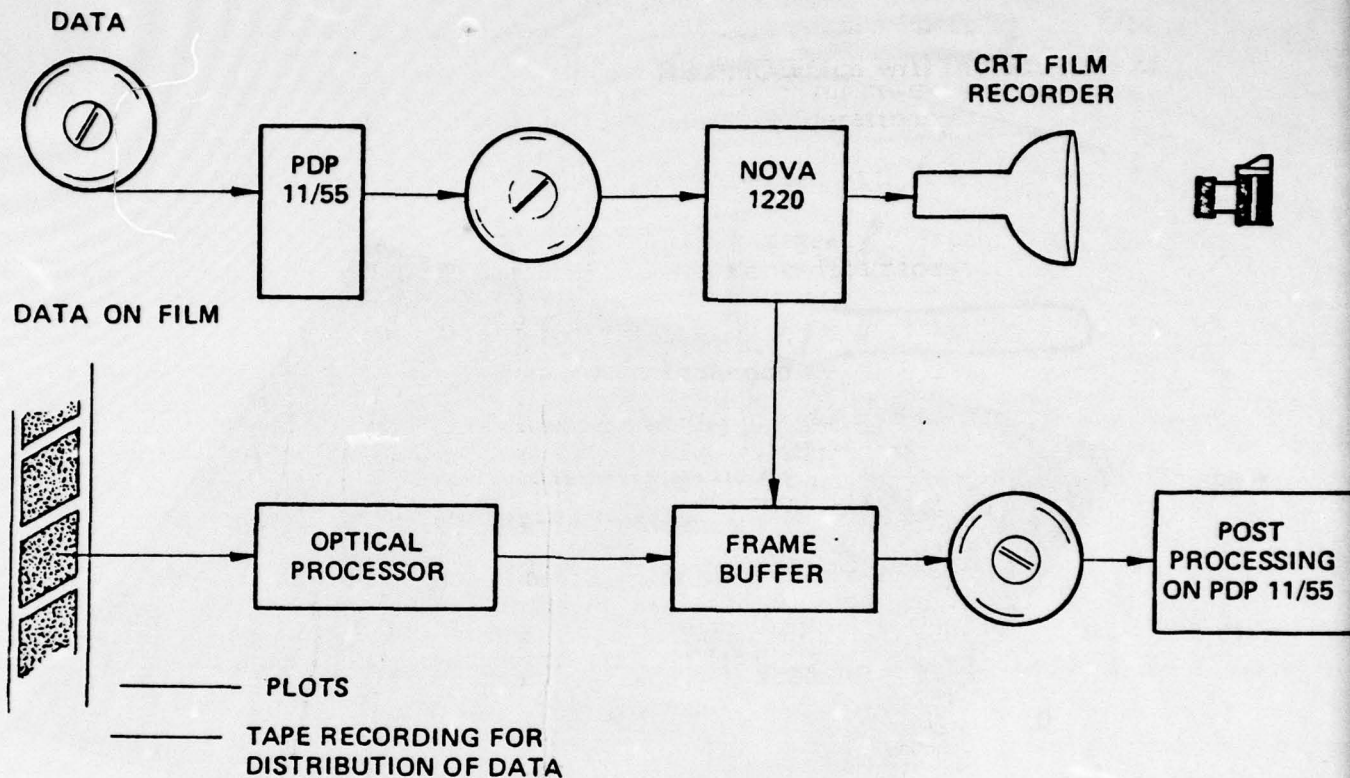


Figure 1.4 Current Processing Hardware

In addition to the examples of optical output that appear in this report, the following two figures are representative of this work. Figure 1.5 shows an optically generated surface which has been digitized and then plotted on the Ampex PDP 11/55 system. It is the result of a cross correlation between a Dopplered and not Dopplered channel. Figure 1.6 demonstrates several concepts at once. As explained in this report, the range direction is easily partitioned so as to be able to form multiple ambiguity surfaces in the same optical frame. Thus, the 256 available range bins can be allocated to different sections of the data. In this figure, the top surface is a correlation displaying a Doppler shift, while the lower surface is an autocorrelation of a single channel. The Doppler shift is clearly indicated by the horizontal markers which were imbedded in the input data. The markers are actually correlations of Barkers codes which were properly formatted on each of the input films and are spaced 0.058 Hz in Doppler and every 80 seconds in range.

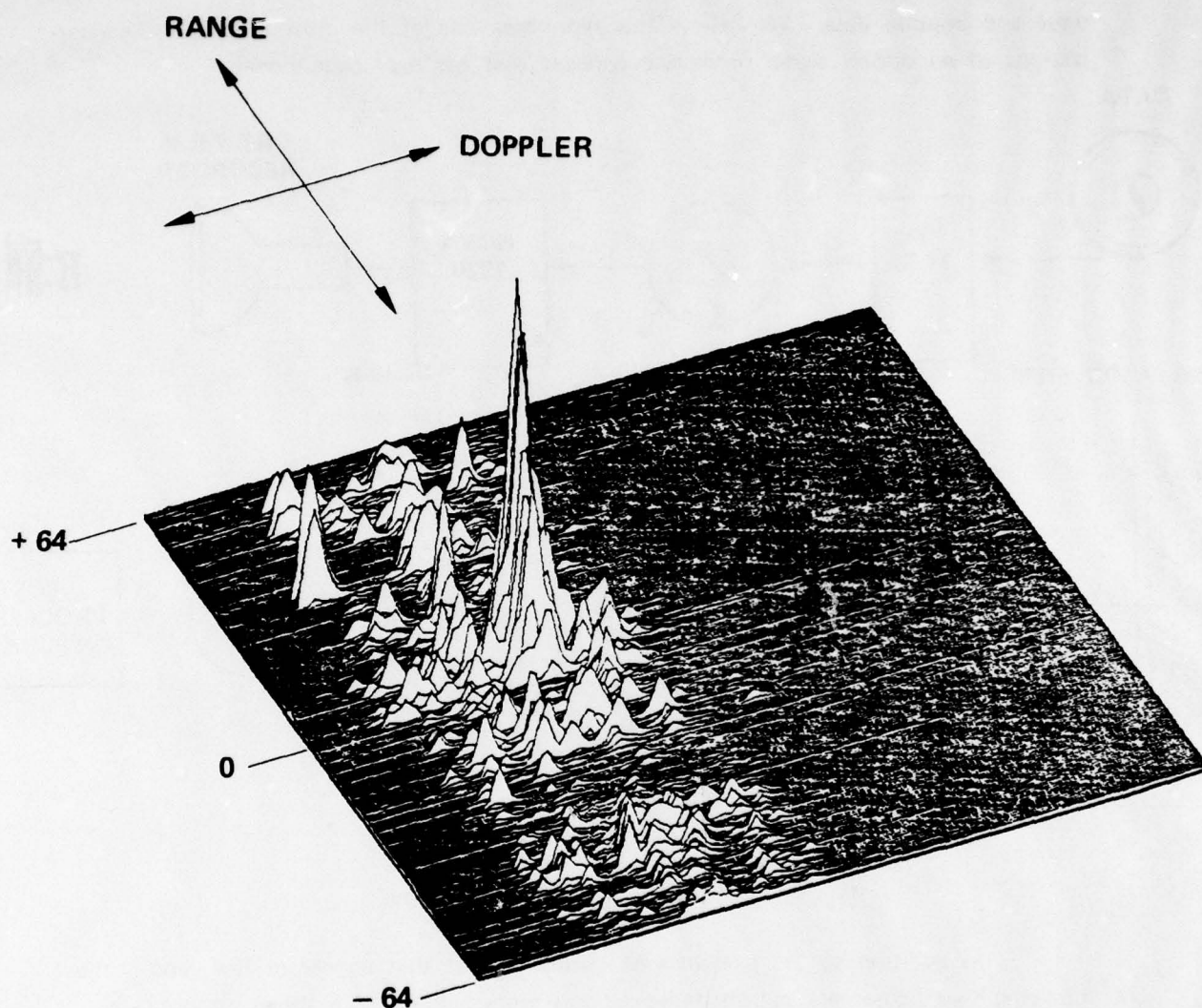


Figure 1.5 Optical Ambiguity Surface - Narrowband Noise Source (256 Second Integration Time)

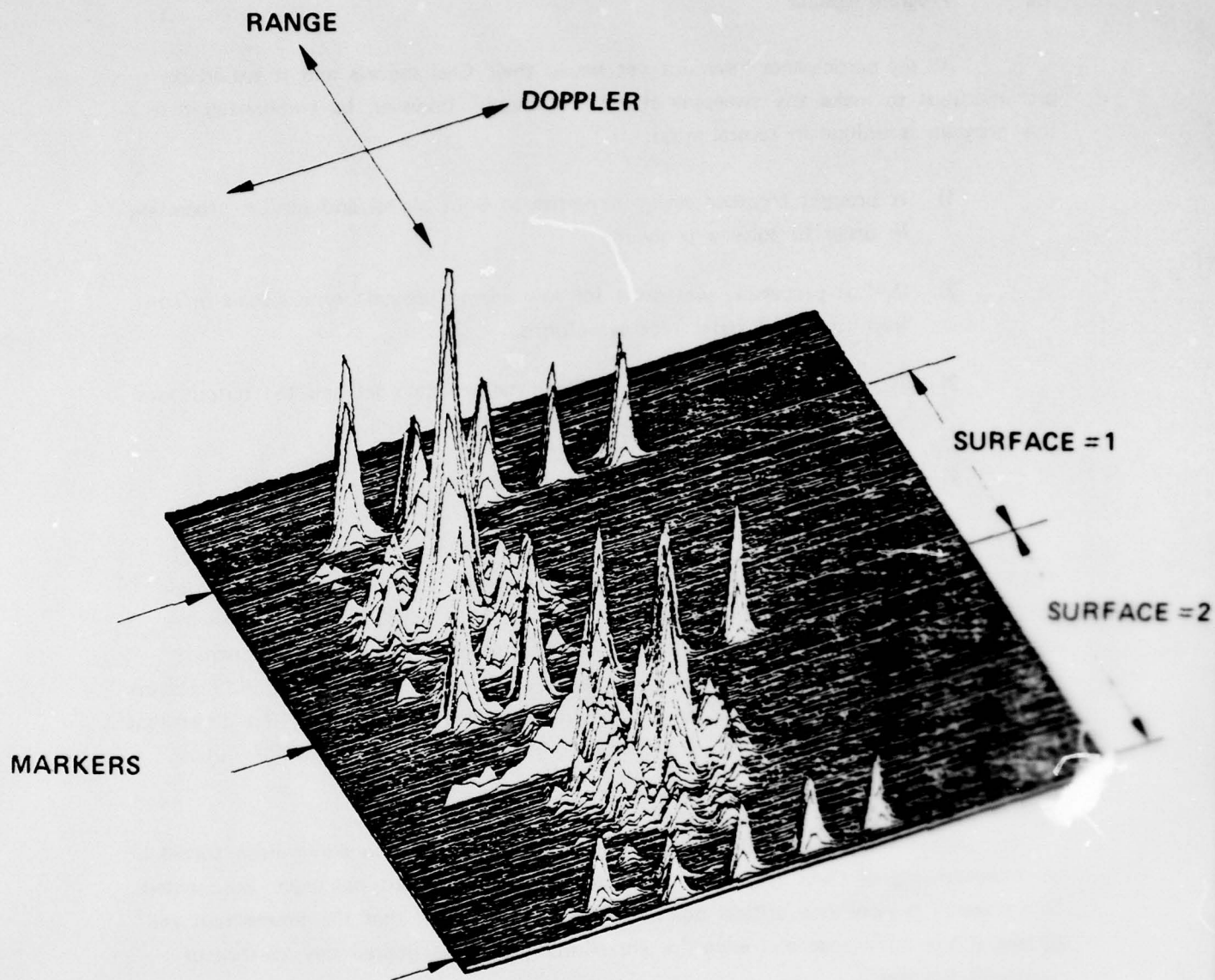


Figure 1.6 Multiple Ambiguity Surfaces per Frame (with Calibration Markers in Range and Doppler)

1.2 Program Results

All the participants have not yet issued their final reports and it would be presumptuous to make any sweeping claims. It should, however, be emphasized that this program is unique in several ways.

- 1) It brought together strong expertise in both digital and optical processing in order to solve a problem.
- 2) Optical processing was done for low energy acoustic type signals in contrast to pulsed radar type waveforms.
- 3) The processing was done on a sophisticated data set and the output was redigitized for direct comparison to digital methods.
- 4) The algorithm employed will accept complex pair data samples.

The major problems that we've encountered during this effort can be attributed to two causes. Foremost was the failure of the 1" vidicon camera to provide adequate resolution of the optical surfaces. This led to a critical uncertainty in the measurements of Doppler resolution and contributed to a reduction in the apparent processing gain by lowering the correlation peak height. The second group of problems are related to the difficulties that were originally encountered in deriving the dimensional scales to be applied to the range, Doppler and correlation height axis in the optical output.

These problems are discussed within this report and have either been solved or an understanding of their ultimate impact on future development has been documented. This research is now at a critical point and there is a danger that the momentum will be lost if the knowledge and expertise are allowed to be redirected due to lack of continued funding.

2.0 ALGORITHM FOR FORMING OPTICAL PASSIVE AMBIGUITY SURFACES

As a first step in the development of an optical processor for the LENS program, several optical correlator architectures were studied. One configuration, the Image Plane Correlator (IPC) was singled out for intensive analysis. In this section, the mathematical theory of the IPC will be developed and comments on the hardware implementation will be made.

2.1 Image Plane Correlator Theory

Although a number of different forms of optical implementation of the correlation function are possible, the scheme that was used, image plane correlation is described here.

It should be noted that the multiplane ambiguity surface generator is very similar to the various forms of image plane correlators reported as early as 1960^[1] and as late as 1977.^[2] Its uniqueness is perhaps limited to the modulation of the complex signal onto a carrier and particularly the optical (spatial) filtration to explicitly produce complex illumination in the "time" domain rather than producing a complex frequency domain filter.

Since we have complex signals, they must be converted to real signals before recording on film since film responds to light power. Therefore, each signal consisting of X^R and X^I was modulated onto a carrier. This is performed by two "multipliers" as shown schematically in Fig. 2.1. The actual multiplication was performed digitally in a Nova minicomputer which was used to pre-process the signals. The carrier frequency, w_c , should be at least twice the signal bandwidth of, X . A bias term B , is added to produce a real and positive signal. Replacing X by X_1 , denoting the output from sensor No. 1, the immediately interesting signal

$$X_1(t) = X_1^R \cos(w_c t) + X_1^I \sin(w_c t) + B \quad (2.1)$$

will be generated

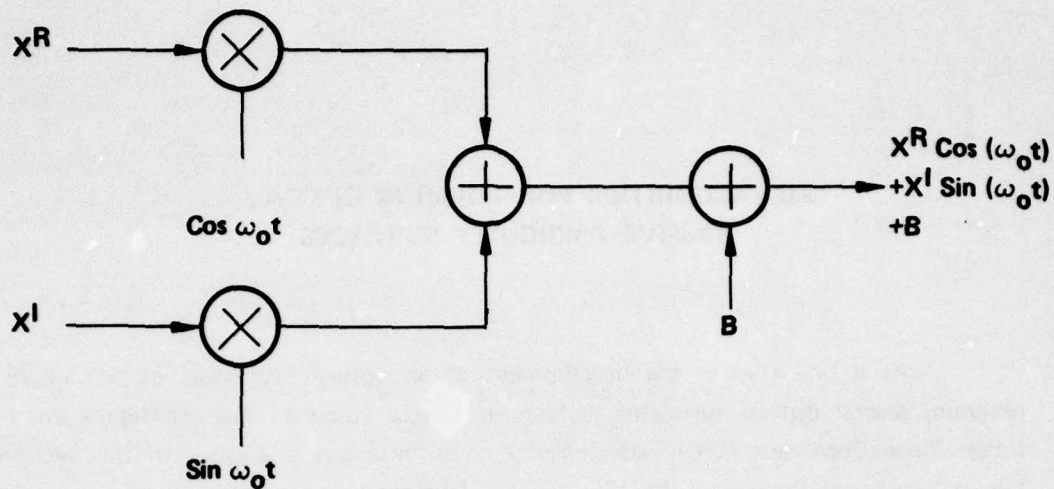


Figure 2.1 Up Conversion to Produce Real Signals from Two Complex Functions.

Since $\cos \omega_c t = (e^{j\omega_c t} + e^{-j\omega_c t})/2$ and $\sin \omega_c t = j(e^{j\omega_c t} - e^{-j\omega_c t})/2$, equation (2.1) may be written as

$$X_1(t) = (X_1^R + j X_1^I) e^{j\omega_c t} + (X_1^R - j X_1^I) e^{-j\omega_c t} + B \quad (2.2)$$

if the constant 1/2 is neglected.

This signal is recorded on film using a CRT recorder. The actual pattern consists of 256 lines of identical information.

In practice, the CRT/film combination was first optimized by control of CRT current and bias and film processing to produce a linear relationship between the input voltage and film amplitude transmittance (this technique is described in Section 3).

The resultant amplitude transmittance function of the film is

$$T_0(x, y) = \sum_n X_1(x/v) \cdot \delta(y - nk) \quad (2.3)$$

where v is the scan velocity in x and k is the distance in y between each scan line. By placing this film in the input plane, P_0 , of an optical processor shown in Fig. 2.2, a 1-D transform (transform in x , image in y) is formed at plane P_1 by the action of the lens pair LP_1 . Therefore, at plane P_1 , we will have

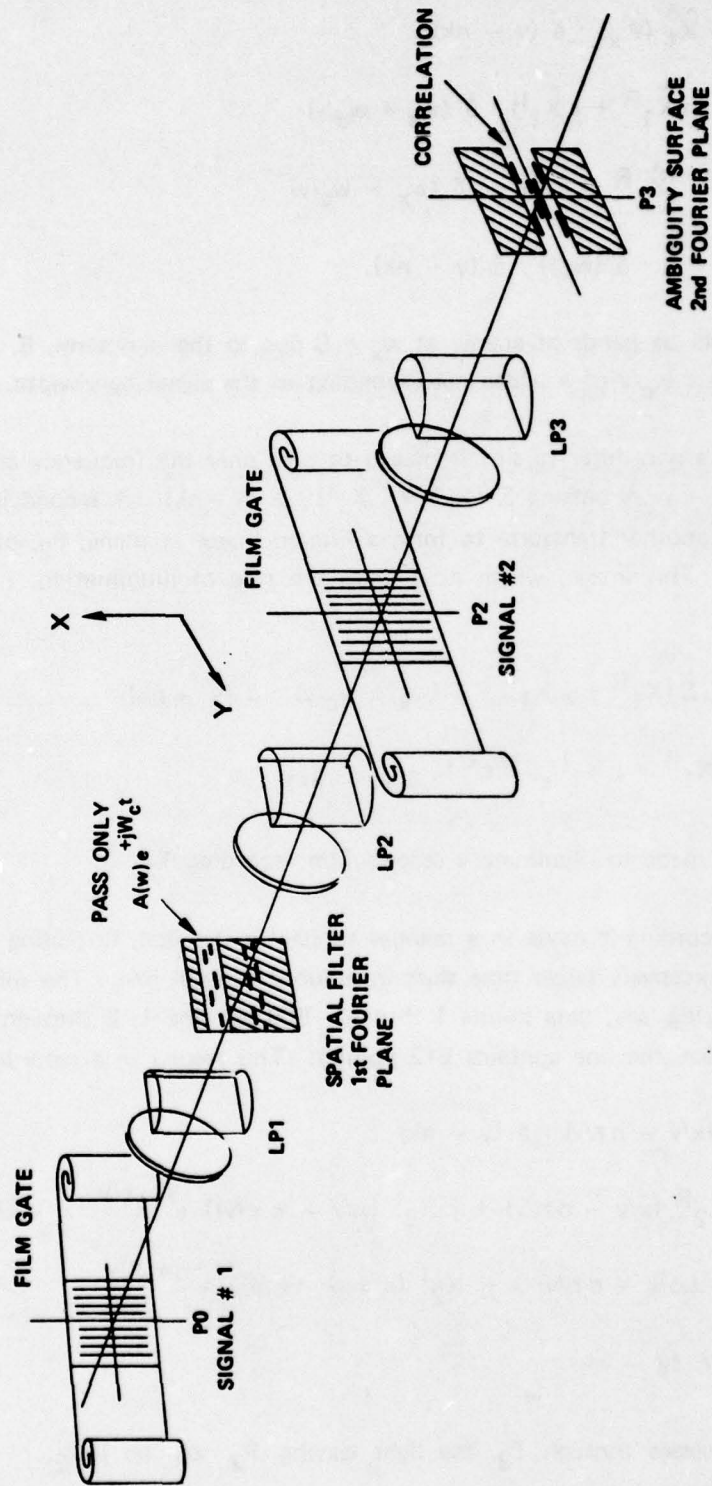


Figure 2.2 Image Plane Correlator as Described

$$\begin{aligned}
 T_1(w_{x,y}) &= \hat{T}_0^x \\
 T_1(w_{x,y}) &= \sum_n \hat{X}_1^x(w_x) \cdot \delta(y - nk) \\
 &= \sum_n [(\hat{X}_1^R + j \hat{X}_1^I) \cdot \delta(w_x + w_c/v) \\
 &\quad + (\hat{X}_1^R - j \hat{X}_1^I) \cdot \delta(w_x - w_c/v) \\
 &\quad + B \cdot \delta(w_x)] \cdot \delta(y - nk).
 \end{aligned} \tag{2.4}$$

Thus, there will be bands of energy at $w_x = 0$ due to the bias term, B , and bands centered at $w_x = \pm w_c/v$ of a width corresponding to the signal bandwidth.

At plane, P_1 , a pass filter (a slit) is placed to pass only the frequency components centered about $-w_c/v$ passing $\sum (\hat{X}_1^R + j \hat{X}_1^I) \cdot \delta(y - nk)$. A second lens pair, LP_2 , will perform another transform to form a filtered image at plane, P_2 , of the recording at plane, P_0 . This image, which now takes the role of illumination, will be

$$\begin{aligned}
 I_2(x,y) &= \mathcal{F}_x^{-1}[\sum (\hat{X}_1^R + j \hat{X}_1^I) \cdot \delta(w_x + w_c/v) \cdot \delta(y - nk)] \\
 &= \sum_n (X_1^R + j X_1^I) e^{-jw_c x/v} \cdot \delta(y - nk).
 \end{aligned} \tag{2.5}$$

This illumination, I_2 , is made to illuminate a second film recording T_2 .

The second recording is made in a manner similar to the first, but using signal No. 2 with a progressively larger time shift introduced in each line. The shift is accomplished by utilizing, say, data points 1 through 500 on line 1, 2 through 501 on line 2, etc. (in practice, the line contains 512 points). This results in a recording

$$\begin{aligned}
 T_2 &= \sum_n X_2(x/v - n\tau/v) \cdot \delta(y - nk) \\
 &= \sum_n \left\{ [X_2^R(x/v - n\tau/v) + j X_2^I(x/v - n\tau/v)] e^{jw_c x/v} \right. \\
 &\quad \left. + [X_2^R(x/v - n\tau/v) - j X_2^I(x/v - n\tau/v)] e^{-jw_c x/v} \right. \\
 &\quad \left. + B \right\} \cdot \delta(y - nk).
 \end{aligned} \tag{2.6}$$

After illumination I_2 passes through T_2 , the light leaving P_2 will be $I_2 T_2$.

Now by introducing lens pair LP_3 in order to form a 1-D Fourier transform, at plane P_3 , of plane P_2 , we will get

$$\begin{aligned}
 I_3 &= F [I_2 T_2] \\
 &= \hat{I}_2 * \hat{T}_2 \\
 &= \sum_n \left\{ \left[\hat{X}_1 \cdot \delta (w_x + w_c x/v) \right] \cdot \delta (y - nk) \right\} \\
 &\quad * \left\{ \hat{X}_2 (x/v - n\tau/v) \cdot \delta (w_x + w_c x/v) \right. \\
 &\quad + \hat{X}_2^* (x/v - n\tau/v) \cdot \delta (w_x - w_c x/v) \\
 &\quad \left. + B \right\} \cdot \delta (y - nk) \\
 &= \sum_n \left\{ \left[\hat{X}_1 * \hat{X}_2 (x/v - n\tau/v) \cdot \delta (w_x + 2 w_c/v) \right. \right. \\
 &\quad + \hat{X}_1 * \hat{X}_2^* (x/v - n\tau/v) \cdot \delta (w_x) \\
 &\quad \left. \left. + \hat{X}_1 B \cdot \delta (w_x + w_c/v) \right] \right\} \cdot \delta (y - nk)
 \end{aligned} \tag{2.7}$$

By passing only the components located at $w_x = 0$ (i.e., containing $\delta (w_x)$), we get

$$I_3' = \sum_n \left[\hat{X}_1 * \hat{X}_2^* (x/v - n\tau/v) \right] \cdot \delta (y - nk) \tag{2.8}$$

This, if transformed once more with another cylindrical lens, would produce

$$I_4 = \hat{I}_3' = \sum_n \left[X_1 (x/v) \cdot X_2^* (x/v - n\tau/v) \right] \cdot \delta (y - nk) \tag{2.9}$$

But to produce the ambiguity function

$$\chi (\tau, \phi) = \int_{-\infty}^{\infty} f_1(t) \cdot f_2^*(t + \tau) e^{-j2\pi\phi t} dt \tag{2.10}$$

we need merely take the transform of the product $f_1(t) \cdot f_2(t + \tau)$ i.e.,

$$\begin{aligned}
 \chi (\tau, \phi) &= F [f_1(t) \cdot f_2^*(t + \tau)] \\
 &= f_1(t) * f_2^* (t + \tau)
 \end{aligned} \tag{2.11}$$

Equation (2.8), expressing the spatially filtered illumination, I_3' at plane P_3 , is of this form and is therefore the passive ambiguity surface (PAS) of signals X_1 and X_2 , accomplishing the desired result.

A power detector at plane, P_3 , detects the squared modulus of I_3 , i.e., $|x|^2$. In practice, a television camera (vidicon) produces graphic and visual output and is digitized for further analysis. The results were distributed to NOSC and Ensco on digital magnetic tape, for comparison of performance with digital processing.

The algorithm that has been described is also approached in a more intuitive fashion in Appendix C which contains a paper entitled "Optical Ambiguity Surface Formation". See also [3].

2.2 Optical Implementation

In practice, the IPC algorithm was implemented in a slightly different fashion as is illustrated in Fig. 2.3. The modified design uses only one cylindrical lens. This results in a simple 2 lens imaging system between the two film planes which is much easier to align for focus and unity magnification. Cylindrical lenses are generally less accurate and more difficult to obtain for large apertures and long focal lengths. Therefore, they should be used sparingly in optical designs. The mathematical treatment remains virtually unaltered, but should reflect the fact that P_1 is a 2-D Fourier Transform plane and that the spatial filter must be altered accordingly.

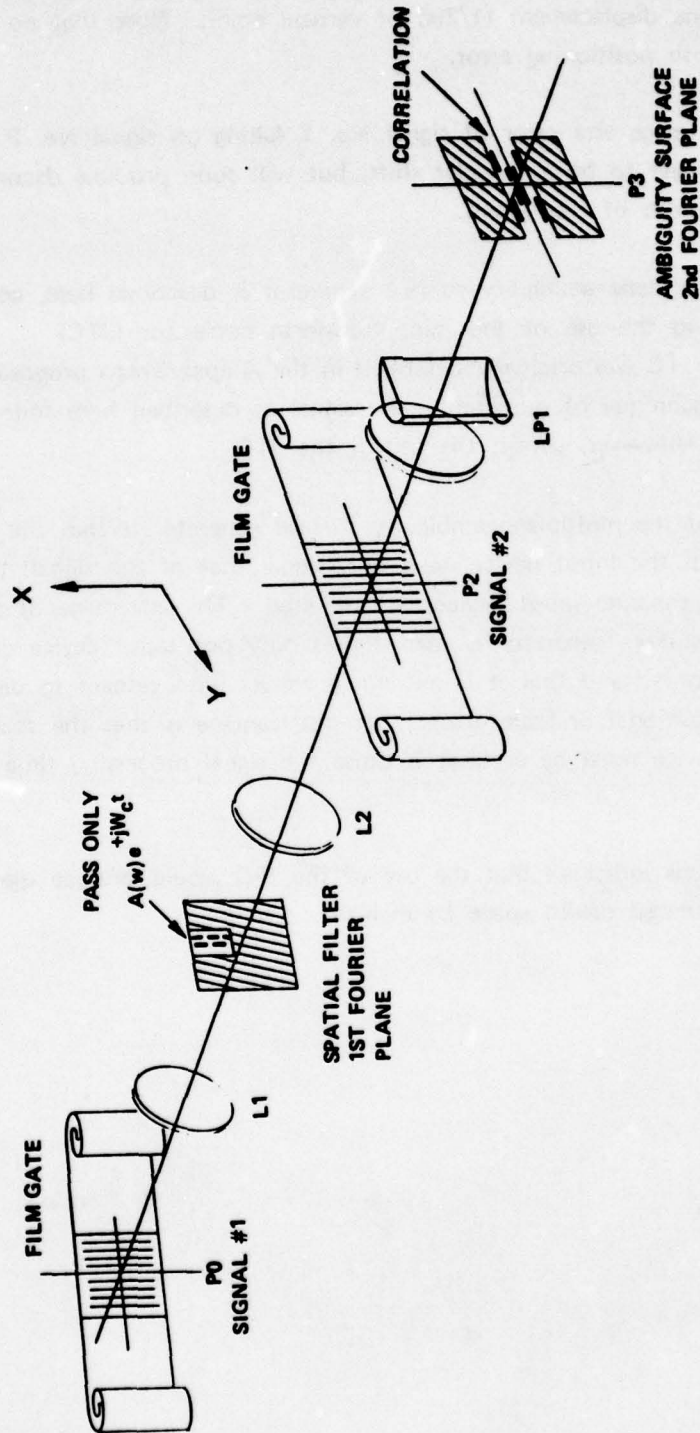
2.3 Alignment Tolerance

Two errors should be considered, positioning error and scale error.

A positioning error in, x , of signal No. 1 will introduce an apparent signal time shift (delay), and will produce $\Delta\tau$ measurement error, i.e., vertical spot motion in the output plane. If, as in the example, each line of signal No. 2 was shifted by one data sample, then "1 sample motion" displacement in, x , will produce a $\Delta\tau$ error corresponding to a movement of the ambiguity surface vertically by 1 line.

A position error in, y , of signal No. 1 will produce no error since all the lines are alike. It will reduce the extent of the τ window.

In the case of signal No. 2, a positional error in, x , will have the same effect as in the case of error in signal No. 1.



L1, L2 - 495 MM SPHERICAL
 LP1 - 300 MM CYLINDRICAL AND 300 MM SPHERICAL
 FILM GATES ARE DECOLENE FILLED AND PUMPED
 FOR LAMINAR FLOW

Figure 2.3 Image Plane Correlator Modified Design

Positional error in, y , will produce a τ translation, of the magnitude of 1 line of τ equivalent per line displacement (1/256 of vertical scan). Note that no decorrelation will occur with positioning error.

Scale error, i.e., image size error of signal No. 1 falling on signal No. 2 will produce what will first appear to be a Doppler shift, but will soon produce decorrelation, depending upon the bandwidth of the signals.

Although the multiplane ambiguity surface generator is described here, consideration was also given to the use of the joint transform correlator (JTC) approach. [4] The use of JTC was originally described in the Ampex/Ensco proposal and later was rejected. The technique of modulating the signal as described here followed by similar filtration might, however, permit the use of the JTC.

The advantages of the multiplane ambiguity surface generator is that the linear space bandwidth product of the input device need only equal that of the signal; the disadvantages are that two separate input devices are required. The advantage of the joint transform ambiguity surface generator is that it uses only one input device on which both signals are recorded and that it is extremely robust with respect to decorrelation produced by positional or scale errors. Its disadvantage is that the space bandwidth of the input device must be at least 3 times the signal processing time bandwidth.

These considerations indicated that the use of the IPC would provide maximum optical performance with limited device space bandwidth.

3.0 RECORDING SIGNALS ON FILM

The evaluation of the film inputs is of extreme importance in quantifying the performance of the LENS correlator. All of the important specifications for the system are related to the quality of the film recordings.

Range and Doppler accuracy is dependent on the spatial linearity of the signals on film since the two film masks must register so that each line of one film mask can be optically multiplied by the corresponding line in the other mask. Any curvature in the recorded raster can contribute to offsets in the output plane or decorrelation of the signal. Process integration times and number of time alignments per frame have to be compatible with the resolution of the film recording process. All processing parameters should be chosen so that spatial frequencies fall within the bandpass of the film as defined by the Modulation Transfer Function (MTF). The MTF is a measure of how the percent modulation of the film behaves with spatial frequency. The light power budget and system dynamic range are largely determined by the diffraction efficiency (DE) of the film. This is a measure of how much of the incident light is actually linearly modulated by the amplitude grating which is written on the film media.

Because of the importance of these film attributes, the following sections will review some technical concepts that pertain to recording electrical signals on film for use as a coherent light modulator.

3.1 Temporal-Spatial Analogies

Converting electrical signals to spatial modulation in raster form is analogous to the operation of a television receiver. The baseband TV signal intensity modulates the current of the electron beam that illuminates the phosphor of the screen. The beam is swept across the screen at a line rate of approximately 16 kHz and swept vertically to form 525 lines in a frame. The electrical signal contains frequencies up to 4 MHz. Dividing the temporal bandwidth by the line rate gives a maximum linear space bandwidth product of 267 cycles along a horizontal line. The TBP of

the electrical information contained in a standard TV picture is 267 cycles/line x 525 lines or 1.4×10^5 . Using a 21 inch diagonal screen as an example, the picture tube and scanning system must be able to resolve 267 cycles/378 mm or .71 cycles/mm along a scan line. This resolution should be concomitant with the maximum visual acuity of a viewer situated at a comfortable distance from the screen.

We have introduced by means of this analogy, some of the important concepts relating the temporal characteristics of an electrical signal to its spatial characteristics as a raster image. In general, a temporal frequency can be converted to a spatial frequency by

$$f_s = \frac{f_T \cdot T_L}{X_L} = \frac{f_T}{f_L \cdot X_L}$$

where T_L is the time aperture along a recorded line and X_L is the linear dimension of the aperture. The reciprocal of T_L is the scan rate f_L . The linear space bandwidth product ($f_s \cdot X_L$) is then equivalent to the time bandwidth product ($f_T \cdot T_L$) along a line. For the film recordings done during this program, a maximum linear space bandwidth product (LSBP) of 200 was used with X_L typically 12.5 mm, resulting in a f_s -3 dB modulation of 16 cycles/mm. With 256 recorded lines, the total SBP available was 5.12×10^4 cycles.

3.2 Film Recorder System

The task of transferring the synthetic data signals to film was assigned to Ampex because of the existence of a film recorder that had been successfully used on previous programs. Although many parts of the system were upgraded during the performance period, a major design effort was avoided and expenditures were minimized. Some features of the original design such as programmable raster line spacing and a servo loop to lock to an external clock were not used. The system block diagram is depicted in Fig. 3.1. Data to be recorded on film can be calculated "on the fly" or read from RK05 disk storage.

A software instruction causes a word of data to be transferred to the device number of the data acquisition board where it is converted to an analog voltage and a clock pulse is derived. A separate instruction causes a field start pulse which is used to initialize the sweep logic in the recorder for each new frame. Digital sample values

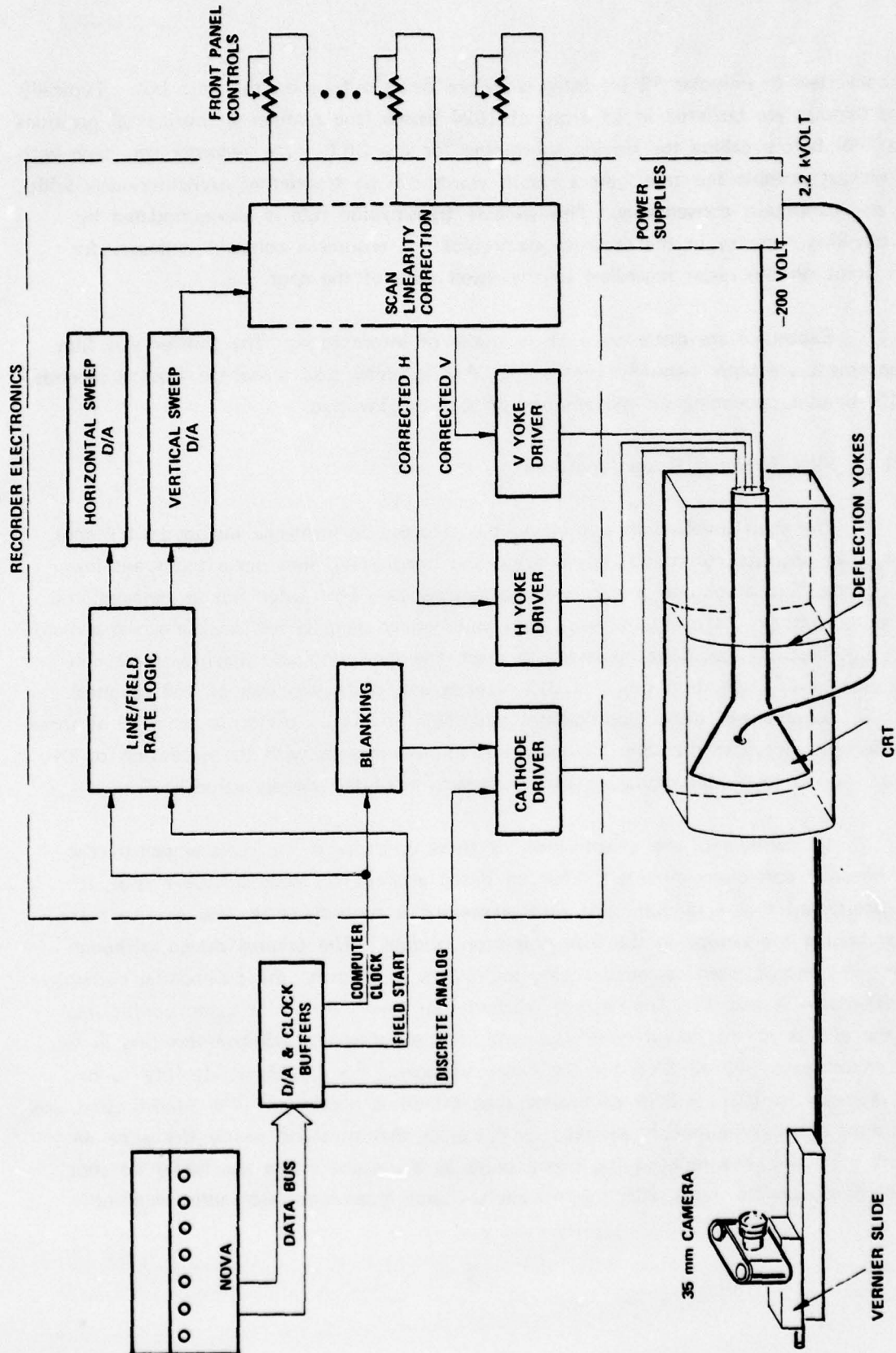


Figure 3.1 Film Recording System Block Diagram

are converted to unipolar 12 bit integers before being output on the data bus. Typically these samples are buffered in an array of 1024 words (the number of horizontal positions in a line) before calling the driving subroutine for the CRT. The recorder can cope with the highest possible bus rate. As a result, words can be transferred asynchronously without any handshake conventions. This variable transmission rate is accommodated by the blanking circuitry in the recorder electronics. It ensures a constant exposure for each point on the raster regardless of the dwell time of the spot.

Exposures are made on a single frame of information. The shutter and film advancement are both manually controlled. A mask may take anywhere from 5 seconds to 10 minutes depending on the amount of software involved.

3.2.1 Film Recorder Setup Procedure

The steps involved in optimizing the recorder performance included CRT spot focus, scan linearity correction, raster sizing and positioning, film plane focus and linearizing of the film amplitude transmission characteristics. This latter task is detailed in a following section. As many of these steps were undertaken, it was ascertained that hardware modifications would be necessary to reach the resolution and linearity goals concomitant with integration times of 512 seconds and range windows of 256 seconds. Table 3.1 summarized these modifications and their effects on performance. All of these modifications provided dramatic improvements in performance (with the exception of the switch from 8 to 12 bit digital to analog conversion of the sample values).

An example of the effectiveness of these upgrades is the replacement of the scan linearity correction module. After an initial attempt to focus the CRT spot, it was ascertained that a random spot jitter exceeding 4 spot diameters was due to noise contaminating the sweeps in the scan corrector module. The original design, although elegant in concept, used cascaded analog multipliers to generate the polynomial correction coefficients in X and Y. The cascade reached four layers deep (for cubic coefficients) and the effects of the device noise was both multiplicative and additive resulting in less than an estimated 46 dB SNR for the sweep voltages. For positional stability to one spot diameter in 1024, a SNR of greater than 60 dB is necessary. The modification was built around a hybrid module supplied by Intronic that provided nearly the same distortion correction and reduced the sweep noise to the point where absolutely no spot motion is observable under 20X magnification. Spot focus was then easily achieved.

Table 3.1

Hardware Upgrade	Effect on Performance
Scan Linearity Corrector	Significantly reduced noise on the sweep waveforms thereby improving positional accuracy.
Sweep D/A Converters	Ensured monotonicity at data rates compatible with the computer interface.
Camera Carriage	Allowed vernier control of camera focus and alignment.
High Resolution Lens	Removed the resolution limit imposed by common 55 mm f2.0 lens.
12 Bit Analog D/A	Increased the resolution of calculated analog values to 4096 grey levels.
CRT Replacement*	Necessary maintenance due to phosphor blemishes after several hundred hours of use.

*Purchased under contract.

Focussing of the film plane image was an initial problem. The depth of focus allowed before the image departs perceptibly from its optimum is given by:

$$\Delta D = 4 \lambda F^2$$

where λ is the wavelength of phosphor and F is the camera lens f number. [5] For a λ of 460 nm and F of 4.0, an allowable depth of focus is only 30 μ m. This tight tolerance must be held across the entire image plane and, therefore, requires alignment of the camera in every axis. A camera carriage with a vernier slide was constructed which included provisions for positioning a microscope tube behind the film plane to inspect the focus. This greatly aided in the focussing of the image.

3.2.2 Scan Linearity Correction

Figure 3.2 shows some of the distortions that are characteristic to cathode ray tube deflection systems. The physical construction of the deflection yoke will determine the type of distortion characteristics that will be observed at the cathode ray tube screen. One general type of distortion is pincushion which is caused by an unevenly filled distribution of the deflection field. Here the magnetic-field density increases from the deflection axis toward the outer parameter of the deflecting field; therefore, the angle with which the electron beam is deflected increases with the deflecting angle.

The opposite geometric problem is barrel distortion. A deflection system to compensate for pincushion distortion dictates that the deflection yoke be wound in a saddle-type structure. This has a tendency to concentrate the magnetic field outward from the center of the deflecting axis. If the magnetic field is over compensated, it will cause the electron beam to be deflected less as the deflection angle is increased.

A third geometric problem that is introduced by flat-faced cathode ray tubes is called tangent error and is also illustrated in Fig. 3.2. As the scan angle linearity increases, the displacement of the electron beam along flat faceplate also increases, but in an increasingly nonlinear (tangential) fashion.

The errors caused by these geometrical distortions can be approximated by a truncated series as in:

$$\epsilon (X,Y) = ax + by + cxy + dx^2 + ey^2 + fx^2y + gy^2x + hx^2y^2 + \dots$$

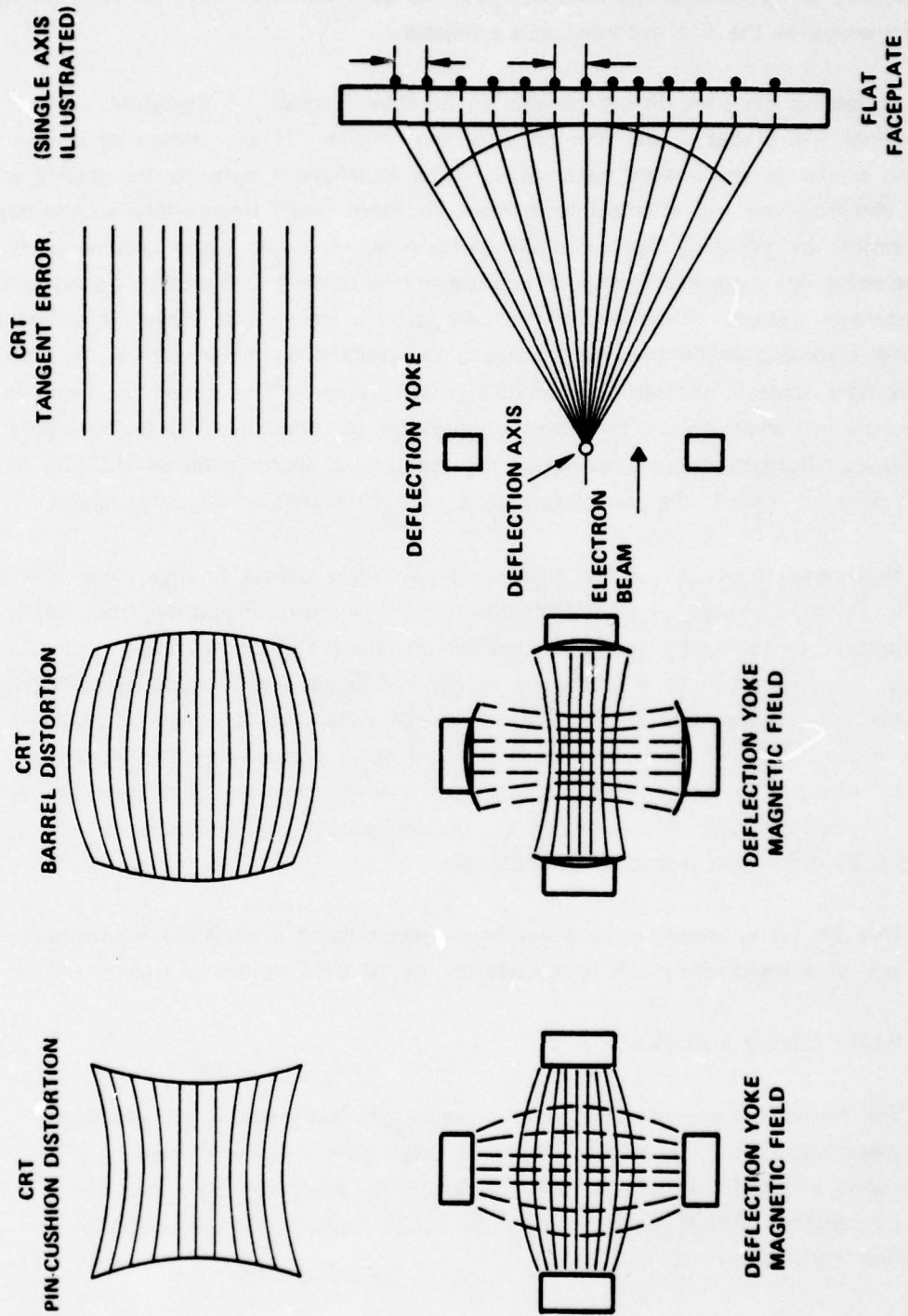


Figure 3.2 Spatial Distortions in CRT Systems

In practice, not all of these terms are necessary and only the first eight terms as shown were implemented in the film recorder scan corrector.

Correcting the scan distortions was an iterative process. A precision grating (Ronchi ruling) was placed in the film plane of the camera. It was chosen to have a line spacing similar to the imaged raster pitch. The interference between the grating and the raster was observed and attempts were made to "zero beat" (completely superimpose) the two gratings by adjusting the correction coefficients. One can easily become proficient at selecting the proper sequence of adjustments to cause a convergence to an optimum interference pattern. Examples of this beat pattern for various errors are shown in Fig. 3.3. A recording would then be made and the residual distortion verified by observing the line rate spots in the optical Fourier transform plane. The spread of the main lobe of these spots indicates the integrated nonlinearity of modulation of the line pitch that is present. Furthermore, by restricting the aperture of illumination of the film, and inspecting different regions, the spatial variations of the distortions can be observed.

Measurements of $\Delta f/f_L$ were made in the enlarged optical Fourier plane which indicated a .5% to 2% range of total scan distortion. This variation stems from the fact that the linearity of the sweep system is sensitive to changes in the scanning rate. As an example, a software call to a subroutine in the middle of a raster pattern stalls the sweep at the last recorded point. Some decay of the sweep voltages may be observed during this period and will result in a start-up transient in positioning when scanning is resumed. Fortunately, the synthetic data masks were precalculated and could be recorded at a constant rate, limited mainly by the uncertainty in disk access time. Therefore, a 1% total scan distortion is applicable.

This 1% figure translates to a maximum accumulated uncertainty in position along an axis of approximately 2.5 lines vertically or 10 CRT points horizontally.

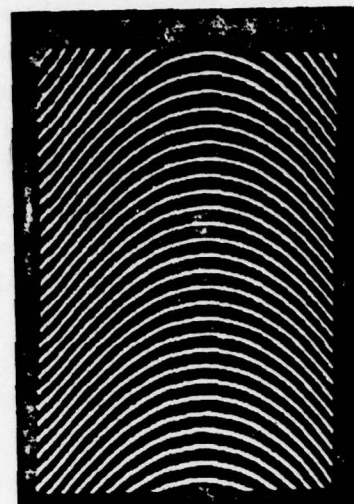
3.2.3 Raster Library Software

The Raster Library was created to generate the test patterns and alignment aids that were used during the effort. Many of these were initially suggested by David Cassasent of CMU and proved to be invaluable in measuring important film recording parameters. Others were developed to aid in rapid and accurate alignment of the optical components.

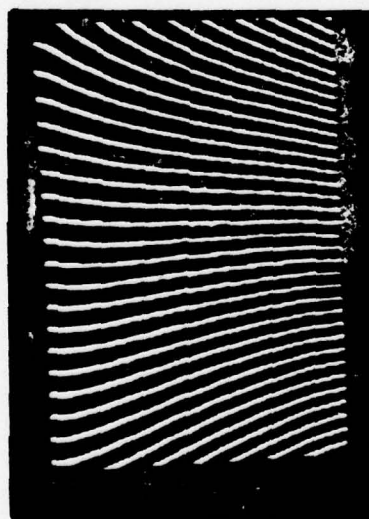
Additional software was created to format the synthetic data set and will be discussed in Section 4.



(a) No Scan Error



(b) Excess X^2 term
(horizontal parabola)



(c) Excess XY term (trapezoid)

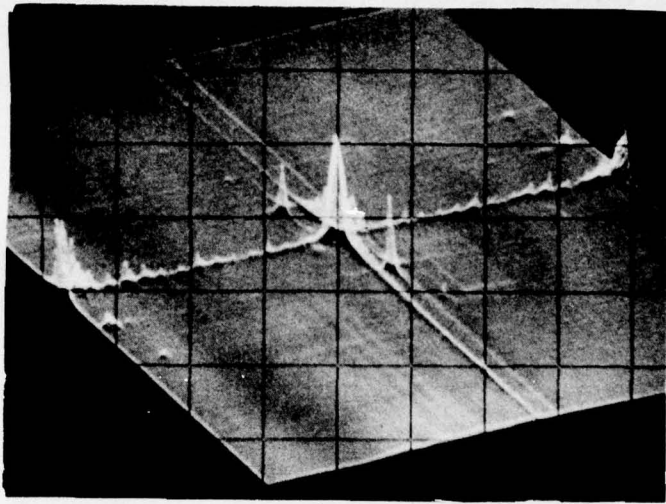


(d) Excess X^2Y term (barrel
and pincushion)

Figure 3.3 Examples of Common CRT Scan Errors (grossly exaggerated)

Two examples of these test pattern generating utility programs are shown in Fig. 3.4. At the top is the optical Fourier transform for a RASTER7 pattern. The input pattern was a two-dimensional film with a single sinusoid at low frequency (3.2 cycle/mm) that had a small shift in starting phase from line to line. This rotating phase causes the fundamental of the 2-D transform to be displaced at an angle to the fine frequency axis so as to avoid the lobes of the zero order sinc function. As shown in Fig. 3.4A, this pattern can be used to measure the harmonic power of a recorded sinewave and thereby help to achieve linear amplitude recording.

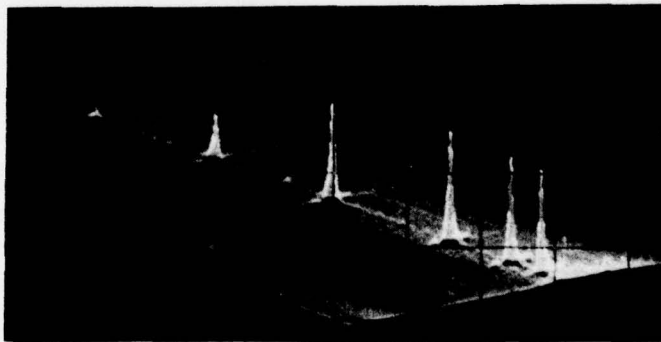
The second example was a pattern used to measure the film recorder MTF called IPC2. This pattern is the sum of six frequencies of sinewaves. Again a phase shift is employed so that power measurements in the transform plane can be taken without interference from the zero order. As shown in Fig. 3.4B, the relative spectral powers of these components can be measured. These can be related through diffraction efficiency to how the film modulation falls off with increasing spatial frequency. This results in a measure of the film recording resolution or MTF.



(a)

FOURIER TRANSFORM OF RASTER7

32 CYCLE/LINE SHIFTED SINEWAVE
NOTICE 2nd HARMONIC



(b)

FOURIER TRANSFORM OF IPC2

FREQUENCIES FROM RIGHT ARE 20.5 40.5 80.5
160.5 240.5 and 320.5 CYCLES/LINE

Figure 3.4A & B

AMPEX

The next pages show a sample main program from the library and the sub-routine "CRT" which is the assembly language driver that controls the film recorder. The pages immediately following these are a summary of the main programs contained in this library.

PAGE 1
10/24/78

RASTER2.
17:37:59

DIRECTORY DP0
DISK PACK #1 - RASTER LIBRARY

```

C      RASTER1
C      MAIN CALLS @SUBR2@
C      LATEST REVISION 12 4 77
C      DONE BY LARRY WEINER
C
C      THIS PROGRAM OUTPUTS A CRT RASTER COMPOSED OF FOUR
C      DIFFERENT FREQUENCIES OF SINEWAVES. OUTPUT IS ORGANIZED INTO
C      FOUR BLOCKS OF 60 LINES SEPARATED BY FOUR
C      LINES OF BLACK. FREQUENCY IS DOUBLED BLOCK TO
C      BLOCK STARTING WITH ENTERED VALUE OF FREQ.
C      *NOTE* AMPLITUDE+DC<256.
C
C
C      COMMON /GEORGE/IOUT(1024)
C      INTEGER AMP,DC
C      ACCEPT "AMPLITUDE (0-256)",AMP
C      ACCEPT "DC OFFSET (DC+AMP256)",DC
C      ACCEPT "FIRST LINE FREQUENCY",FREQ
X      CALL INITT(120)
C      CALL START
C      AMP=AMP/2
C      DO 8 M=1,4
C      AUG=2*FREQ*3.1415926/1024
C      DO 10 IZ=1,1024
C      IOUT(IZ)=AMP*(SIN(AUG*IZ)+1)+DC
10      CONTINUE
C      DO 11 IX=1,60
C      CALL DTA(1)
11      CONTINUE
X      CALL OPLO(M)
C      DO 2 NI=1,4
C      CALL BLACK
C      CALL DTA(1)
2      CONTINUE
8      FREQ=FREQ*2
X      CALL FINIT(0,780)
C      STOP
C      END

```

AMPEX

PAGE 1
11/10/78

CRT.
14 09 42

DIRECTORY DPG
DISK PACK #3 SYNTHETIC DATA

	TITL	CRT	
	EXTU		
	NREL		
	ENT	START, DTA	
	COMM	GEORGE 1024	
	FS.		
START:	JSR	@.CPYL	
	NICC	60	
	JSR	@.FRET	RETURN
DTA	JSR	@.CPYL	
	LDA	0, @T.+0,3	
	STA	0, LUUP	
	LDA	0, MASK	MASK OUT RTC
	MSKO	0	AND A/D INTERRUPTS
LUP	LDA	0 THOSND	
	STA	0 THOSAND	
	LDA	2, DAT	LOAD ADDRESS OF COMMON AREA
LOOP	LDA	0, 0, 2	LOAD DATA FROM COMMON AREA
	NIOS	60	SEND START PULSE TO CRT
	DOA	0, 60	SEND OUT DATA
	INC	2 2	NEXT ADDRESS
	DSZ	THOSAND	DONE YET?
	JMP	LOOP	
	DSZ	LUUP	
	JMP	LUP	
	JSR	@.FRET	RETURN
JP	.BLK 1		
THOSND	2000		
THOSAND		2500	
MASK	204		
DAT	.GADD	GEORGE, 0	
	FS =	1	
	T. =	-167	
	END	START	

AMPEX

XPLAIN
13:14:46

DIRECTORY DPO

SUMMARY OF RASTER LIBRARY
THESE PROGRAMS ARE USED TO CREATE PATTERNS FOR THE CRT
FILM RECORDER.

LATEST REVISION 12/28/77
DONE BY L.R.W.
AMPEX-ADVANCED TECHNOLOGY DEPT-

****RASTER1****

THIS PROGRAM OUTPUTS A CRT RASTER COMPOSED OF FOUR
DIFFERENT FREQUENCIES OF SQUAREWAVES. OUTPUT IS ORGANIZED INTO
FOUR BLOCKS OF 60 LINES SEPARATED BY FOUR LINES OF BLACK.
FREQUENCY IS DOUBLED BLOCK TO BLOCK STARTING WITH
ENTERED VALUE OF FREQ. *NOTE* AMPLITUDE+DC<256.
AMPLITUDE AND DC ARE ENTERED FROM KEYBOARD

****RASTER2****

THIS PROGRAM OUTPUTS A CRT RASTER COMPOSED OF FOUR
DIFFERENT FREQUENCIES OF SINEWAVES. OUTPUT IS ORGANIZED INTO
FOUR BLOCKS OF 60 LINES SEPARATED BY FOUR
LINES OF BLACK. FREQUENCY IS DOUBLED BLOCK TO
BLOCK STARTING WITH ENTERED VALUE OF FREQ.
AMPLITUDE AND DC ARE ENTERED FROM KEYBOARD.
NOTE AMPLITUDE+DC<256.

****RASTER3****

THIS PROGRAM GENERATES A GREY SCALE WITH VALUES GIVEN IN
DATA STATEMENT.
DATA AMP/0,32,64,96,128,160,192,224/

****RASTER4****

RASTER4 CREATES THREE BANDS OF SINEWAVES 82 LINES
LONG. THE SINE AMPLITUDES VARY IN EACH BAND AS 64,128,
192 POINTS OUT OF 256. THIS CORRESPONDS TO 25%,50%
AND 75% SATURATION.EACH BAND IS SEPARATED BY 5 LINES OF BLACK.
FIELD FREQUENCY IS ENTERED FROM THE KEYBOARD.

****RASTER5****

RASTER5 CREATES THREE BANDS OF LFM SINEWAVES 82 LINES
LONG. THE SINE AMPLITUDES VARY IN EACH BAND AS 64,128,
192 POINTS OUT OF 256. THIS CORRESPONDS TO 25%,50%
AND 75% SATURATION. EACH BAND IS SEPARATED
BY FIVE BLACK LINES.
LFM STARTING FREQUENCY AND BANDWIDTH ARE ENTERED FROM
KEYBOARD.

****RASTER6****

RASTER6 CREATES THREE BANDS OF LFM SQUAREWAVES 82 LINES LONG. THE CHIRP BANDWIDTH AND STARTING FREQUENCY IS CHANGED THREE TIMES PER FIELD AS INPUT FROM THE KEYBOARD.

****RASTER7****

THIS IS A GENERAL PROGRAM TO GENERATE A PAIR OF PHASE SHIFT CORRELATION MASKS FOR OPTICAL PROCESSING USING THE CRT FILM RECORDER. BOTH A SHIFTED AND NONSHIFTED VERSION OF THE SELECTED SIGNAL IS AVAILABLE. SIGNAL TYPE, AMPLITUDE, AND DC OFFSET ARE KEYBOARD SELECTED.

****RASTER8****

THIS PROGRAM IS USED TO OUTPUT PRECALCULATED DOPPLER SHIFT SINUSOIDAL TEST PATTERNS TO A CRT. THE 1024X256 ARRAY SHOULD RESIDE ON DISK AT CPART "T". A NONSHIFTED VERSION IS ALSO AVAILABLE.

****RASTER9****

THIS PROGRAM IS USED TO OUTPUT PRECALCULATED DOPPLER SHIFT LFM TEST PATTERNS TO A CRT. THE 1024X256 ARRAY SHOULD RESIDE ON DISK AT CPART "U". A NONSHIFTED VERSION IS ALSO AVAILABLE.

****DGEN8****

THIS PROGRAM GENERATES A 1024 POINT BY 256 LINE ARRAY OF SINUSOIDS IN THE DOPPLER TEST PATTERN FORMAT. THIS ARRAY IS TEMPORARILY STORED ON DISK (CPART "T") BEFORE TRANSFER TO MAG TAPE. THIS DATA MAY THEN BE CALLED BY *RASTER8*.

****DGEN9****

THIS PROGRAM GENERATES A 1024 POINT BY 256 LINE ARRAY OF CHIRPS IN THE DOPPLER TEST PATTERN FORMAT. THIS ARRAY IS TEMPORARILY STORED ON DISK (CPART "U") BEFORE TRANSFER TO MAG TAPE. THIS DATA MAY THEN BE CALLED BY *RASTER9*.

****IPC1****

PROGRAM TO GENERATE MASKS FOR THE IMAGE PLANE CORRELATOR. PROGRAM CALCULATES A SINE OR LFM DOPPLER SHIFTED PATTERN FOR THE INPUT PLANE OF THE IPC. THE SECOND PLANE MASK WILL ALSO BE AVAILABLE. SIGNAL TYPE, AMPLITUDE AND DC ARE ENTERED FROM THE KEYBOARD.

IPC2

THIS PROGRAM IS USEFUL IN MEASURING THE MTF FOR THE CRT FILM RECORDER. SIX DIFFERENT FREQUENCY SINUSOIDS ARE SUMMED TOGETHER. EACH COMPONENT IS APPROXIMATELY 10% OF TOTAL AMPLITUDE. FREQUENCIES ARE 20.5, 40.5, 80.5, 160.5, 240.5, 320.5 CYCLES/CENTIMETER.

RASTER

SLIGHT VARIATION ON RASTER3. PRESENT AMPLITUDES ARE: 64, 64, 128, 128, 192, 192, 255, 255.

3.3 Idealized Film as a Coherent Light Modulator

A coherent optical system processes both amplitude and phase of the modulated laser beam. In order to use photographic film as an amplitude modulator, we must describe its amplitude transmittance characteristic versus exposure. Conventional photographic processing relies on describing film in terms of the density resulting from a combination of light exposure and development technique. The fact that density is related (although nonlinearly) to recorded amplitude allows us to exploit well known film parameters so as to find an optical operating point for maximally linear amplitude transmittance versus exposure. The most common characteristic curve for film is the Hurter-Driffeld (HD) plot of density versus log exposure as shown in Fig. 3.4A. Once exposed, the film density can be defined by:

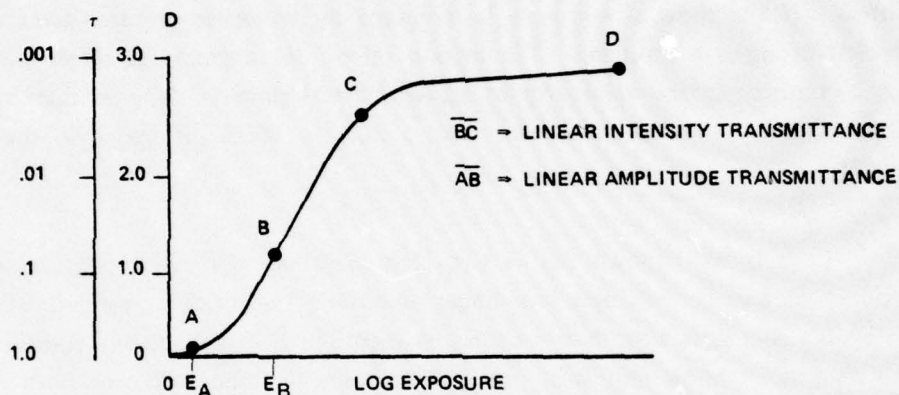
$$\begin{aligned} D &= \log (1/\tau_n) \\ \tau_n &= \text{intensity transmittance} \\ &= \text{local average } \left[\frac{I \text{ transmitted}}{I \text{ incident}} \right] \end{aligned} \quad (3.3.1)$$

The relationship between intensity transmittance and amplitude transmittance is a square law mapping which must include any phase deviations due to local emulsion thicknesses.

$$T(x,y) = \sqrt{\tau_n(x,y)} \exp(j\phi(x,y)) \quad (3.3.2)$$

The phase term can be neutralized by index matching. The purpose of the liquid gates in the LENS correlator is to provide a laminar flow of deca/tetrahydronaphthalene across the film. This combination of liquids is chosen because its optical index comes close to forming a uniform phase front for the film/glass/air interface. Because of this precaution, the phase term in Eq. 3.3.2 can be dropped.

By comparing Fig. 3.4A and B, several important points should be noted. The linear amplitude region of the curves, AB, exists in the low density region, therefore contributing to the subjective opinion that linear recordings lack contrast or appear washed out. Secondly, the corresponding density change over this region is restricted to about one order of magnitude^[6] (as will be later demonstrated by our experimental results). At the same time, this linear amplitude region represents a considerable range of exposure energy. For our experiments, this range was perhaps 400 ergs/cm². The last observation



- { D => DENSITY
- { E => EXPOSURE
- { τ => INTENSITY TRANSMITTANCE
- { T => AMPLITUDE TRANSMITTANCE
- { γ_n => GAMMA FOR NEGATIVE FILM

$$\gamma_n = \frac{D_C - D_B}{\log E_C - \log E_B}$$

Figure 3.4A

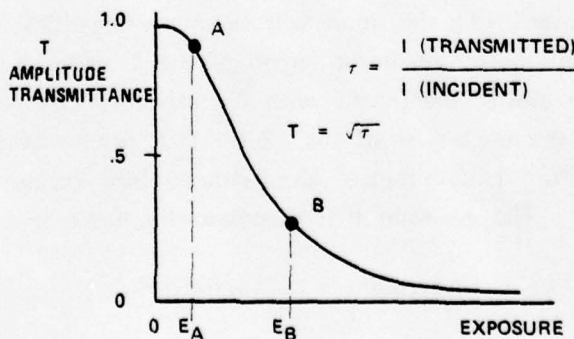


Figure 3.4B

is that since we are developing a linear model for amplitude versus exposure, the density curve is of little use other than to initially get our bearings by means of conventional densitometry.

Attempts to utilize the linear intensity segment BC on the HD curve by "pre-distorting" or square rooting the electrical drive signal are undesirable for two reasons. The necessary exposures required in region BC increase by an order of magnitude. Since both the CRT spot size and the developed film spot grow with intensity, the resolution suffers. If the time of exposure is increased by an order of magnitude, fogging and haloing becomes a problem. The second reason for avoiding schemes that attempt to use this region is the variability of γ_n with development. One minute of development time or 10°F in temperature can make a 20% to 100% difference in the final value of γ_n . [7]

It is well known that a two step, negative to positive process, with a gamma product of two [8] will also give linear amplitude results over segment BC. This process unfortunately, suffers from the problems mentioned above and, in addition, narrows the choices of films and developers and requires tight control over both resolution and illumination during the reversal imaging. [6]

It is for these reasons that the film recorder was constrained to operate in region AB in order to provide linear amplitude recordings.

3.3.1 Biasing for Linear Operation

Referring to the T-E curve in Fig. 3.5A, a close analogy can be developed between choosing a bias point for maximizing the linear swing of a transistor amplifier and determining the correct range of exposures for linear film recording. A drastic shift in the bias point or overdriving the input will cause nonlinearities in the output. Figure 3.5A shows the equation for the linear region of the T versus E curve and Fig. 3.5B shows this region plotted exclusively with the exposure axis given in units corresponding to the 4096 discrete values of the 12 bit D/A drive voltage. The vertical axis is marked in amplitude transmittance values derived from measured density readings of grey scale steps. The equation that describes this linear segment is then

$$T = C - BE = .78 - (.42/4095)E \quad (3.3.3)$$

If E is:

$$E = E_b + E_s \cos 2\pi\phi X \quad (3.3.4)$$

then

$$T/C = (1 - BE_b/C) - BE_s/2C (e^{+j2\pi\phi X} + e^{-j2\pi\phi X}) \quad (3.3.5)$$

Normalizing by C accounts for the reduced transmittance at our minimum exposure. The quantity $(1-C)$ can be considered the absorption of the film at this minimum exposure.

By definition;

$$T = \frac{\text{Amplitude Transmitted}}{\text{Amplitude Incident}} = \frac{A_T}{A_0} = (I_T/I_0)^{1/2} \quad (3.3.6)$$

The terms in Eq. 3.3.5 represent the components of the light amplitude that are passed by a transparency with transmittance T and incident illumination A_0 . Note that if amplitudes are observed in the Fourier domain, that $(1 - BE_b/C)$ is the amplitude of the zero order focussed spot and $(BE_s/2C)$ will be the amplitude of each of the spots at $\delta(f \pm \phi)$.

If we measure the intensity of a diffracted spot in the transform plane and divide by the intensity of the incident beam we have formed a ratio commonly known as the diffraction efficiency. This ratio describes the percent of input intensity that is converted to signal intensity. By measuring the diffraction efficiency, we can derive the amount of modulation that was recorded by the relationship.

$$\frac{I_{\text{signal}}}{I_0} = \left(\frac{BE_s}{2C} \right)^2 \Rightarrow \text{Diffraction efficiency} \quad (3.3.7)$$

As an example, diffraction efficiency as measured for a single sinewave recording at low spatial frequencies was 1.6%. Referring to Fig. 3.5B, the input exposure for this recording was $E_b = 2048$ units and $E_s = 2047$. The calculated diffraction efficiency, as given by Eq. 3.3.7, is 1.8%.

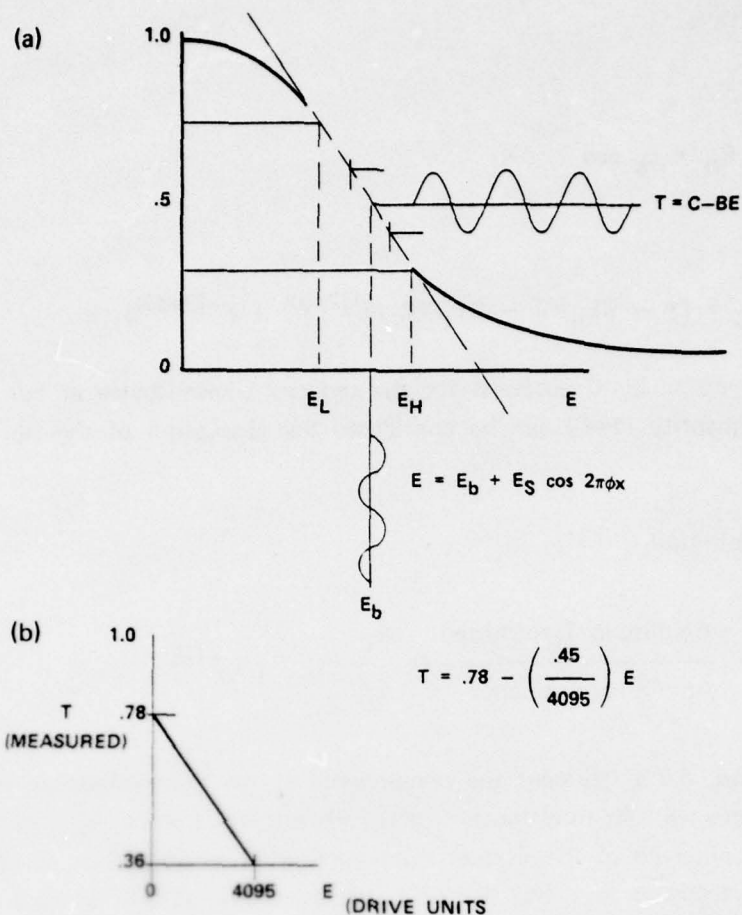
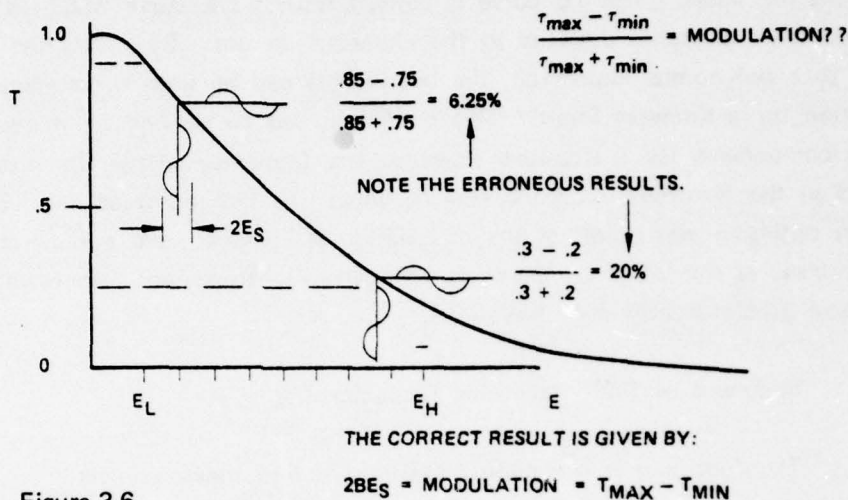


Figure 3.5A & B

By measuring the diffraction efficiency and knowing B and C by densitometry, we can have an unambiguous measurement of $T_{\max} - T_{\min}$ or the actual depth of modulation. In our example, the modulation was $(.78 - .36)$ or 42%. Notice also that 100% modulation would only occur if a linear swing in T were to occur from 0 to 1 (or from fully opaque to fully transparent). In this case, $C = 1$, $E_b = 0.5$, $B = 1$ and $E_s = 0.5$. The diffraction efficiency limit is then found to be from Eq. 3.3.7, $(1/4)^2$ or 6.25%. This also corresponds to 100% modulation using $2 BE_b$ as a criterion.

Caution must be used in applying the conventional definitions of modulation in cases where the bias point is not fixed. A standard definition of modulation, $\frac{T_{\max} - T_{\min}}{T_{\max} + T_{\min}}$ predicts erroneous differences in modulation for shifts in the bias point

as shown in Fig. 3.6. It should be obvious that a small signal should be converted with the same efficiency through a linear element regardless of bias and this is true for our linear model, but not for the standard definition.



3.3.2 Modulation Transfer Function

After defining modulation as the peak to peak linear recorded amplitude transmittance and showing its proportionality to diffraction efficiency, we can proceed to show how these quantities behave as a function of spatial frequency ϕ . We start by introducing the term $K(\phi)$ into Eq. 3.3.7 so that:

$$\frac{I_{\text{signal}}}{I_0} = K(\phi) \left(\frac{BE_S}{2C} \right)^2 \quad (\text{for low spatial frequency } E_S) \quad (3.3.8)$$

The variable $K(\phi)$ is then the variation in useful modulation normalized to the modulation at low frequencies. By recording a series of sinusoids with fixed modulation and at a fixed bias point, but with increasing frequencies, we can derive a true Modulation Transfer Function, $K(\phi)$, from the measurement of the diffracted light intensity. [2]

$$K(\phi) = \frac{\left(\frac{I_{\text{signal}}}{I_0} \right)^{1/2}}{\left[\left(\frac{I_{\text{signal}}}{I_0} \right)^{1/2} \right]_{\text{LF}}} \quad (3.3.9)$$

Results will be shown in a later section.

3.3.3 Prediction of Harmonic Distortion from the T vs. E Curve

Harmonic distortion at a certain modulation and bias can also be predicted from the TE curve. The TE curve is derived from a DE curve which in turn is constructed from measured densities at the exposures in use. By fitting the observed TE curve to a polynomial expression, the coefficients can be used to estimate the harmonic distortion for a sinewave input. This prediction can be verified by measuring the harmonic components for a sinewave input in the frequency plane. The distribution of harmonics in the transform is also a clue to where the bias point on the TE curve lies. For an optimum bias point, as the modulation is increased, the odd harmonics will predominate as the waveform becomes symmetrically truncated. An offset in bias will introduce predominantly even harmonics.

3.4 Summary of Film Recording Characteristics

The following is a concise collection of film measurements that are pertinent to the performance of the LENS correlator. Although these thorough results are taken from only one of more than 120 rolls of film that were recorded (about 2400 frames), the results are typical of those consistently achieved after and including the 8/28/78 data set (with the exception of the most recent dramatic improvements discussed in Appendix A).

All spectral power measurements in the Fourier plane were made of spots off the axis of the zero order to avoid contamination with the sidelobes of its sinc function.

The film that was used exclusively was 35 mm Kodak High Contrast Copy, also known as AHU Microfilm. The developer was a gelatinous contact process known as Bimat. This simple developer is wound in intimate contact with the exposed film, separated after 3 minutes at room temperature, washed and rinsed in PhotoFlow. The rate of this developer "times out" after about 2.5 minutes assuring good repeatability.

Table 3.2 shows the density measurements from a RASTER3 eight-step grey scale and the derived measurements of intensity transmittance and amplitude transmittance.

Table 3.2

Exposure Level (0 - 4095)	D	τ_n	T
Clear	.08	.83	.91
0	.22	.60	.78
512	.30	.50	.71
1024	.38	.42	.65
1536	.46	.35	.59
2048	.58	.26	.51
2560	.67	.21	.46
3072	.76	.17	.42
3584	.88	.13	.36
dark	2.12	.01	.09

Figure 3.7 is a plot of the TE curve with the dashed line being a fit to a quadratic equation:

$$T = .097E^2 - .56E + .78 \quad (3.4.1)$$

The second harmonic to fundamental ratio can be calculated by forming the ratio of quadratic to linear coefficients to get:

$$\frac{.097}{2(.56)} = -21.9 \text{ dB}$$

Table 3.3 shows the harmonic intensities measured in the optical Fourier plane for a low frequency (2.6 cy/mm) sinusoid occupying this same region of the TE curve. From this information, we can calculate 2nd harmonic ratio, total harmonic distortion, diffraction efficiency, and D.C. transmission ratio. These values are shown with the predicted values in Table 3.4.

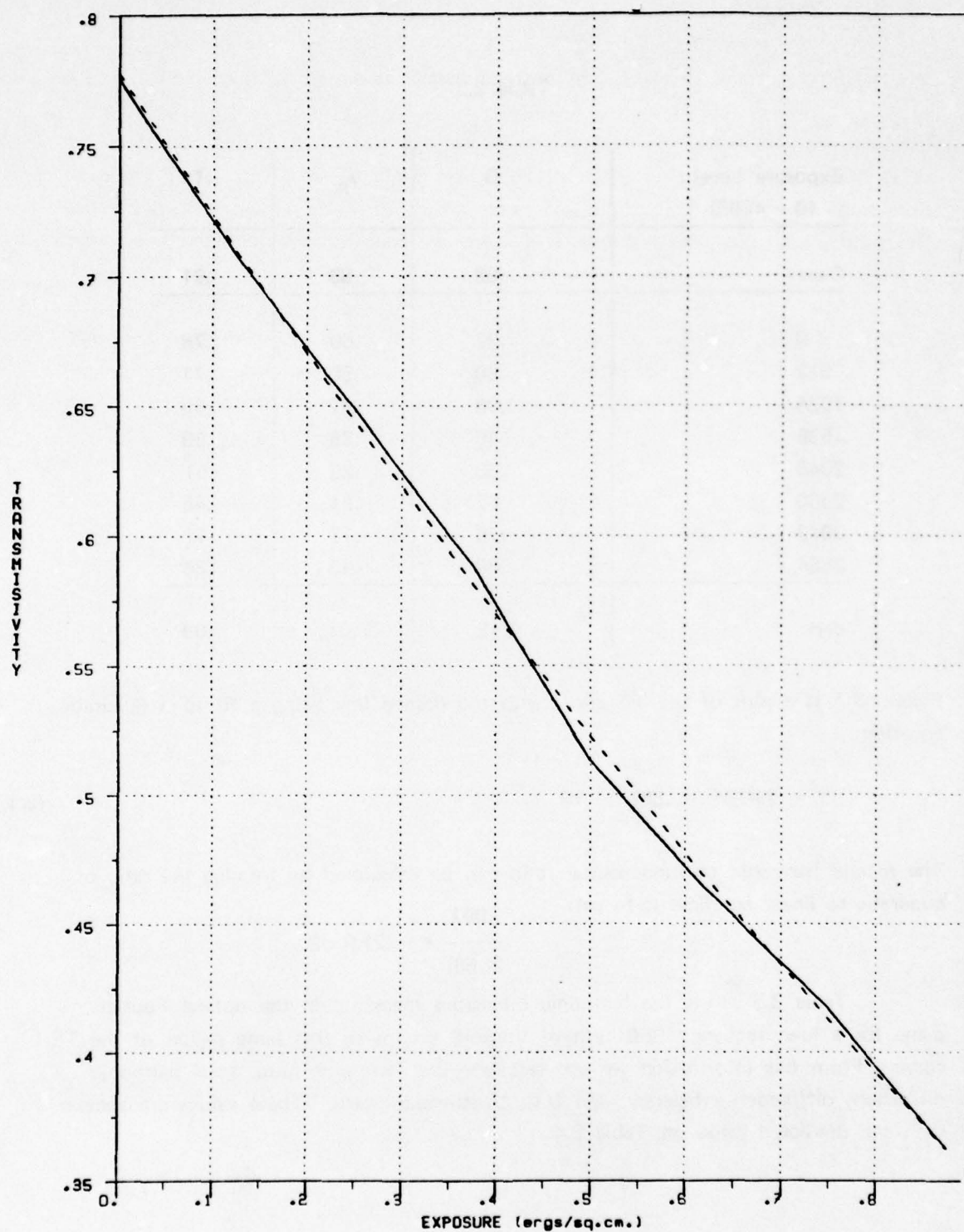


Figure 3.7

Table 3.3

Intensity	Value
Input	.5 mw
D.C. Spot	.42 mw
Fundamental	7.8 μ w
2nd Harmonic	.11 μ w

Table 3.4

Parameter	Observed	Calculated
Diffraction Efficiency	1.6%	1.8%
D.C. Transmission Ratio	84.0%	53.0% (78.0%)*
2nd Harmonic Ratio	-18.5 dB	-21.9 dB
Total Harmonic Distortion	-18.5 dB	- - - -

* So far, no mention has been made of the raster nature of the recordings. Assuming no exposure coupling between lines and assuming a line to space width ratio of 1:3, this number was calculated by $1/3 (.53) + 2/3 (.91)$.

MTF was measured by using the IPC2 program which generates the sum of 6 sinusoids of equal amplitude, all of which are chosen to have a 1/2 cycle excess per line. This causes a displacement in the Fourier plane away from the D.C. locus. Figure 3.8 gives the results.

3.5 Raster Recording Realities

The measurements presented in Section 3.4 are immutable indicators of the film performance. It is not surprising that most of these characteristics can be predicted from the simple linear model of Eq. 3.3.5, but some results can only be justified when the raster nature of the recordings are considered. The previous results are valid if the raster is modeled as consisting of recorded lines of width L and spaces between lines of width S with no leakage of exposure into the spaces or adjacent recorded lines. An additional constraint is that L/S is independent of the local exposure level. With this model, the increased DC transmission ratio could be accounted for by simply considering L/S. Signal diffraction efficiency remains unaffected since this measure is independent of the recorded area. (Intensity transmittance is measured in energy/unit area.)

These assumptions progressively weaken with increased exposure. Both the spot on the CRT phosphor and the recorded film spot grow with increased exposure. This results in a spill over of density into the unrecorded areas and eventually a contamination of adjacent recorded lines. A direct result of this can be a change in actual modulation as a result of exposure level or a compression of the amplitude versus exposure characteristic. This can also occur for shifts in bias point for small signal inputs as in Fig. 3.6. But notice that this is not due at all to our definition of modulation, but to considerations of the two dimensional exposure and effects occurring in the direction orthogonal to the raster lines.

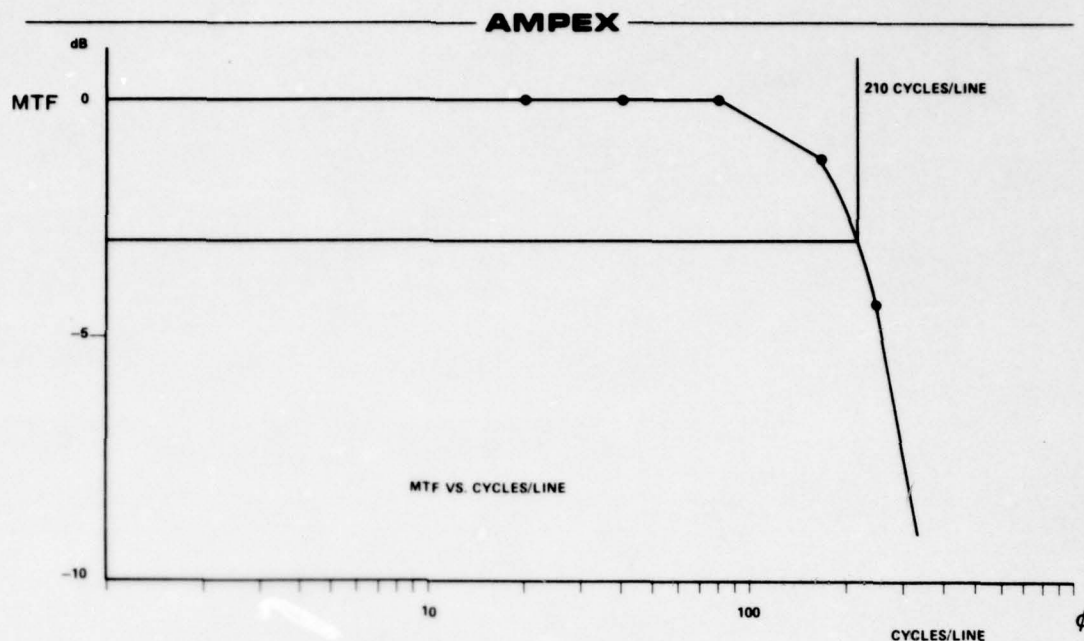
We can rewrite Eq. 3.3.3 as:

$$T(x', y') = C - BE'(x', y') \quad (3.5.1)$$

where x' and y' are continuous variable. Now if the spot is discretely positioned on the raster in increments of (nx, ky) and (X, Y) are the number of samples/line and number of lines respectively, then:

$$E'(x', y') = \sum_{k=0}^Y \left[\int_{x'=0}^{x'=X} \int_{y'=0}^{y'=Y} \sum_{n=0}^X \left(E(x') \cdot \delta(x'-nx) \cdot \exp \left(-\frac{(x'-nx)^2 + (y'-ky)^2}{C\sigma^2} \right) \right) dx' dy' \right] \cdot \delta(y'-ky) \quad (3.5.2)$$

This expression is the effective exposure for a sampled raster pattern with a uniform gaussian spot. It could be substituted into Eq. 3.5.1 and manipulated to show the change in depth of modulation as a function of the exposure, and would also account for the change in average transmittance due to exposure between lines of the recording. This, however, is the beginning of a study in itself and would not change the results obtained in Section 3.4. Figure 3.9 is a visual aid to understanding Eq. 3.5.2.



Cycles/line	Cycles/mm	Measured Intensity	$10 \log \left(\frac{I}{I_0} \right)_{LF}$
20.5	1.64	.16	0dB
40.5	3.38	.16	0dB
80.5	6.44	.16	0dB
160.5	9.64	.12	- 1.25 dB
240.5	19.24	.06	- 4.25 dB
320.5	25.64	.02	- 9.03 dB

Figure 3.8 Film Recorder MTF

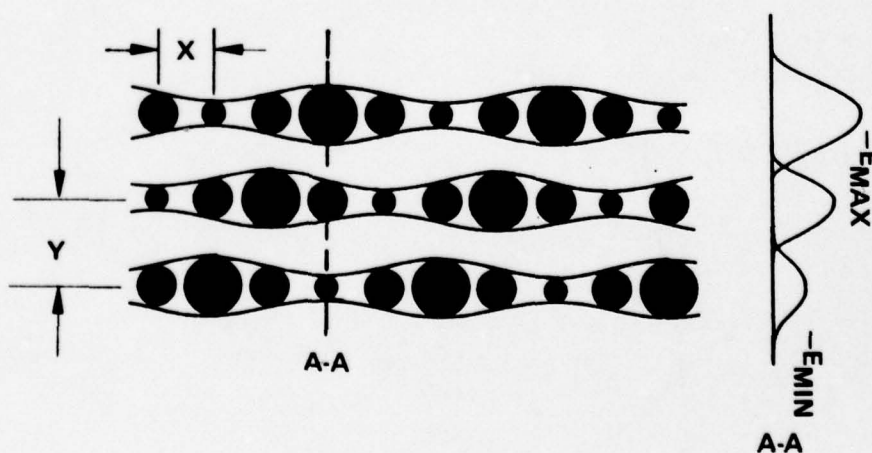


Figure 3.9 Effects of Gaussian Spot Spreading

4.0 SYNTHETIC DATA PROCESSING

A considerable amount of work was involved in the preprocessing of the synthetic data set. This preprocessing included the segmentation, modulation, level shifting, gain control, and conversion to 8-bit positive integer values of the complex, two-channel data that was received from NOSC. In order to accomplish one to one comparisons of optical and digital PAS, it was necessary to trace the data that was recorded on film back to the synthetic data segments.

This section contains a description of the synthetic data characteristics and their effect on the choice of processing parameters for the optical PAS. The film format is also described and a software summary is presented.

4.1 Data Description

The raw data consists of 28 segments each containing 3600 complex data points. The odd segments (1, 3, 5, 27) are the unDopplered channel and the even segments (2, 4, 6, 28) have a .08 Hz relative Doppler. The adjacent odd-even segment pairs vary in SNR from $+\infty$ (1,2) to $-\infty$ (27,28). The complex pairs represent one second samples in time of a single FFT bin with .25 Hz processing bandwidth. The input for this narrowbanding process is assumed to be a noiselike signal centered at approximately 150 Hz. The SNR ratio is reduced by adding noise that is uncorrelated between channels and lowering the signal level in steps until it is zero. It is assumed that the noise fills the .25 Hz bin. The data bandwidth occupies only .1 Hz of the .25 Hz bin. Also included in the data set are sinewave and impulse segments, again with varying SNR and a constant Doppler difference between channels.

Each real and imaginary sample was a 16 integer value. An initial problem of the zero level representation was easily corrected. We were also cautioned to avoid processing the first 256 samples of each segment pair due to a transient effect in the generation of the signal.

4.2 Choice of IPC Processing Parameters

The maximum values for coherent integration time (CIT) and number of time alignments per surface were chosen with regard to the synthetic data parameters and the performance of the film recorder. An easy decision was to maintain a range dimension of 256 discrete time alignments, each one representing successive one second offsets between data channels. Zero range would be at the center of the surface. With a data bandwidth of .1 Hz, the PAS peak would appear on 10 lines of the surface (measured null to null).

The choice of maximum CIT was influenced by the signal bandwidth, the need to remodulate the data (as explained in Section 2) and the available horizontal resolution on film. For the remainder of this discussion, we will refer to the film aperture in temporal terms and the film resolution in terms of cycles across the aperture rather than in cy/mm.

If we were to record 512 one second samples of .1 Hz bandwidth signal across each line of film, there would nominally be 51.2 cycles of signal in the aperture. Arbitrarily choosing a remodulation carrier of 3 times the bandwidth would yield approximately 150 cycles of carrier in the same 512 second period. The re-modulated signal would be $.3 \pm .1$ Hz and display 150 ± 50 cycles of signal for a 512 second CIT. A positive Doppler shift of .08 Hz at baseband would cause a 41 cycle increase within the aperture. Recalling that the -3 dB modulation frequency of the film was approximately 200 cycles/line, 512 second CIT was adopted as a maximum and a carrier of .2929 Hz (exactly 150 cycles/line) resulted. Experiments with 256 second CIT were also performed. In this case, half the modulated data samples were used and each was repeated without interpolation to fill the same spatial dimension. The result was 75 ± 25.6 cycles/line which is well within the resolution of the film recorder. A one second shift from line to line in range was still maintained, for the 256 second CIT data.

It is painfully obvious in retrospect that the criterion for the choice of carrier should have been a frequency at least twice the **processing bandwidth** of .25 Hz and not the **data bandwidth**. Since the data was fairly well contained in the .1 Hz, this is not a fatal error. For SNR of less than $+\infty$ this could have an effect if the noise filled the containment.

The choice of parameters for 512 second CIT resulted in a ± 128 second range dimension that only tests for correlation of the middle half of the CIT as

shown in Fig. 4.1. Because the ± 128 second range search was maintained for 256 CIT, the overlap was 100% complete.

4.3 Film Recorder Format

There are some comments to be made for the sake of completeness, though they are not necessary for understanding the performance of the IPC, that deal with the actual recording of the synthetic data. The CRT in the film recording has 1024 discrete steps (samples) in the horizontal position. To represent 512 seconds at 1 sample per second with 1024 points on the face of the CRT, each modulated sample was duplicated for 2 CRT points. For 256 seconds, each sample was repeated for 4 CRT points. This amounts to a noninterpolative contraction of the time scale where 1 CRT point was either .5 or .25 seconds depending on the CIT. The range shifts from line to line were 1 second in both cases, but either 2 or 4 CRT points respectively.

4.4 Modulation and Traceability

As was reported in Section 2, the modulation was performed in software according to:

$$F(t) = X^R(t) \cos w_c t + X^I(t) \sin w_c t \quad (4.1)$$

For each 1024 sample epoch in a segment, we can emphasize the discrete nature of this processing by writing:

$$R(n) = .707X^R(n)\cos\left(\frac{600\pi n}{1024}\right) + .707X^I(n)\sin\left(\frac{600\pi n}{1024}\right) \text{ for } 0 \leq n \leq 1023. \quad (4.2)$$

The fact that $\sin w_c t + \cos w_c t$ has a maximum of 1.414 is reflected in the .707 normalizing factors. At this point, before adding the bias term and rounding to 8-bit accuracy, each 3600 sample segment was normalized by multiplying each sample by a factor derived from the maximum point within a segment. This had the effect of causing the maximum point for each SNR case to fill the entire 16-bit range. A list of these factors is supplied in Table 4.1. The data was then rounded to integers between - 2048 and + 2047 and a bias of 2048 was added. An example of the appearance of the modulated synthetic data is shown in Fig. 4.2. Figure 4.3A shows

Table 4.1
Gain Factors Applied to Synthetic Data

Segment Number	Largest Value	Relative Gain Factor <u>32768</u> Vimax
1	30078	1.09
2	31628	1.04
3	29574	1.11
4	29370	1.12
5	24193	1.36
6	22858	1.43
7	16517	1.98
8	18794	1.74
9	16625	1.97
10	14987	2.19
11	15442	2.12
12	14253	2.30
13	14776	2.22
14	12098	2.71
15	13067	2.51
16	14118	2.32
27	12903	2.54
28	13558	2.42

AMPEX

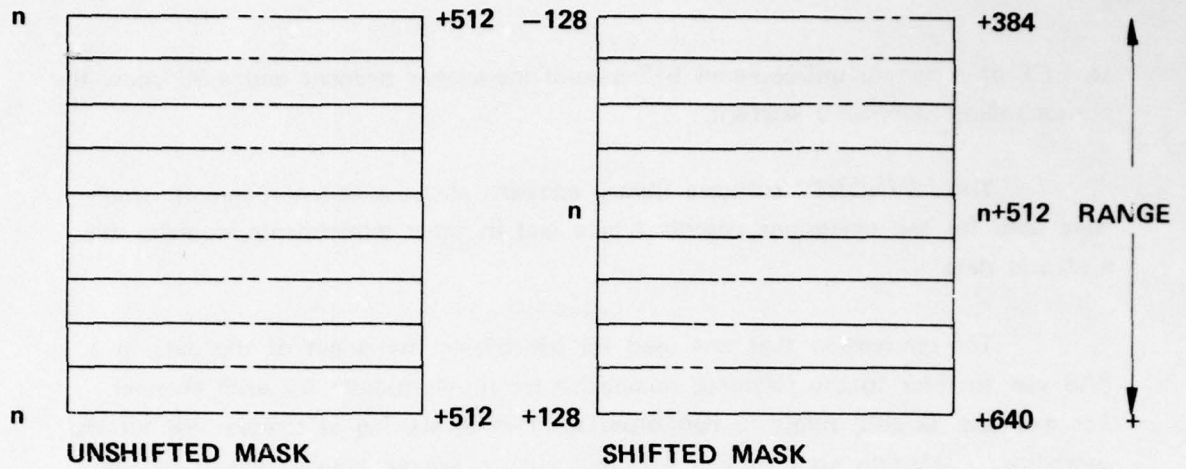


Figure 4.1 Correlation at Zero Range Showing 50% Overlap

NOF DATA BLOCK 0

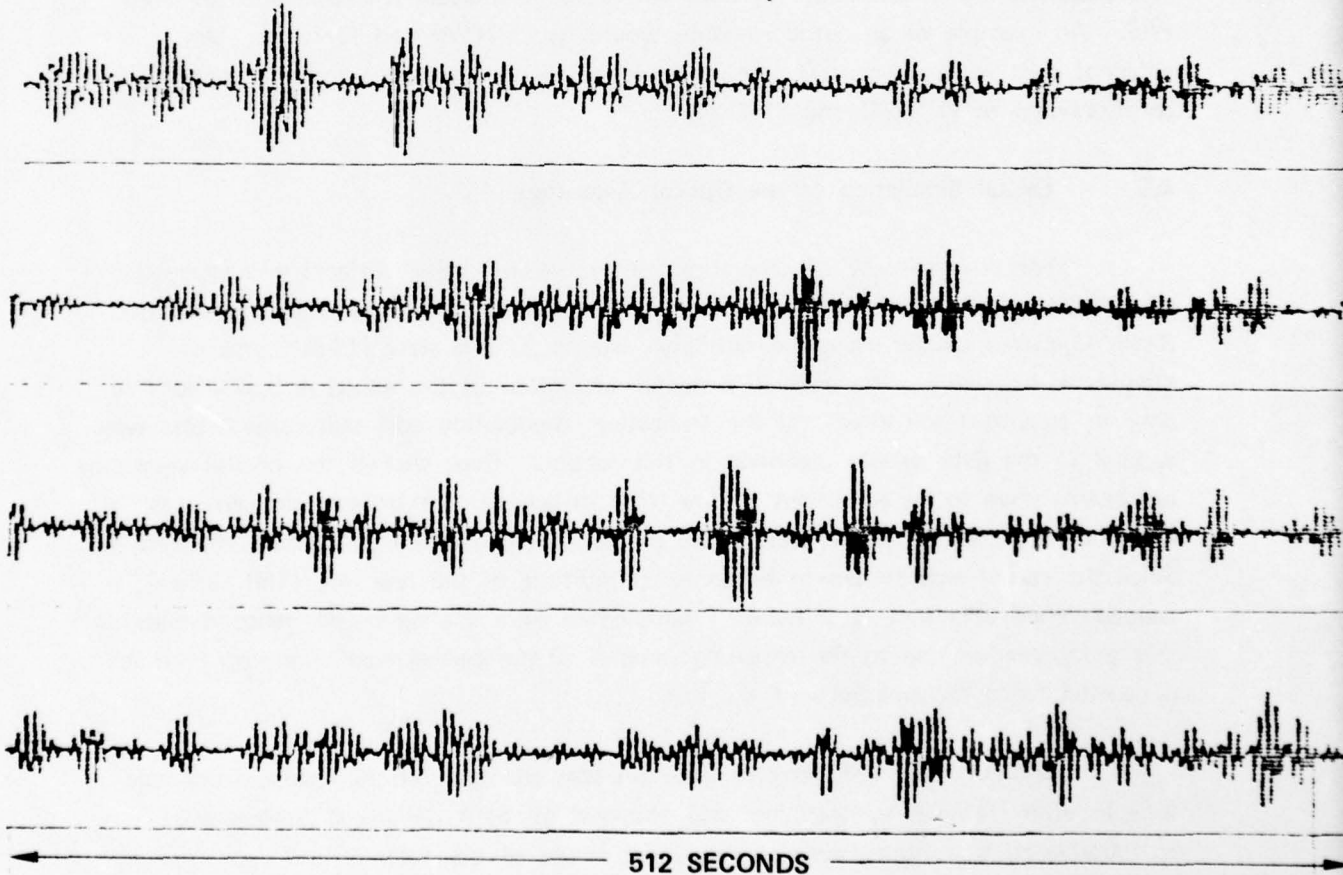


Figure 4.2 Modulated Synthetic Data

an FFT of a sample unDopplered 512 second modulated segment and 4.3B show the corresponding Dopplered segment.

The "SYNDAT" software library contains about a dozen programs which were used for the operations described here and in other experiments involving the synthetic data.

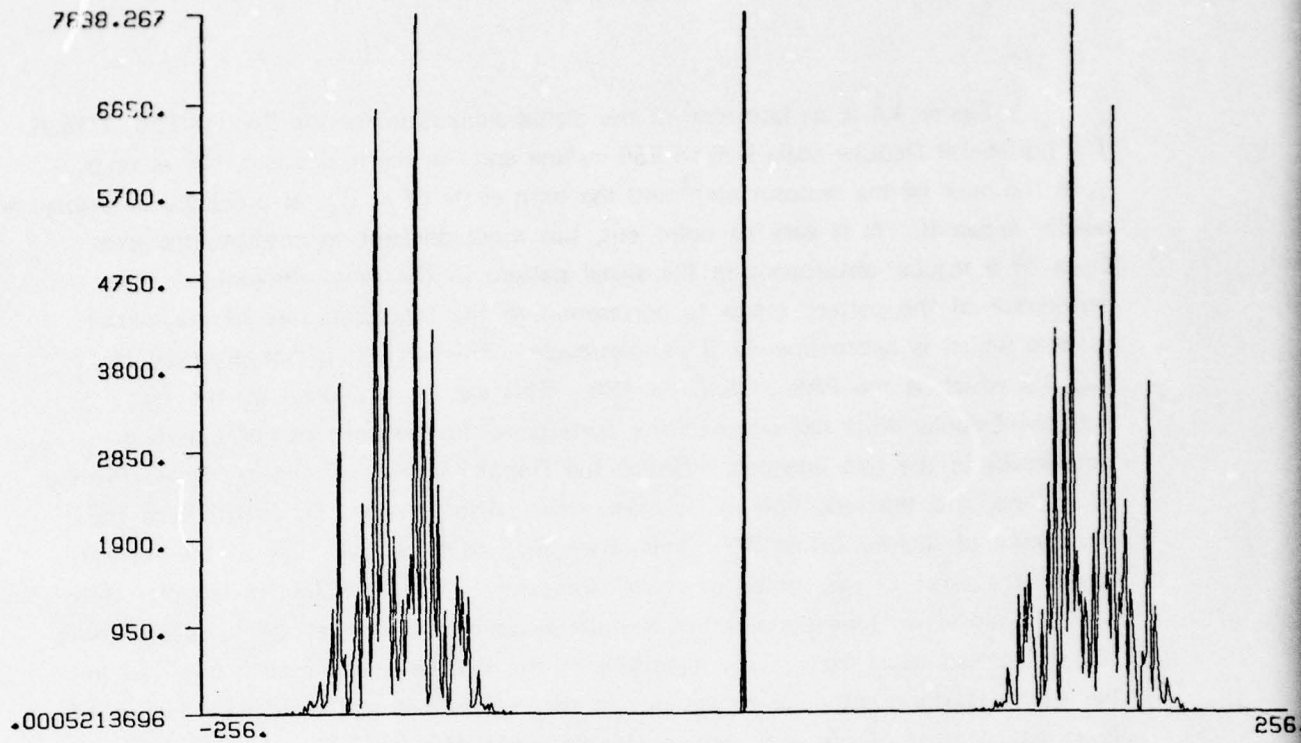
The convention that was used for identifying the origin of the data in a PAS was to refer to the (segment number/centerline startpoint) for each channel. For example, (2/768) refers to data from segment 2, starting at sample 768 for the centerline. Referring back to Fig. 4.1, this starting sample number would be the same for all lines of the unshifted mask (the n^{th} sample), while it corresponds to the first sample of the centerline (line 128) of the shifted mask. As a further convention, the Dopplered (even segments) were always written on the unshifted mask. A crosscorrelation specified by (2/1536) and 1/1536 indicate a Dopplered + ∞ SNR PAS. An example of an autocorrelation would be (1/1024) and (1/1024). An apparent shift in range of 100 seconds could be demonstrated by forming the PAS corresponding to (1/1024) and (1/1124).

4.5 Digital Simulation of the Optical Algorithm

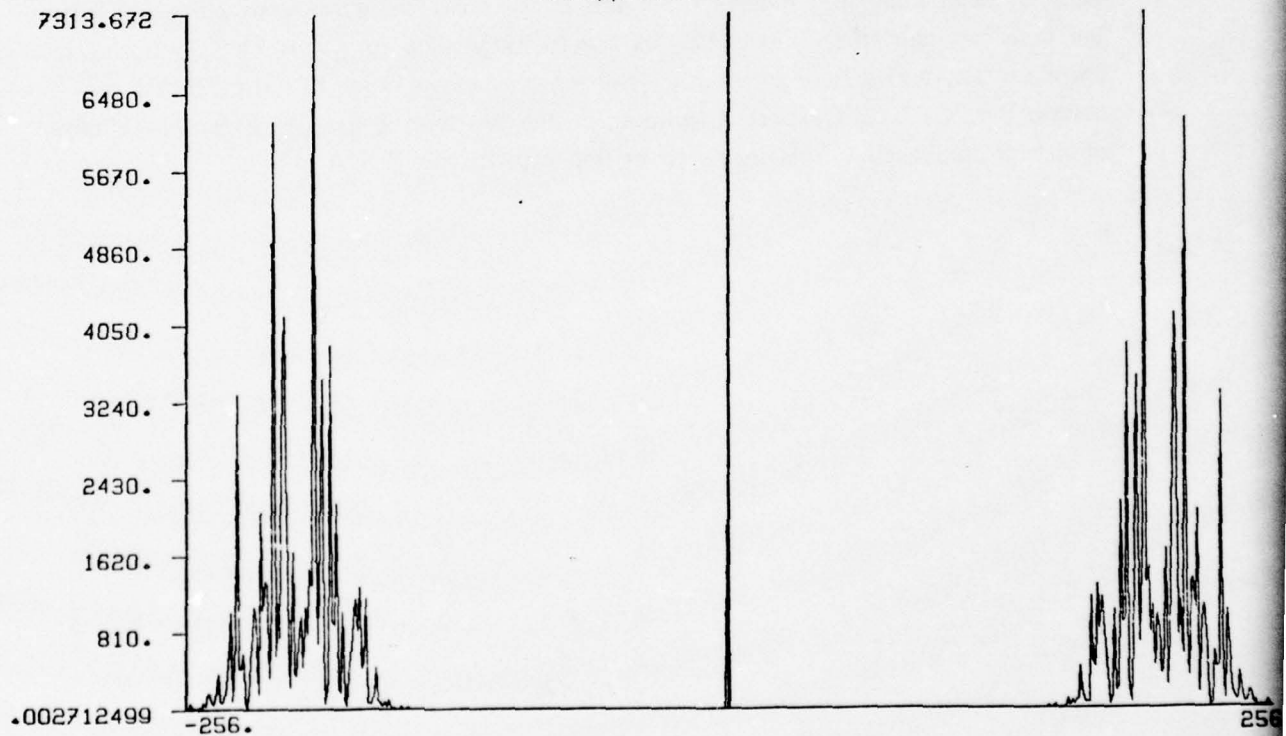
The responsibility of generating the equivalent digital surfaces was assigned to ENSCO. They supplied the matching digital surfaces as calculated by the Narrow Band Algorithm (NBA) using the synthetic data in its raw state (16-bit complex samples as baseband). We pursued a digital simulation of the actual optical algorithm only to document the effects of the truncation, modulation and gain control that were applied to the data as was described in this section. Even though the optical algorithm has been shown to be equivalent to the NBA in general, our primary concern was how the choice of carrier frequency and carrier sampling rate would affect the PAS. Since the carrier was chosen to be an exact multiple of the line rate (150 cy/line), it seemed conceivable that as shifts of 1 sample/line were applied in the range dimension, that a modulation due to the repeating samples of the carrier would develop in that dimension for autocorrelations of the PAS.

Another motivation was to ascertain that the peak height change from epic to epic of the optical surfaces that was observed by both CMU and Ampex was attributable to true fluctuations of the signal power of the data.

AMPEX



Undopplered modulated data

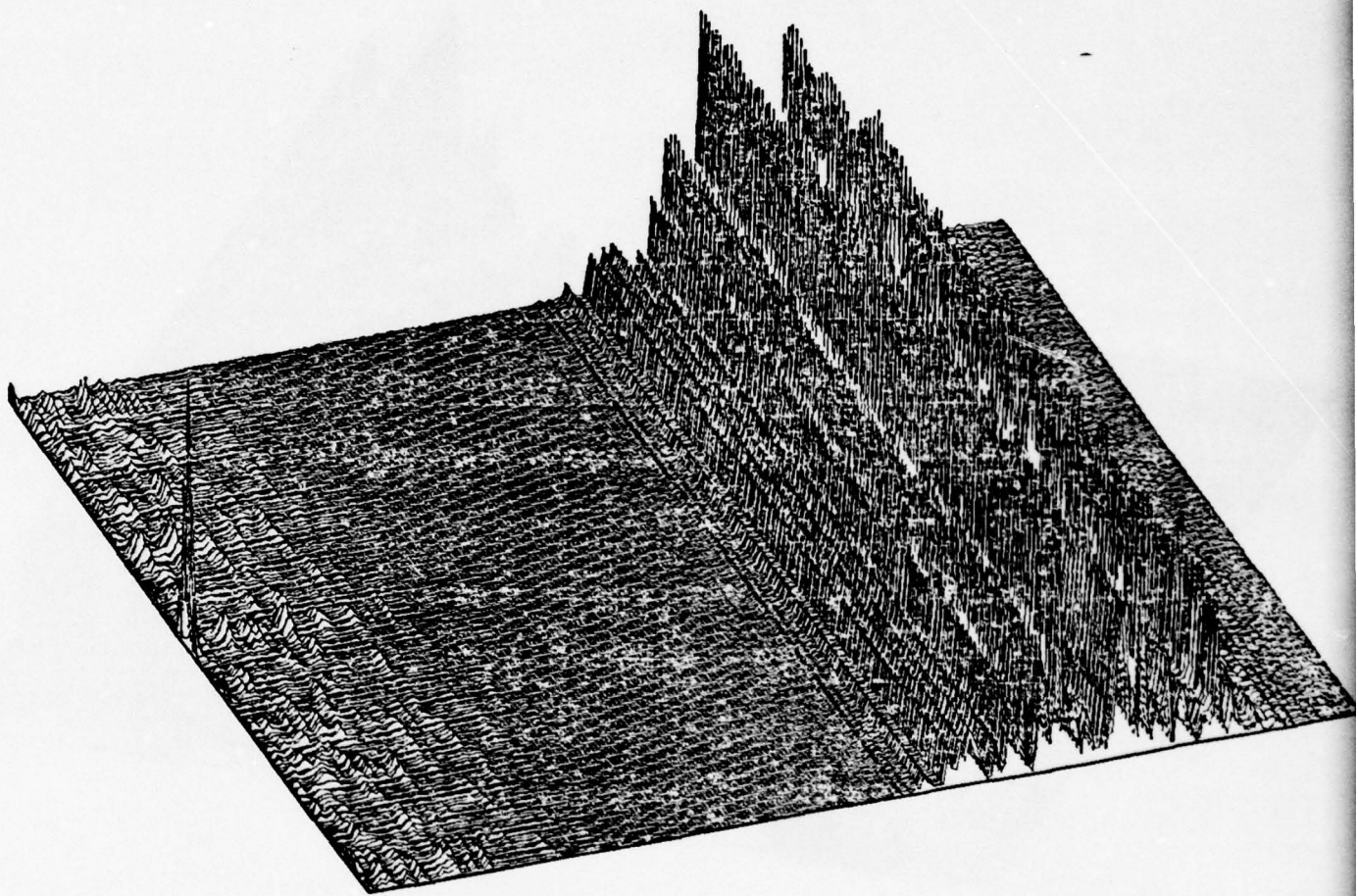


Dopplered modulated data

NOTE* Bias term has been
Truncated

Figure 4.3A & B

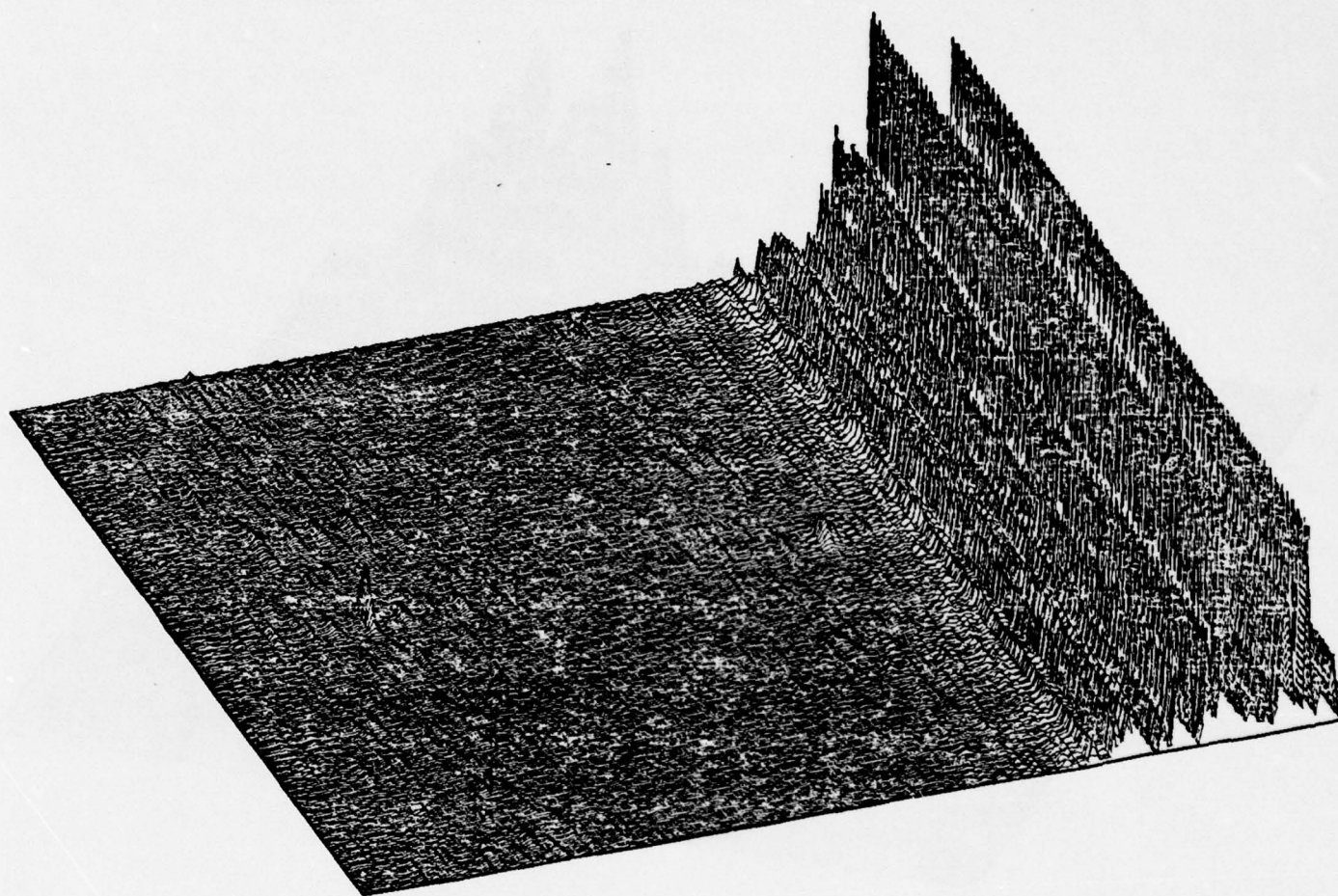
Figure 4.4 is an isometric of the digital simulation for the PAS 1/1536, 1/1536. The horizontal Doppler scale is 0 to 256 cy/line and the range axis is ± 128 seconds. Both the peak of the $|\text{autosurface}|^2$ and the term centered at W_c , as predicted in theory, are readily apparent. It is easy to point out, but more difficult to confirm, the existence of a regular disturbance in the signal pattern in the range dimension. The periodicity of the pattern seems to correspond to the repetition rate of the carrier samples which is approximately 3 samples/cycle. This pattern is not observed in Fig. 4.5 which is the PAS 2/1536, 1/1536. This can be explained by the fact that the Doppler shift has removed the correspondence between carrier sampling frequencies in the two channels. Notice the Doppler shift of the peak, approximately 40 cy/line, and the reduction of its magnitude. Also apparent is repetition of the PAS centered slightly below W_c . This is assumed to be a true alias of the surface due to the error in the choice of carrier frequency. With the .08 Hz Doppler shift, a .3 Hz carrier no longer meets the Nyquist sampling criterion at the bandedge (now .18 Hz instead of .1 Hz). This repetition of the PAS was also clearly observed in the optical surfaces although it was not in the region that was digitized. Figure 4.6 is an enlargement of Fig. 4.5, with a Doppler scale of 0 to 128 cycles/line. The gain has been doubled. Figures 4.7A and B are slices along the zero range loci of the same two surfaces. Figure 4.8A is a zero range slice for 0 dB SNR in both channels. If, as we have previously assumed, the added noise fills the .25 Hz processing BW, we would expect a spillover of the W_c term below $W_c/2$ for our choice of carrier frequency. This seems to be the case in Fig. 4.8 A and B.



-g0.00000000003 -X -s1.5 -md1.5 -ml1.9 -r20 -t30

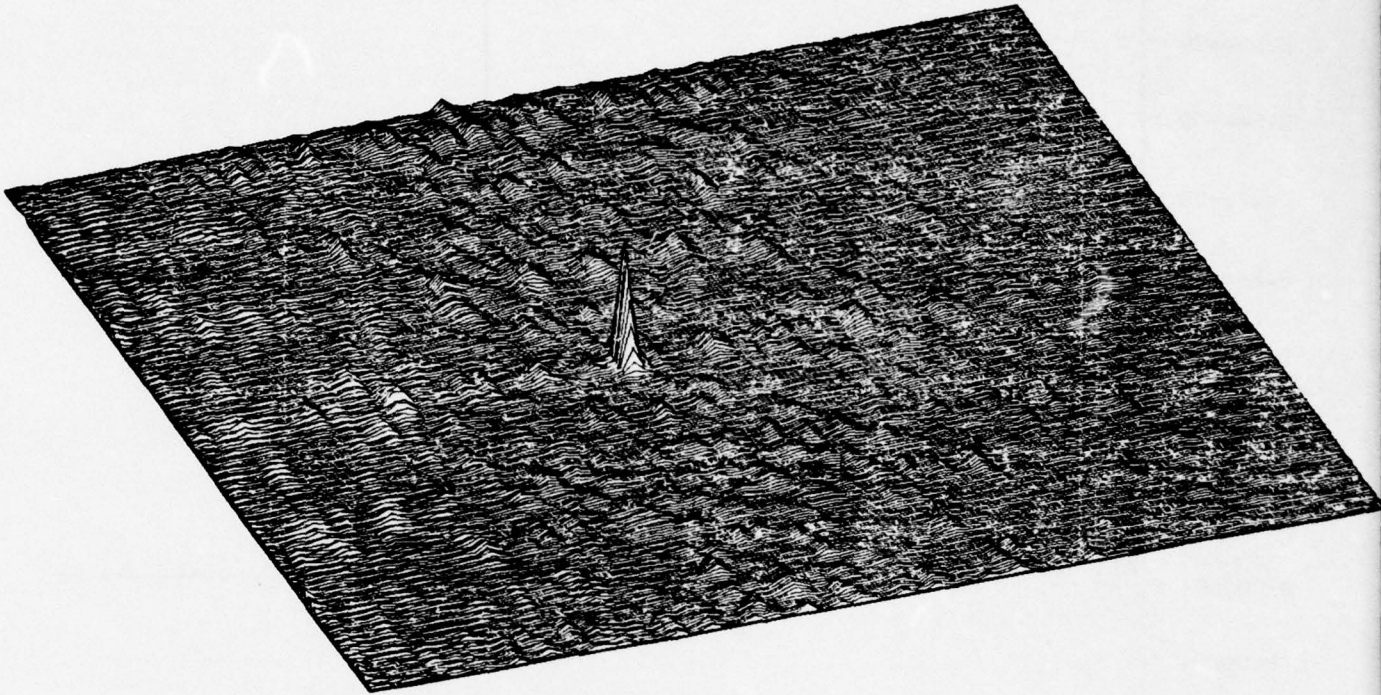
AMPEX Research--Signal Processing Systems Section Wed Aug 29 00:52:25 1979

Figure 4.4



-g0.00000000003 -X -s1.5 -md1.5 -ml1.9 -r20 -t30
 AMPEX Research--Signal Processing Systems Section Wed Aug 29 01:00:49 1979

Figure 4.5



-g0.00000000006 -X -s1.5 -md1.5 -ml1.9 -r20 -t30

AMPEX Research--Signal Processing Systems Section Wed Aug 29 00:46:43 1979

Figure 4.6

AMPEX

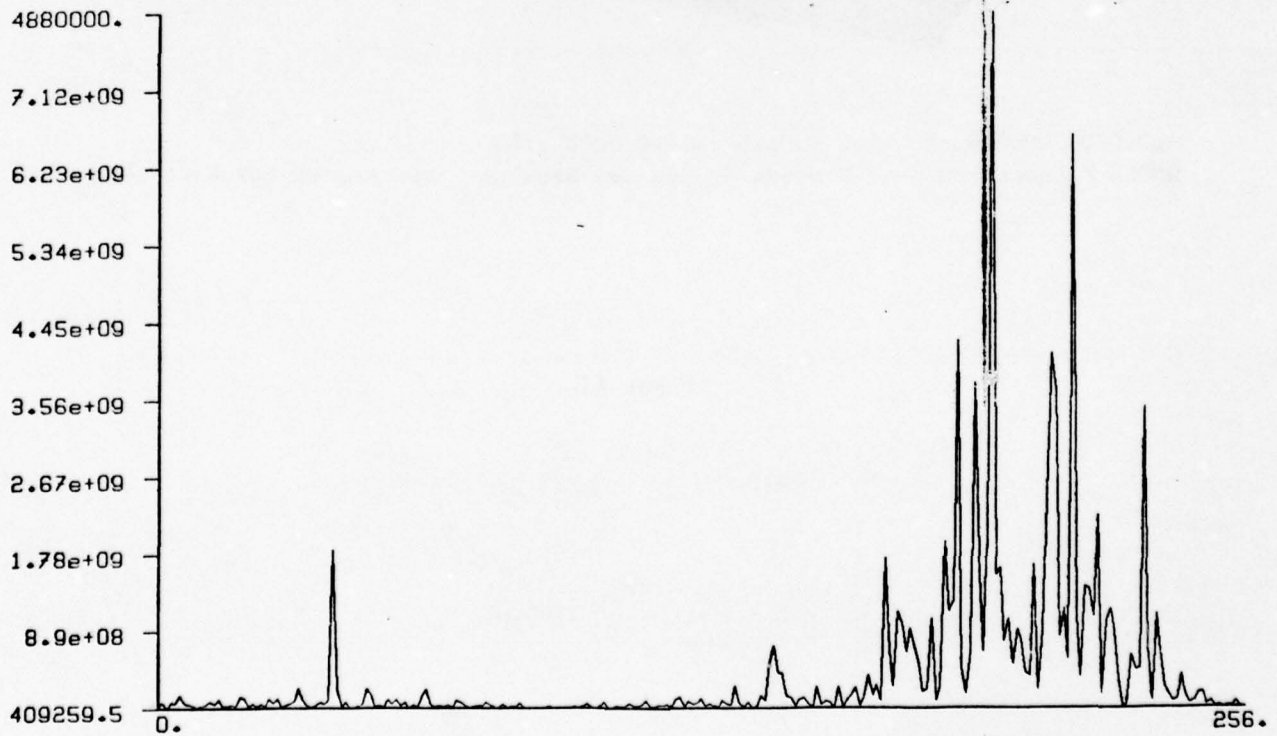
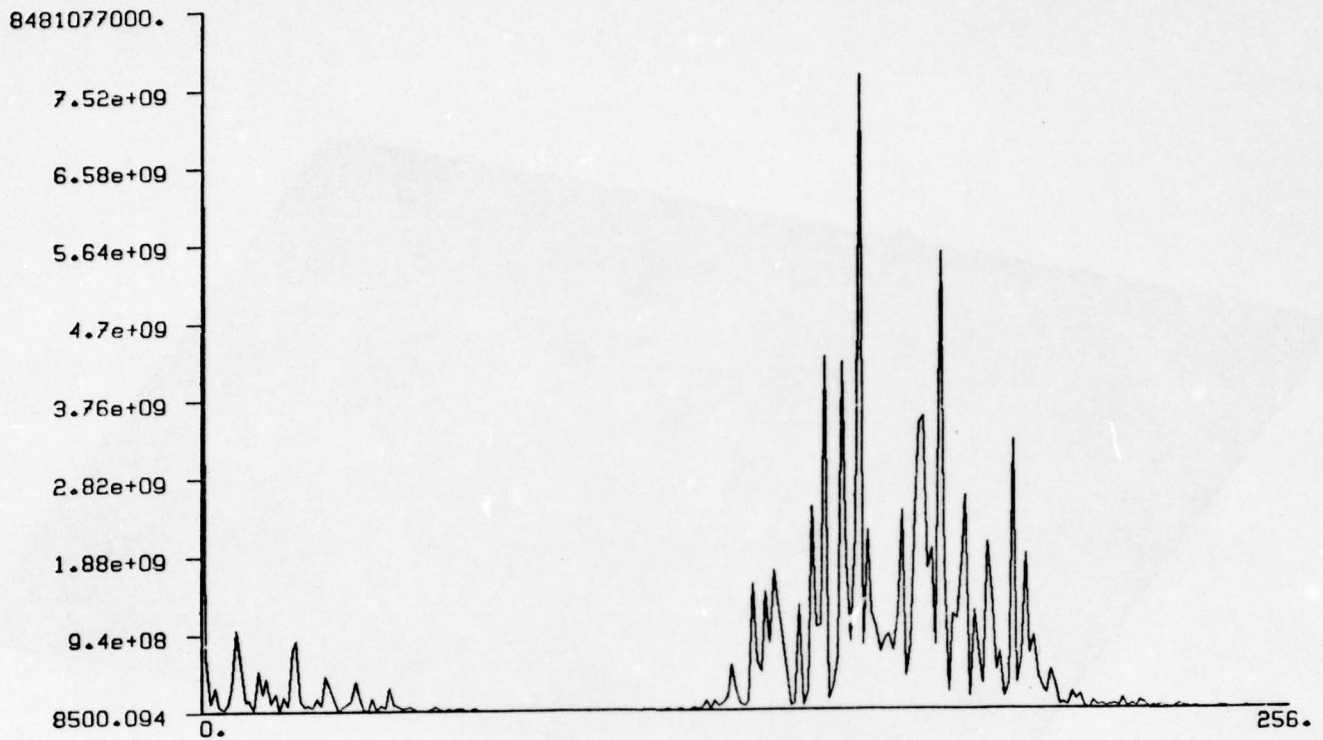
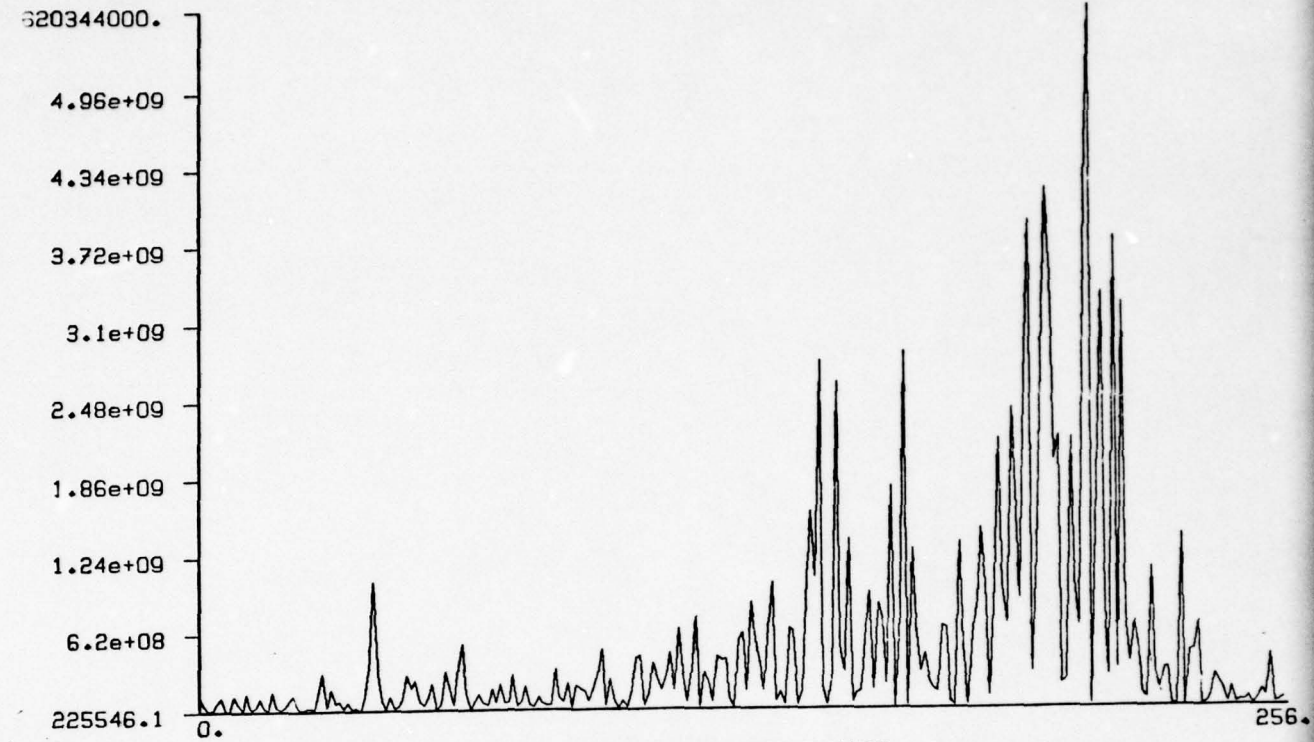
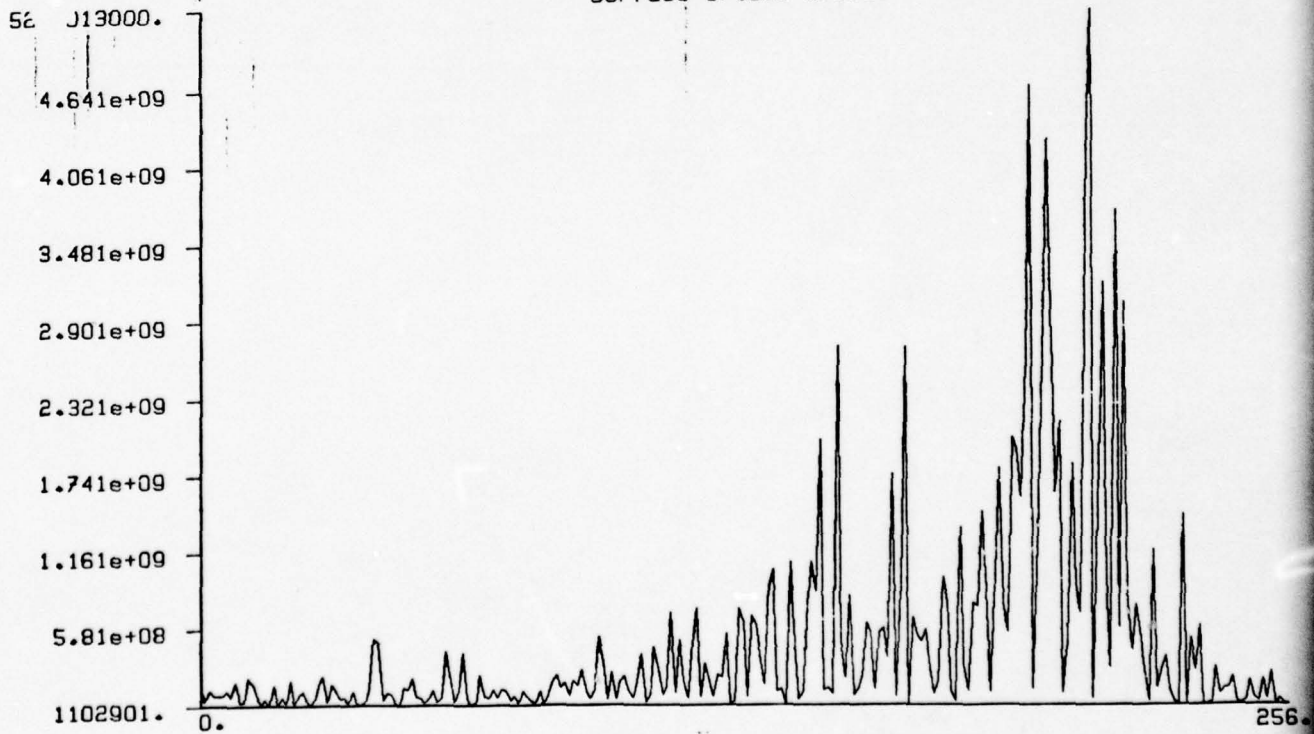


Figure 4.7



Surface 6/1536 5/1536



Surface 6/1536 9/1536

Figure 4.8

5.0 OPTICAL SYSTEM

The three topics to be discussed in this section will be alignment of optical components, scaling and light budget. A detailed analysis of the accuracy of the optical system was not performed under this contract. We can say with some certainty, however, that we concur with the conclusion of the CMU researchers that "the optical PAS system was found to be more than adequate for the available input data". As will become evident in this report, the resolution limitations of the vidicon camera and the residual scan nonlinearities of the input films had a far more drastic effect on the performance than the relatively simple 8 lens optical design of the IPC.

5.1 Component Alignment

The schematic diagram of the correlator is shown in Fig. 5.1. The light entering the correlator has already been collimated and sized to the 1.25 x 1.25 cm aperture of the film. Perhaps the most critical alignment task is to precisely register the two film masks in focus and at exactly unity magnification. This was facilitated by the generation of special alignment masks. The program "ALIGN1" creates a crosshatch pattern with selectable line widths and a positive or negative image option. One positive and one negative pattern was recorded and each installed in a liquid gate. The imaging pair L_1 and L_2 , a matched set of 24" focal length lenses, were approximately positioned and a temporary magnifying lens pair was used to cast a focussed 50X image of the film mask in the second gate onto a screen. L_1 and L_2 were then manipulated to superimpose the film mask in the first gate onto the screen. Elevation, tilt, magnification and focus could then be optimized. Use of the cross-hatch pair proved to be very effective. Registration was repeatedly accomplished to within one line pair of accuracy,

The 1-D transform lens pair was installed one element at a time while the focus onto the plane of the vidicon camera was checked. Sinewave patterns were used to verify the correct placements. Arbitrary refocussing of the system while operating with the test data was avoided.

A few of the most important optical design principles bear mentioning. Attempts are always made to restrict the area of the lens that is used to the axial region and to position all elements "on axis" (centered and at a right angle to the beam). This is accomplished by overlapping the accumulated front surface reflections that appear at various points. A second practice is to avoid placement of mirrors at points where the field of interest is extremely small and thereby prone to the effects of dust or surface defects. The last consideration is to isolate high intensity beam paths from critical lower intensity paths either by design of the layout or by appropriate baffling. These are a sample of the practices that were followed in the optical design of the IPC.

5.2 Scaling of the Optical Output

The size of the PAS in the 1-D transform plane is easily determined. The films represent ± 128 seconds in the vertical range axis and either 512 or 256 seconds of integration time in the horizontal dimension. They are 12.5 mm square. Since this size is preserved by the imaging operation, the only factor in scaling becomes the final 1-D transform lens pair. The configuration shown in Fig. 5.2 was used exclusively while processing the synthetic data. L_1 is the Doppler transform lens with power in the horizontal direction and L_2 is the range imaging lens with power only in the vertical direction. The scaling of the range axis is given by the ratio of image to object distance for L_2 which is $150/350 = .43$. Multiplying by the object dimension of 12.5 mm gives 5.36 mm. The deflection of the surface peak in the Doppler direction is found by applying the relationship given in Fig. 5.2. To find the spatial frequency corresponding to .08 Hz Doppler, we multiply by 512 seconds (or 256 seconds) and divide by the 12.5 mm aperture to get 3.28 cy/mm (1.64 cy/mm). The resultant Doppler deflection is .51 mm (.26 mm). Note that a Doppler difference corresponding to the full processing bandwidth of .25 Hz would give a 1.6 mm (.8 mm) deflection. Since in real life, both positive and negative Doppler differences might be expected, we arrive at a surface which is 5.36×3.2 mm in size. From this surface must be extracted ± 128 points in range by ± 512 points in Doppler. Therein lies a serious problem since nearly seven times the resolution is required of a detector in the Doppler direction. (Interestingly enough CMU encountered a similar problem with a different scheme for forming the 1-D transform.) If a square pattern were to be achieved, the Doppler resolution requirement would still be 4 times as great (2 times for 256 second CIT) as the range resolution. The major constraint in increasing the size of the Doppler axis is the scarcity of cylindrical lenses with focal lengths longer than 300 mm. Equal sizing must then be achieved by decreasing the range dimension which would require a slightly more complex

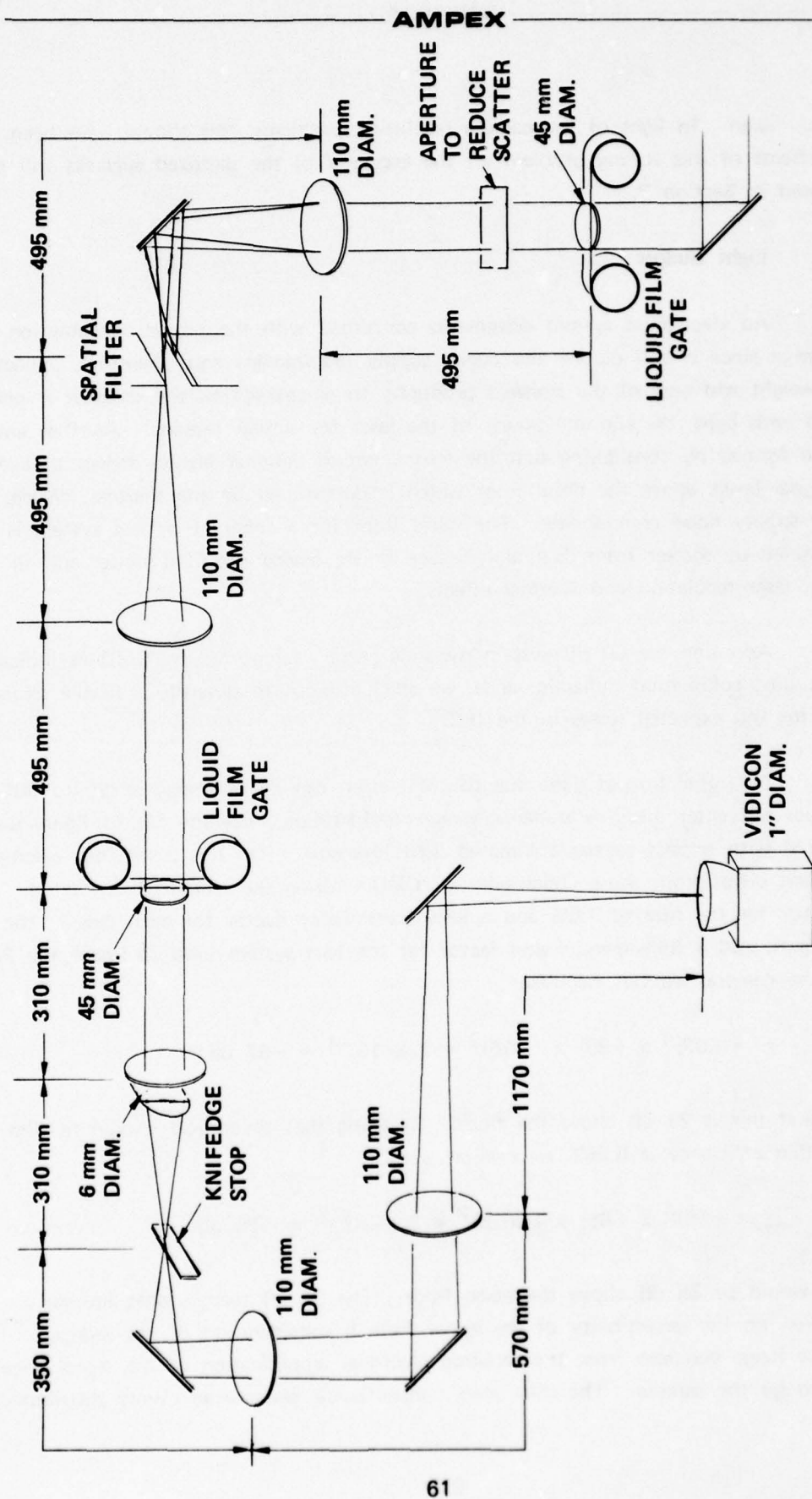


Figure 5.1 LENS Optical Image Plane Correlator

optical design. In light of the camera resolution problems, this should have been done. The effects of this scaling problem on the accuracy of the digitized surfaces will be discussed in Section 6.

5.3 Light Budget

An electronics system designer is concerned with the power consumption of his design since it will dictate the power supply requirement and, therefore, impact the size, weight and cost of the finished product. In electro-optics, the designer is concerned with light loss and the power of the laser for similar reasons. Another analogy can be formed by considering that the analog circuit designer always strives to keep the signal levels above the noise floor which is determined by the thermal, device, and power supply noise components. The noise floor for a coherent optical system is determined by scatter from dust and surface finish, device (or film) noise, and to some extent, laser regulation and thermal effects.

Adopting the 60 dB system dynamic range as reported by CMU as indicative of the post collimation dynamic range, we shall attempt to quantify a usable dynamic range for the expected losses in the IPC.

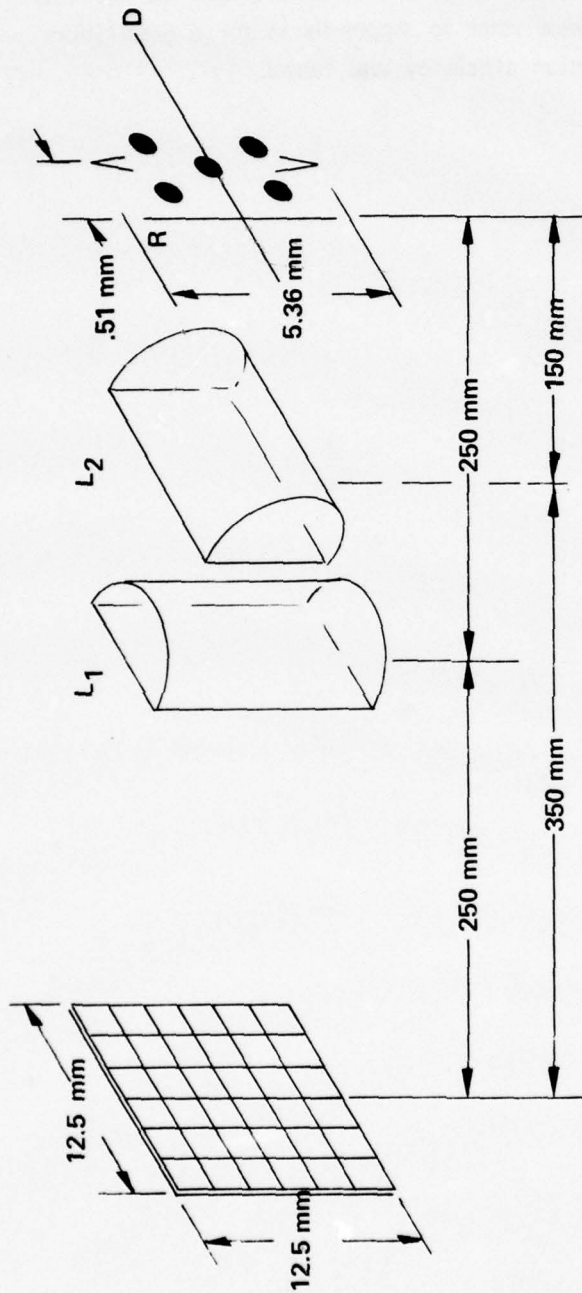
An initial loss of light due to collimation can be estimated at 80 to 90%, but does not enter into the dynamic range consideration since the 60 dB figure was measured with respect to the collimated light intensity. (On this point, our calculations will differ from those conclusions of CMU.) Using the measured diffraction efficiency for the film of 1.6% and a 98% transmission factor for each lens in the signal path and a 85% transmission factor for the lens system used to image the PAS onto the camera, we can calculate:

$$\tau = (.98)^4 \times (.85) \times (.016)^2 = 2 \times 10^{-4} \Rightarrow -37 \text{ dB}$$

Note that this is 23 dB above the floor. Recalling that theoretical maximum film diffraction efficiency is 6.25%, we can calculate:

$$\tau_{\text{max}} = (.98)^4 \times (.85) \times (.0625)^2 \approx 3 \times 10^{-3} \Rightarrow -25 \text{ dB}$$

which would be 35 dB above the noise floor. The 23 dB margin does impose a restriction on the detectability of the signal from a consideration of the reduced dynamic range and also from the required electrical amplification of the signal once detected by the camera. The calculated transmittance assumes an evenly distributed



L₁ IS THE DOPPLER TRANSFORM LENS

L₂ IS THE RANGE IMAGING LENS

SIZE OF THE RANGE IMAGE IS $\frac{150 \text{ mm}}{350 \text{ mm}} \times 12.5 \text{ mm} = 5.36 \text{ mm}$

DOPPLER SCALE: $d = \frac{F \lambda}{D}$

d = DEFLECTION IN CORRELATION PLANE

F = FOCAL LENGTH OF L₁

λ = WAVELENGTH OF LASER LIGHT (514.5 nm)

D = DOPPLER SPATIAL WAVELENGTH AT THE INPUT

Figure 5.2 Final Stage of Image Plane Correlator (Scaling Considerations)

intensity in the output plane. The processing gain for 512 second integration will raise the peak approximately 17 dB above the floor and thereby insure the visibility of the surface features for this case. Please refer to Appendix A for a description of a recent experiment where the diffraction efficiency was raised.

6.0 DETECTION AND DIGITIZATION

The difficulties involved in the proper detection and digitization of the optical PAS were highly underestimated at the beginning of the technical effort. As the program progressed, it became apparent that it was not the accuracy of the optical elements that was in question, but the accuracy of the input films and the quality of the detection. This is not at all surprising, since optical signal processing is almost always constrained by the input-output devices.

For 512 second CIT and 256 time alignments in range, the PAS requires the detection of ± 256 1 mHz Doppler bins and ± 128 range bins. This calls for a detector with a TBW of greater than 10^5 . The optical PAS is continuous in Doppler and discrete in range, and the TV camera which was used exclusively as a detector is also continuous in one axis and discrete in the other. This also poses some problems. If the fast scan axis of the camera is perfectly aligned along the Doppler axis, the range axis is resampled by the frequency of the raster lines. There must be a minimum of 512 raster lines and smoothing of the data in the vertical direction is then necessary. When video signal is digitized in Doppler, it must also be sampled according to Nyquist which requires a minimum of 2×512 cycles of 1024 samples per scan line. This corresponds to an A/D conversion rate in excess of 15 Megasamples/sec.

Although we believe that these detection requirements can be presently met with the proper equipment, the example given most likely is an upper design limit and larger surfaces are not likely to be adequately handled. Unfortunately, the equipment available for the effort fell short of meeting these criteria and as a result, the digitized optical surfaces were not properly replicated. In this section, we will discuss each item in the detection and digitization system as shown in Fig. 6.1.

6.1 Camera and Video Processing

A 1 inch television camera with a Newvicon tube was used exclusively as the detector. The Newvicon is advertised as a linear intensity transfer device, as

opposed to a vidicon which has a rather nonlinear transfer function. The optical output was imaged directly onto the photosensitive layer of the tube. The camera was operated in a 525 line interlaced mode with a line rate of 15 kHz. The camera as set up, had a specified resolution of 850 TV lines or 425 cycles per line. As our measurements showed, this proved to be very misleading. Figure 6.2A shows the response for a bar chart pattern graduated in 100 cycles increments. The 50% modulation point was estimated at 300 cycles. (It was later found that the specification sheet was referring to resolution at 20% modulation.) The -3 dB modulation point of about 150 cycles fell far short of the required 512 cycle requirement. A further restriction on resolution was the fact that the surface did not fill the screen in the Doppler dimension. For the 2/28/79 data set, the Doppler range of interest filled only 110 points of the 512 that were digitized. This shows that, exclusive of the camera resolution problem, each sample covered 4.5 mHz of Doppler. A later test of camera resolution showed no increase in peak width for a magnification of less than 15 times the size of the 2/28/79 surfaces. This agrees with the measured resolution of the camera as follows. The data utilized 29% of the full screen. At full screen magnification, the resolution of the camera would still have a shortfall of 150 cycles (measured)/512 cycles (required) = 20%. So the total deficit was $.20 \times .29 = .06$, requiring a magnification of $1/.06$ or 16.7. The optical peak width as reported by NOSC, was on the order of 19 mHz. It is obvious that the detection resolution was largely responsible for this 19:1 discrepancy.

A 2 inch vidicon camera was measured for resolution and the result is shown in Fig. 6.2B. Using a 2 inch camera will give approximately double the resolution. With proper scaling of the optical surfaces to fill the useful area of the target, a 5 x improvement would be achieved. Finally, aperture correction ("phaseless peaking") could be applied to the camera video signal to double the apparent resolution. This is a standard video practice. The product of all these factors would just relieve the 16 x shortfall in resolution. Therefore, the present PAS size, 512 x 256 represents a maximum for practical detection. It remains to be seen if the 800 x 800 element photodiode arrays that have recently been reported by Texas Instruments will offer an alternative to the TV camera as a detector.

The video signal from the camera can be adjusted in gain and D.C. level from the camera control unit (CCU). These controls are equivalent to the contrast and brightness adjustments of a TV receiver. This signal was buffered and the synchronizing pulses removed before digitization. Video amplitude at normal setup

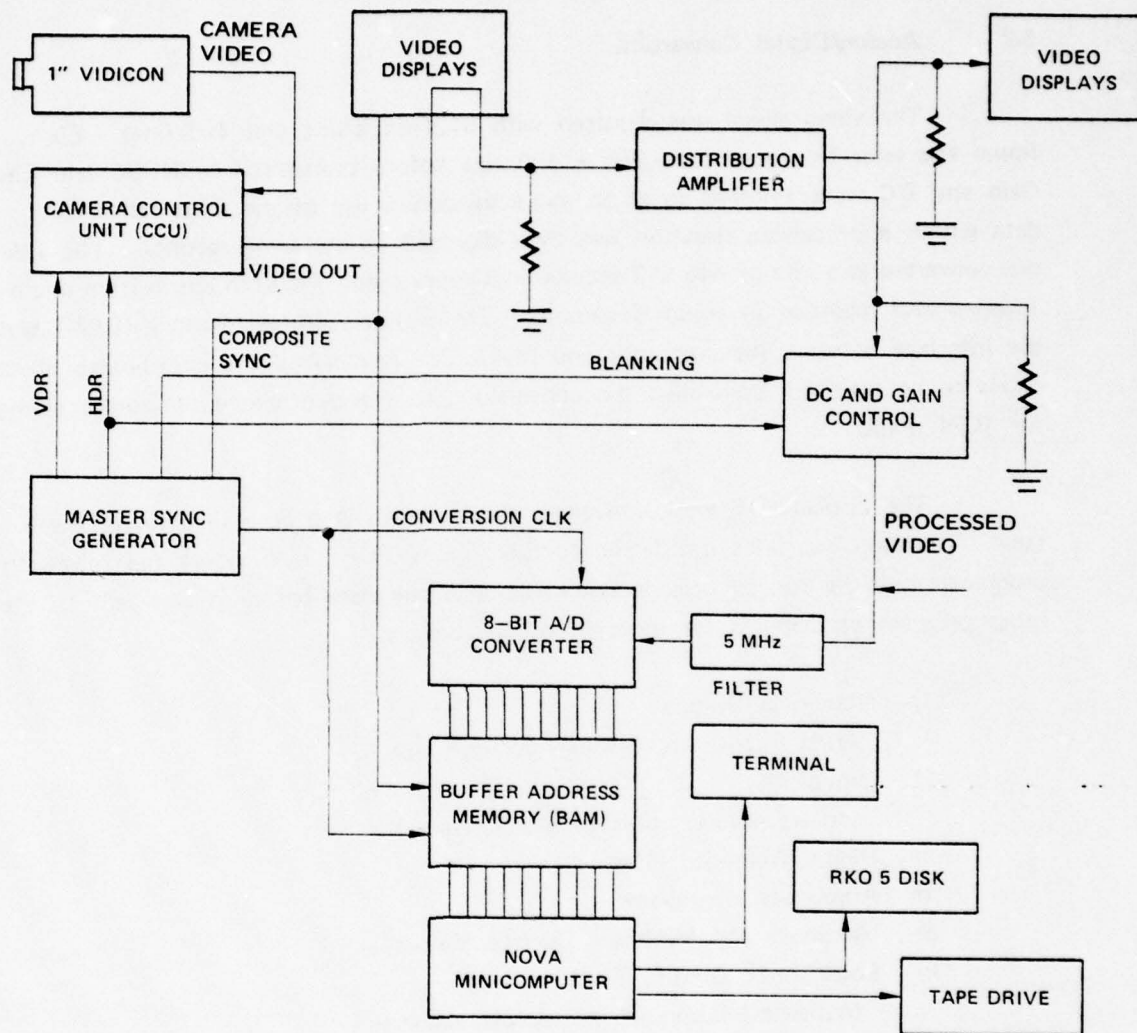


Figure 6.1

values is 29% sync pulse, so the process of removing them before digitization better utilizes the 8-bit range. A 5 MHz filter immediately preceded the 10.24 MHz A/D.

6.2 Analog/Digital Conversion

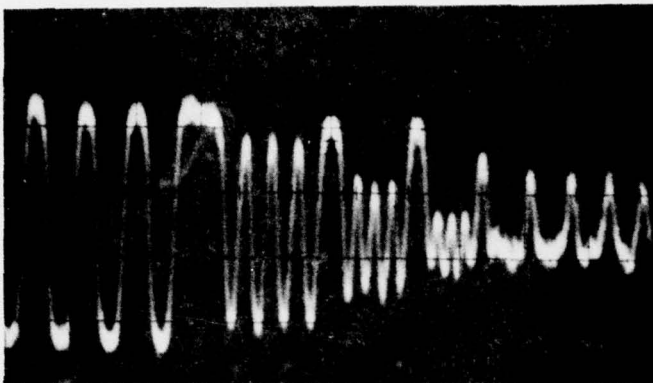
The video signal was digitized with 512 pixels/line and 490 lines. Each frame was later truncated to a 256 x 400 size before transmittal to NOSC and Ensco. Gain and DC were adjusted so as to make maximum use of the 8-bit range. All data within a processing iteration was then digitized at the same settings. The video was converted at a rate of two 512 sample lines every field. Thus, an entire frame could be scanned and recorded in about 5 seconds. The Buffer Address Memory (BAM) was the interface between the computer and the A/D. It received the coordinates of the pixels to be digitized, controlled the conversion clock and provided temporary storage for 1024 pixels.

The optical PAS were converted and recorded one at a time on magnetic tape. The tape was later transferred to the Ampex PDP 11/55 where the following programs could be run to provide quick looks at the data before it was sent to the other program participants for more thorough analysis:

- 1) Numerical Dumps
(first 4 and last 4 values of each line.)
- 2) Greyplots
(coarse density plots of the surfaces.)
- 3) Digital Isometric Plots
- 4) Amplitude Histograms
- 5) Maximum and Minimum Surface Values
- 6) Logarithmic Density Plots
(numerical dump of log sample values)

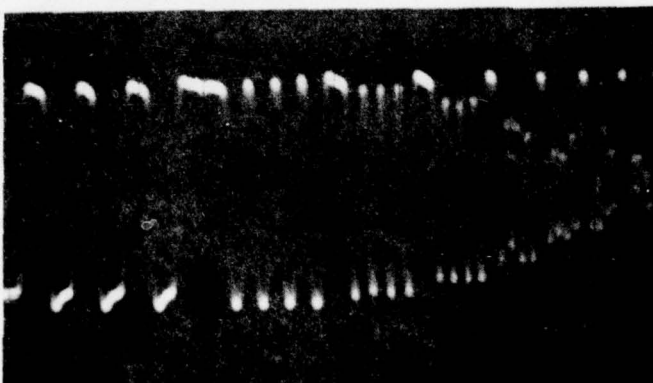
All of these aids with the exception of 5 and 6 were routinely supplied for each surface along with the data tape for each iteration.

The following pages show example outputs for each of these utility programs.



(a)

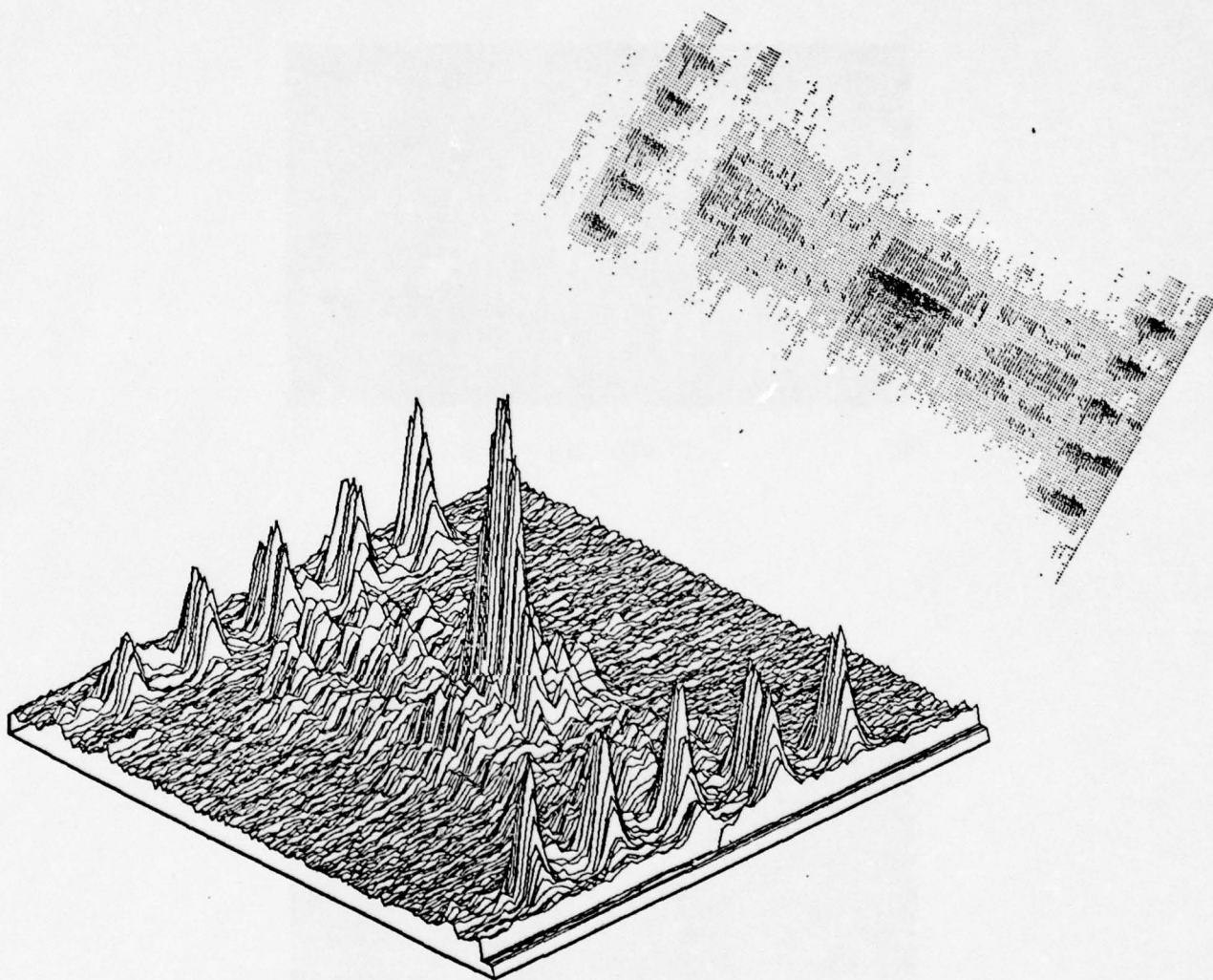
1" VIDICON



(b)

2" VIDICON

Figure 6.2A & B Camera Response to Squarewave Test Chart. Leftmost Packet 100 Linepairs - Graduated in 100 Linepair Increments.



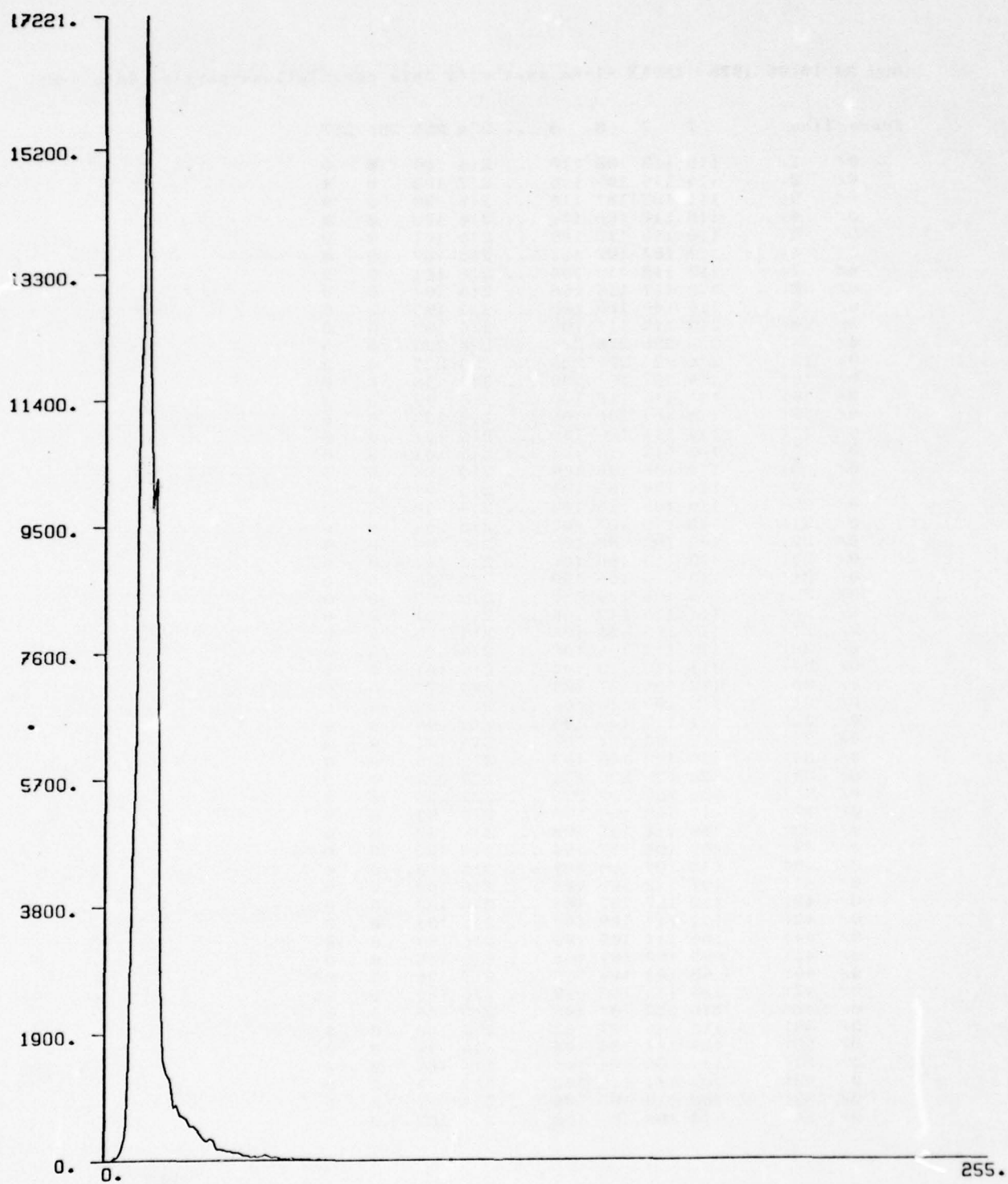
Digital Isometric & Greyplot

AMPEX

Aug 29 10:06 1978 AMPEX -lens synthetic data correlations-partial data dump

frame/line:	1	2	3	4	...	254	255	256	257
0/ 1:	118	112	108	110	...	216	106	0	0
0/ 2:	114	116	109	106	...	217	102	0	0
0/ 3:	111	107	107	110	...	215	190	0	0
0/ 4:	118	113	108	110	...	216	103	0	0
0/ 5:	110	113	112	109	...	216	101	0	0
0/ 6:	114	107	107	111	...	215	189	0	0
0/ 7:	113	112	113	104	...	216	101	0	0
0/ 8:	112	117	114	108	...	216	101	0	0
0/ 9:	116	109	108	108	...	215	196	0	0
0/ 10:	113	112	111	106	...	216	109	0	0
0/ 11:	226	226	226	226	...	225	225	0	0
0/ 12:	226	226	226	226	...	225	225	0	0
0/ 13:	114	109	109	109	...	216	98	0	0
0/ 14:	111	116	112	106	...	216	99	0	0
0/ 15:	112	109	106	106	...	214	183	0	0
0/ 16:	114	114	109	104	...	216	101	0	0
0/ 17:	106	113	110	101	...	216	101	0	0
0/ 18:	115	108	106	109	...	214	188	0	0
0/ 19:	114	109	108	104	...	215	99	0	0
0/ 20:	110	109	113	103	...	216	99	0	0
0/ 21:	98	100	107	107	...	215	164	0	0
0/ 22:	102	103	108	106	...	216	94	0	0
0/ 23:	108	113	108	106	...	216	101	0	0
0/ 24:	113	110	106	108	...	215	158	0	0
0/ 25:	115	106	109	110	...	215	102	0	0
0/ 26:	111	115	112	106	...	216	101	0	0
0/ 27:	110	105	105	106	...	215	185	0	0
0/ 28:	115	112	106	108	...	216	101	0	0
0/ 29:	111	113	113	104	...	216	101	0	0
0/ 30:	112	105	107	109	...	214	172	0	0
0/ 31:	113	109	110	106	...	215	99	0	0
0/ 32:	111	112	108	108	...	216	96	0	0
0/ 33:	112	105	107	107	...	214	191	0	0
0/ 34:	113	110	106	107	...	215	103	0	0
0/ 35:	226	226	226	226	...	225	225	0	0
0/ 36:	226	226	226	226	...	225	225	0	0
0/ 37:	111	108	109	108	...	215	99	0	0
0/ 38:	109	110	107	102	...	216	102	0	0
0/ 39:	109	104	107	104	...	214	182	0	0
0/ 40:	113	109	106	109	...	215	103	0	0
0/ 41:	107	112	109	102	...	216	100	0	0
0/ 42:	112	107	107	106	...	214	183	0	0
0/ 43:	111	111	109	109	...	215	101	0	0
0/ 44:	106	111	109	103	...	216	99	0	0
0/ 45:	95	100	109	106	...	215	155	0	0
0/ 46:	98	101	106	108	...	215	96	0	0
0/ 47:	106	113	108	107	...	216	101	0	0
0/ 48:	110	112	107	105	...	215	154	0	0
0/ 49:	113	111	107	107	...	215	100	0	0
0/ 50:	109	111	106	105	...	216	99	0	0
0/ 51:	111	106	104	106	...	214	185	0	0
0/ 52:	109	111	110	102	...	215	99	0	0
0/ 53:	108	114	108	106	...	216	99	0	0
0/ 54:	110	106	104	108	...	214	182	0	0

AMPEX



PAS Amplitude Histogram

AMPEX

Mar 1 1:24 1979 Histogram Dump for LENS 3/7/79 Page 1

```

*****
segment # 0
256 samples, 0 columns, 1
type '1', typesize 2, pro
0:      0
1:      0
2:      10
3:      45
4:      54
5:      167
6:      389
7:      1490
8:      4368
9:      6415
10:     11313
11:     12433
12:     17221
13:     12025
14:     9776
15:     10224
16:     3032
17:     1514
18:     1298
19:     1221
20:      797
21:     833
22:     687
23:     667
24:     633
25:     520
26:     527
27:     465
28:     409
29:     333
30:     299
31:     342
32:     305
33:     181
34:     182
35:     172
36:     141
37:     148
38:     124
39:     119
40:     109
41:      78
42:      83
43:      54
44:      72
45:      63
46:      71
47:      97
48:      83
49:      47

50:      60
51:      49
52:      28
53:      33
54:      29
55:      44
56:      24
57:      26
58:      22
59:      24
60:      22
61:      16
62:      14
63:      29
64:       9
65:      10
66:      13
67:      14
68:      14
69:      17
70:       6
71:      10
72:       4
73:      14
74:       9
75:       4
76:       4
77:       4
78:       3
79:       8
80:      11
81:       5
82:       5
83:       3
84:       4
85:       4
86:       1
87:      10
88:       2
89:       1
90:       5
91:       4
92:       7
93:       4
94:       3
95:       8
96:       5
97:       3
98:       5
99:       1
100:      4
101:      0
102:      0
103:      2
104:      2
105:      4

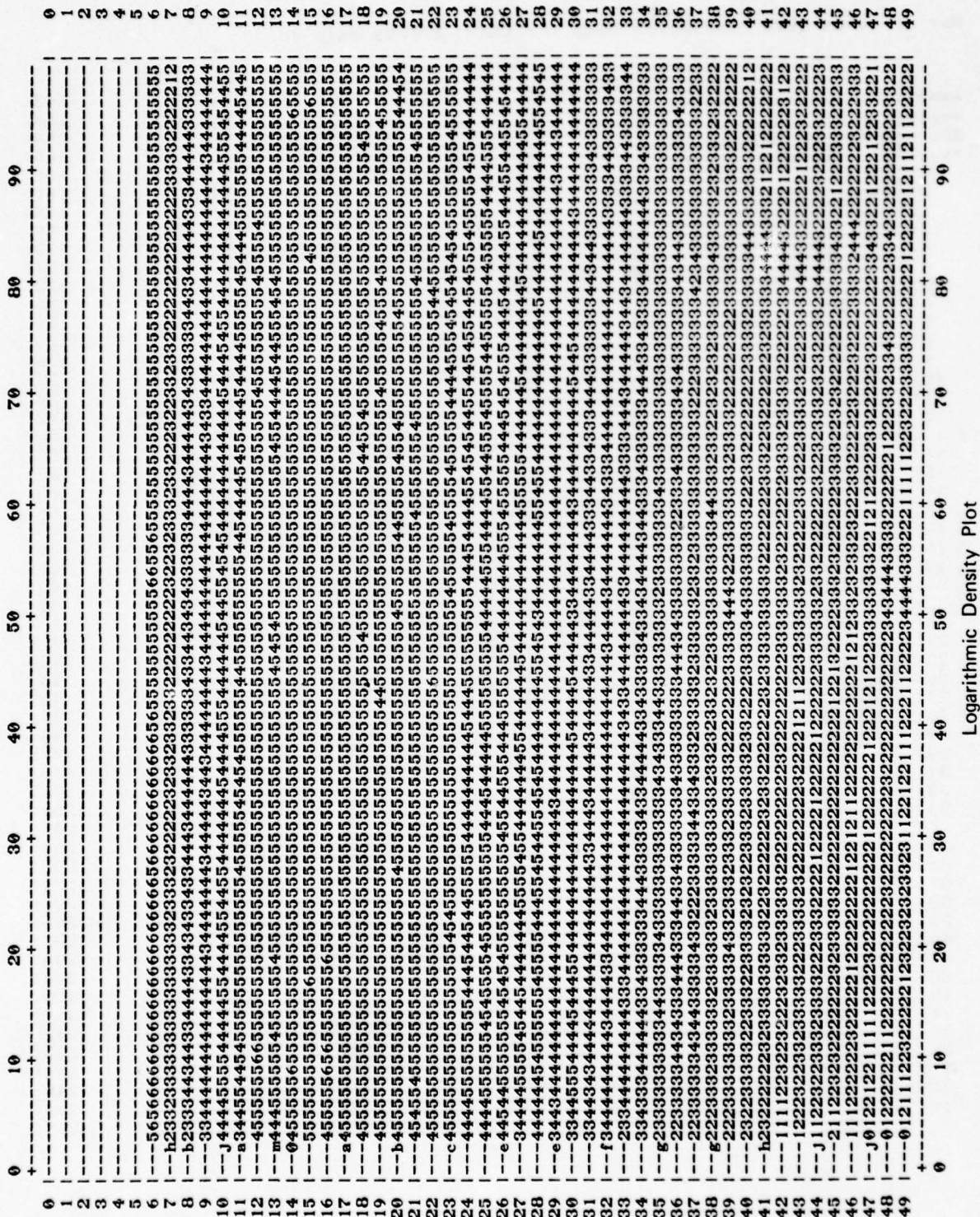
106:      3
107:      2
108:      3
109:      1
110:      4
111:      9
112:      1
113:      2
114:      2
115:      2
116:      1
117:      1
118:      1
119:      1
120:      1
121:      4
122:      1
123:      1
124:      1
125:      1
126:      0
127:      3
128:      2
129:      1
130:      0
131:      1
132:      0
133:      1
134:      2
135:      2
136:      1
137:      2
138:      1
139:      1
140:      2
141:      1
142:      0
143:      2
144:      0
145:      0
146:      1
147:      1
148:      0
149:      0
150:      0
151:      1
152:      0
153:      0
154:      2
155:      1
156:      0
157:      0
158:      0
159:      0
160:      0
161:      0

162:      1
163:      0
164:      1
165:      1
166:      2
167:      1
168:      0
169:      2
170:      0
171:      0
172:      0
173:      1
174:      0
175:      2
176:      1
177:      0
178:      0
179:      1
180:      1
181:      0
182:      1
183:      1
184:      0
185:      0
186:      0
187:      0
188:      0
189:      0
190:      0
191:      2
192:      1
193:      1
194:      0
195:      0
196:      1
197:      0
198:      0
199:      0
200:      0
201:      0
202:      0
203:      0
204:      1
205:      0
206:      0
207:      0
208:      2
209:      0
210:      0
211:      0
212:      2
213:      0
214:      1
215:      0
216:      1
217:      0

```

AMPEX

Ampe. Research--Signal Processing Section Wed Jul 4 22:22 1979
 Zero dB reference point = 211.000000
 Segment 0 of /scr/lens/cjuly2.slg



7.0 DISTRIBUTION OF DIGITIZED OPTICAL DATA

Digitized optical information was distributed on four different occasions to NOSC and Ensco. Each iteration was performed in response to feedback from the other program participants or significant improvements in system performance. With each iteration, the exchange of data went smoother and the surfaces showed constant improvement. Both NOSC and Ensco were extremely cooperative in promptly supplying measurements that they had extracted from the data, so that problems could be solved and new experiments could be performed. We believe that we have supplied all the data and information that was requested in the test plan as well and additional information to help evaluate the optical surfaces. This section contains a brief description of each of the iterations. Additional information on the distribution of data is contained in Appendix B.

7.1 April 21, 1978

This first iteration served mainly to work out problems in the transfer of data. The quality of the data was disappointing due to hardware problems in the FAG*, the A/D and poor film modulation. For this experiment, the fast scan axis of the camera was aligned with range. This proved to be unsatisfactory since the maximum resolution was required in the Doppler direction. It was corrected for the following iterations. Seven surfaces were transmitted as described in Table 7.1. Following this experiment, the FAG was replaced and a new lens was installed on the film recorder. It was also decided to abandon the hope of doing 1024 second CITs and 512 seconds was adopted as a maximum.

7.2 August 28, 1978

The bulk of the analysis that was done on the digitized optical surfaces is based on this data set. Twenty surfaces were transmitted as described in Table 7.2. They included 10 successive 512 second epochs with 50% overlap at $+\infty$ SNR and 4 successive epochs at ODB SNR. Also included were sinewave correlations as

* The FAG was a predecessor to the BAM with only 256 point per line digitizing capability.

prescribed in the test plan. A report followed the test data to describe the range-Doppler scaling of the surfaces. The calculated scale factors were approximately correct, but some of the empirical assumptions about the camera aspect ratio and scan sizes left much to be desired. It was decided to develop a way of imbedding correlating markers in the data to achieve scaling in future iterations. ENSCO suggested that there was a problem with the monotonicity of the A/D. This was verified by observing irregularities in the amplitude distributions. The A/D was subsequently replaced.

7.3 February 28, 1979

This data set included surfaces of both 512 and 256 second CIT, surfaces composed of mixed SNR signal segments, the inclusion of range-Doppler calibration markers and impulse correlations. These surfaces were listed in Table 7.3. The 256 second CIT data looked very promising since increased light efficiency was achieved with the lowered spatial frequencies on film; This resulted in a signal to system noise advantage. A further improvement in SNR was achieved due to the replacement of the faulty A/D. This allowed us to make better use of the 8-bit dynamic range. The peak signal to mean value of the amplitude distributions improved as reported by ENSCO.

This measurement was calculated as:

$$SNR = \log \frac{A_{\max} - A_{\min}}{A_{\text{turn}} - A_{\min}} \quad \text{where } A_{\max} \text{ is the peak height, } A_{\min} \text{ is}$$

the lowest point in the plane and A_{turn} is the mean of the distribution. The table below shows this measurement for the two data sets.

	8/28/78	2/28/79
Lowest	31	6
Turnover	53	11
Peak	255	231
Ratio	1	1.65

The lower baseline value for 2/28/79, which was made possible by the new A/D, contributed to this improvement. The Doppler resolution remained a serious problem. Flexibility of the IPC design was demonstrated by experimenting with multiple surfaces/frame. The range dimension was partitioned into three, 64 second range intervals. Thus it was demonstrated that the frames could be arbitrarily divided into any number of

surfaces as long as they were the same CIT and the total number of range samples was less than 256.

7.4 March 7, 1979

This data set was transmitted immediately following the February 28 run to rectify some problems in that data. The first few surfaces in the 2/28/79 were inadvertently clipped at the baseline due to a misadjustment of the camera setup level. Seven surfaces were redigitized and transmitted as described in Table 7.4.

7.5 Additional Experiments

A data set was prepared on July 3, 1979 just prior to a working meeting with Mr. James Teeter of NOSC. Four identical surfaces were digitized to demonstrate the temporal stability of the system. A transient scan size change had previously been discovered in the camera control unit. We believe it was satisfactorily demonstrated that the features remained stationary to within a sample from frame to frame. (The transient effect has earlier been demonstrated with digitized test charts and then disappeared.) These four surfaces had also been magnified by about 250% and showed a Doppler width of 13 mHz, a 32% improvement over the previous data.

This result only reflects the fact that the useful Doppler range was sampled by the same number of points, but each point now representing 1.87% mHz or 40% of less Doppler. The sampled points were still not resolved by the vidicon as evidenced by the fact that the physical size of the peak did not noticeably increase.

The final data iteration was performed after a dramatic increase in film modulation and a concomitant decrease in system noise was achieved. This is documented in Appendix A.

Table 7.1

LENS TAPE CONTENTS (4/21/78)

Surface No.	Origin	Comments
1	Block 1, point 512 → 1023	Autocorrelation shifted ± 128 points wrt itself.
2	Block 2, point 512 → 1023 Block 1, centerline of τ Shifts at point 512 → 1023	Cross correlation one epoch. $S/N = \pm \infty$
3	Block 2, point 550 → 1061 Block 1, centerline of τ Shifts at point 512 → 1023	Cross correlation $S/N = + \infty$ Data offset to show shift in range.
4	Block 5, point 1024 → 1535	Autocorrelation shifted ± 128 points wrt itself.
5	Block 6, point 1024 → 1535 Block 5, centerline of τ Shifts at point 1024 → 1535	Cross correlation $S/N = 0$ dB one epoch
6	Baseline optical noise	Sample 1
7	Baseline optical noise	Sample 2

Table 7.2
SURFACE DATA 8/28/78

SURFACE NO.	1ST BLK/2ND BLK/DATA PTS.	S/N	REMARKS
0	- - - - -	- - -	TV Crosshatch
1	1/1/256-767	+INF	Autocorrelation
2	2/1/256-767	+INF	EPOCH NO.1
3	2/1/512-1023	+INF	EPOCH NO.2
4	2/1/768-1279	+INF	EPOCH NO.3
5	2/1/1024-1535	+INF	EPOCH NO.4
6	2/1/1280-1791	+INF	EPOCH NO.5
7	2/1/1536-2047	+INF	EPOCH NO.6
8	2/1/1792-2303	+INF	EPOCH NO.7
9	2/1/2304-2815	+INF	EPOCH NO.9
10	2/1/2560-3071	+INF	EPOCH NO.10
11	6/5/512-1023	0 dB	EPOCH NO.1
12	6/5/768-1279	0 dB	EPOCH NO.2
13	6/5/1024-1535	0 dB	EPOCH NO.3
14	6/5/1280-1791	0 dB	EPOCH NO.4
15	30/29/512-767	+INF	SINEWAVE
16	30/29/768-1279	+INF	SINEWAVE
17	- - - - -	- - -	BASELINE NOISE
18	- - - - -	- - -	BASELINE NOISE
19	- - - - -	- - -	BASELINE NOISE
20	- - - - -	- - -	UNCORRELATED SIGNAL (2 FILM MASKS AT RANDOM)

Table 7.3

SURFACE DATA 2/28/79

FRAME NO.	1ST BLK/2ND BLK/DATA POINTS	S/N	REMARKS
0	1/1/768-1023 2/1/768-1023 2/2/768-1023	+INF	MULTIONE 3 Surfaces/frame
1	1/1/1024-1279 1/2/1024-1279 2/2/1024-1279	+INF	MULTIONE 3 Surfaces/frame
2	5/5/768-1023 6/5/768-1023 6/6/768-1023	0dB	MULTIONE 3 Surfaces/frame
3	2/1/768-1023	+INF	256 Second
4	1/1/512-767	+INF	Autocorrelation
5	2/1/512-767	+INF	Crosscorrelation
6	2/1/1024-1279	+INF	
7	6/5/768-1023	0dB	
8	1/1/768-1279 2/1/768-1279 2/2/768-1279	+INF	MULTI 3 Surfaces/frame
9	1/1/768-1279	+INF	Autocorrelation
10	2/1/768-1279	+INF	
11	6/5/1024-1535	0dB	
12	Impulse 4 cycles, 32 points	±INF	

Table 7.3 Continued

FRAME NO.	1ST BLK/2ND BLK/DATA POINTS	S/N	REMARKS
13	1/1/1024-1279	+INF	Autocorrelation
14	2/1/1024-1279	+INF	
15	6/5/1024-1279	0dB	
16	2/7/1024-1279	+INF/-3dB	Mixed S/N
17	6/7/1024-1279	0dB/-3dB	Mixed S/N
18	2/1/1024-1535	+INF	
19	8/7/1024-1535	-3dB/-3dB	Mixed S/N

Table 7.4

SURFACE DATA 3/7/79

FRAME NO.	1ST BLK/2ND BLK/DATA POINTS	S/N	REMARKS
0	1/1/1024-1279	+INF	MULTIONE
	2/1/1024-1279		3 Surfaces/frame
	2/2/1024-1279		
1	1/1/768-1023	+INF	MULTIONE
	2/1/768-1023		3 Surfaces/frame
	2/2/768-1023		
2	5/5/768-1023	0dB	MULTIONE
	6/5/768-1023		3 Surfaces/frame
	6/6/768-1023		
3	2/1/1024-1279	+INF	256 Seconds
4	2/1/768-1023	+INF	256 Seconds
5	2/1/1024-1535	+INF	512 Seconds
6	2/1/768-1279	+INF	512 Seconds
7	—	—	Camera Black (Laser Off)

8.0 BIBLIOGRAPHY

CITED REFERENCES

Section 2

1. Cutrona, L. J., et. al., "Optical Data Processing and Filtering System", IRE Trans. Info. Theory, Vol. 6, pp 386-400, 1960.
2. Sprague, R. A., "A Review of Acousto-Optic Signal Correlators", Opt. Eng., Vol. 16, No. 5, pp 467-474, 1977.
3. Cassasent, D., et. al., "A Coherent Optical Signal Processor for Passive Ambiguity Function Generation", Inter. Opt. Comp. Conf., pp 96-101, 1978.
4. Nisenson, P. and Sprague, R., "Real-Time Optical Correlation", Appl. Optics. Vol. 14, No. 11, pp 2602-2606, 1975.

Section 3

5. Techniques of Microphotography, Eastman-Kodak, Publication No. P-52.
6. Kozma, A., "Film Recording for Coherent Optical Systems and Holography, Univ. of Michigan Short Course on ODP, 1968.
7. RCA Electro-Optics Handbook, RCA Solid State Div., Chapter 13.
8. M. Borne and E. Wolfe, Principles of Optics, McMillan Co., p 454.

ADDITIONAL REFERENCES

- Woodward, P. M., Probability and Information Theory with Applications to Radar, Pergammon Press, 1953, p 120.
- Bendat, J. S. and Piersol, A. G., Measurement and Analysis of Random Data, John Wiley & Sons, Chapter 3.
- Van Trees, Harry L., Detection, Estimation and Modulation Theory, J. Wiley & Sons, Part 1, p 173, 1968.
- Weaver, C. S. and Goodman, J. W., "A Technique for Optically Convolving Two Functions", Appl. Optics, Vol., 5, No. 7, p 1248, 1966.

APPENDIX A

IMPROVEMENTS OF FILM RECORDING CHARACTERISTICS

While preparing Section 3 (Recording Signals on Film) of this report, an experiment was run to see how close the film recording system could come to the theoretical maximum diffraction efficiency of 6.25%. After inspecting the computer generated TE curves, it was decided that the modulation could almost be doubled while only increasing the harmonic distortion by 6 dB. Recalling that in Section 5 it was shown that the film was the most inefficient component in the light budget calculations, the payoff in improving the film modulation would be an optical output that was much higher above the noise floor. A doubling in modulation index would result in a 12 dB improvement in signal to optical noise.

The electrical signal to be recorded was doubled in amplitude and new densitometry measurements were taken on recorded grey scale charts. An optimum bias point was selected and the new grey scale density values are shown in the following table:

Exposure Level (0-4095)	D	τ	T
clear	.08	.83	.91
0	.09	.81	.90
1	.14	.72	.85
2	.25	.56	.75
3	.38	.42	.65
4	.52	.30	.55
5	.67	.21	.46
6	.85	.14	.38
7	.98	.10	.32
dark	1.94	.01	.11

The values for the amplitude transmittance (T) were plotted and fit to both a linear and quadratic curve with the following results:

Linear fit $T_A = -.70E + .915$

Quadratic fit $T_A = .053E^2 - .75E + .92$

The 2nd harmonic to fundamental power ratio can be calculated by $10 \log \left(\frac{.053}{2(.75)} \right)$ or -14.5 dB.

Using the relationships derived in Section 3.3, the diffraction efficiency and D.C. Transmission Ratio could similarly be predicted from this data. From the linear fit of the densitometry data, it appeared as though a 64% modulation had been achieved. Figure A-1 is the computer generated plot of the measured and linear fitted T-E curve.

The film characteristics were then measured experimentally for a sinewave input and found to be:

Intensity	Value
Input	.54 mw
D.C. Spot	.28 mw
Fundamental	20 μw
2nd Harmonic	.44 μw
3rd Harmonic	.07 μw

From this experimental information we can now compare the 2nd harmonic ratio, diffraction efficiency and D.C. transmission ratio as was done in Section 3. The new comparisons are shown below:

Parameter	Observed	Calculated
Diffraction Efficiency	3.7%	3%
D.C. Transmission Ratio	52%	44% (75%)
2nd Harmonic Ratio	-16.6%	-14.5 dB

This should be compared to Table 3.4. Notice that the observed diffraction efficiency has more than doubled while the harmonic content has only increased by 2 dB. Since the measured modulation is now 64% rather than the old value of 42%, we would expect an increase of $(64/42)^2$ or 230% in diffraction efficiency. We observed exactly that. So even though we fell short of doubling the modulation

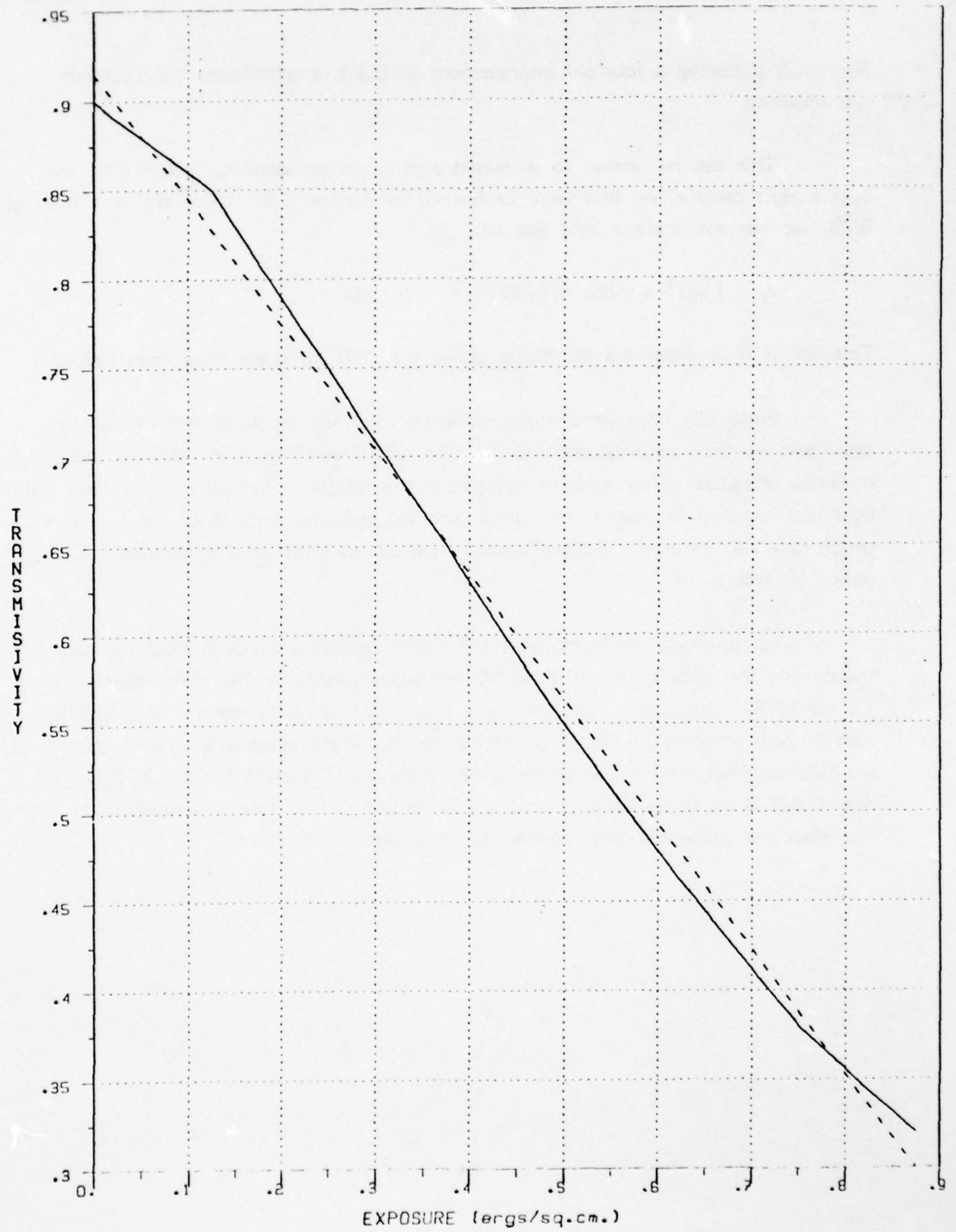


Figure A-1

(and thus obtaining a fourfold improvement in D.E.), a significant improvement was obtained.

This can be related to increased system performance by referring to the light budget calculations that were performed in Section 5.3. Using the new D.E. of 3.7%, we can anticipate a light loss of:

$$\tau_l = (.98)^4 \times (.85) \times (.037)^2 \Rightarrow -29.7 \text{ dB}$$

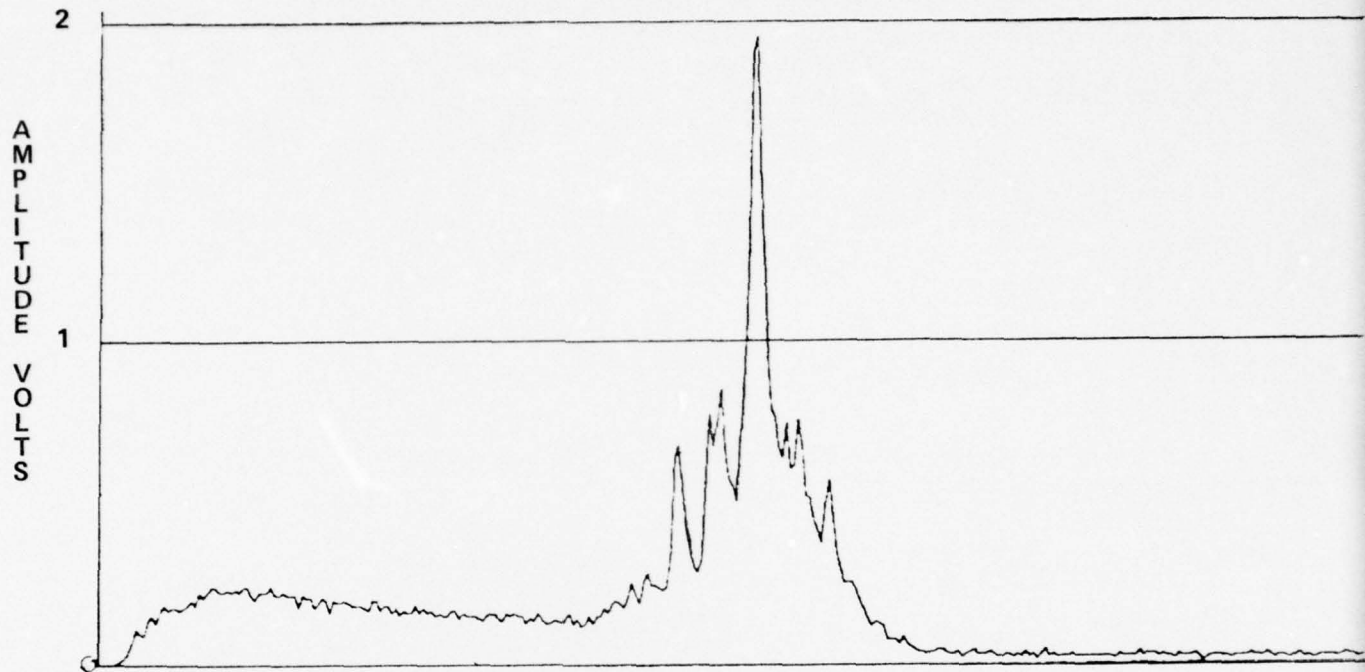
This results in a signal 7.3 dB higher above the -60 dB noise floor than before.

Since this improvement was obtained after the technical end of contract, there was no time to distribute new data to NOSC and Ensco for analysis. We did, however, redigitize a few surfaces to observe the results. Significantly less laser input light was required to observe an output and the required amount of video amplification was also reduced. Both effects are certain to improve the detectability of the optical surfaces.

An untimely malfunction in the GASP tape drive has prohibited us from transferring this data to the PDP 11/55 for quantitative analysis. The estimate of a 7.3 dB SNR improvement will have to suffice. We can only show a 1-D digitized scan at zero range as in Fig. A-2. It clearly shows the magnitude of the noise floor, the sidelobe level, and the peak for a 512 second CIT surface (1/768 2/768). Figure A-3 is an analog isometric of a 256 second CIT surface with calibration markers. The floor has purposely been clipped to emphasize the features.

DATE 9/6/79

TIME 14:51:45



AMPLITUDE VS FREQUENCY SAMPLE POINTS FROM 1 TO 320

Figure A-2

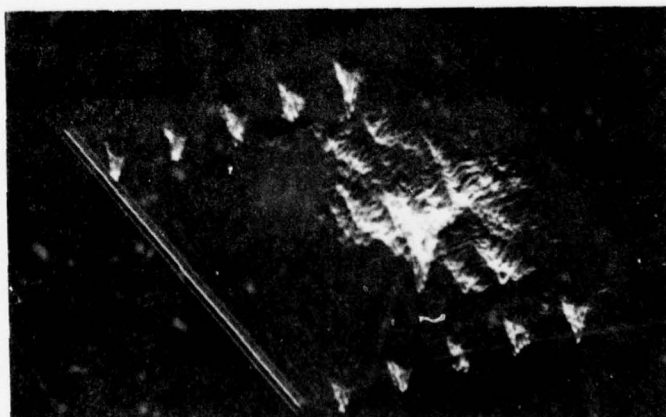


Figure A-3

**APPENDIX B
SELECTED CORRESPONDENCE**

NAVAL OCEAN SYSTEMS CENTER
San Diego, California 92152

7114/NP/gh
711/238/77
02 September 1977

MEMORANDUM

From: Norman D. Pos, Code 7114
To: Neal J. Martini, Code 7114

Subj: LENS Data Tape

1. The tape of synthetic data will contain a total of 28 blocks of 7200 words each.
2. The blocks are in sequential pairs: blocks N and N+1 represent respectively the undopplered and dopplered signals, where N=1,3,5,....,27.
3. Each block contains, in sequence, the real, then the imaginary parts, of a data point. That is, the sequence goes:

WORD#	DATA POINT#	
1	1	REAL
2	1	IM
3	2	REAL
4	2	IM
5	3	REAL
6	3	IM
-	-	-
-	-	-
-	-	-
7199	3600	REAL
7200	3600	IM

Thus, each 7200 word data block contains 3600 data points.

4. A table of S/N for each block follows:

(ODD Block# = Undopplered signal)

Even Block# = Dopplered signal)

BLOCK #	S/N (DB)	BLOCK#	S/N (DB)
1-2	Infinity	23-24	-21
3-4	3	25-26	-30
5-6	0	27-28	-Infinity
7-8	-3		
9-10	-6		
11-12	-9		
13-14	-10.5		
15-16	-12		
17-18	-13.5		
19-20	-15		
21-22	-18		

AD-A082 073

AMPEX CORP REDWOOD CITY CA ADVANCED TECHNOLOGY DIV
OPTICAL CORRELATION STUDIES. CONTINUATION OF LENS PROGRAM. (U)
OCT 79 L R WEINER

F/G 20/6

N00014-77-C-0447

UNCLASSIFIED

RR-79-23

NL

2 OF 2

AD-

A082073

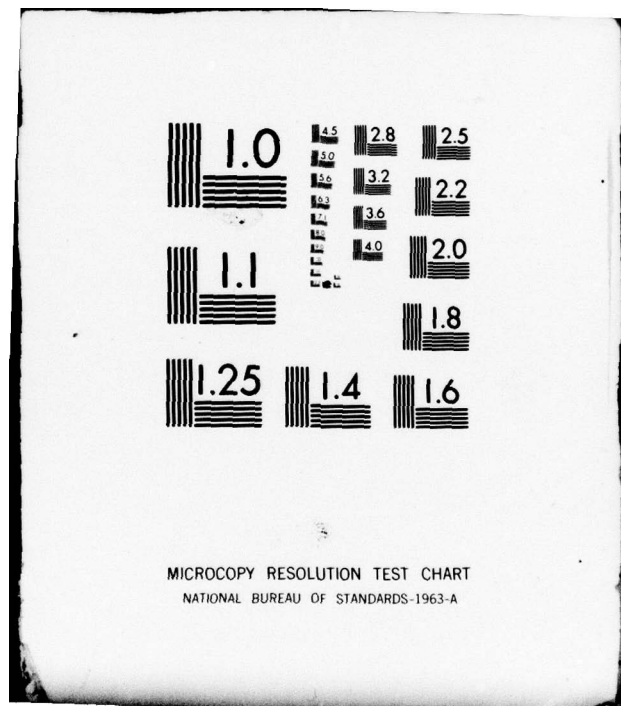


END

DATE
FILMED

4-80

DTIC



MICROCOPY RESOLUTION TEST CHART
NATIONAL BUREAU OF STANDARDS-1963-A

7114/NDP/gh
711/238/77
02 September 1977

Subj: LENS Data Tape

5. The data is DC shifted and normalized so that the words on the tape are integers N such that:

$0 \leq N \leq 2^{16} - 1 = 65535$, with a translated zero at

$N = 32767.5$ (literally, though not represented with N an integer).

6. The tape has been prepared with 1600 BPI density 9 track, odd parity, each two successive BYTES of 8 bits each representing one 16 binary bit word.

7. The synthetic signal contained on this tape is of .1 Hz BW; 149.975 Hz center; .06 Hz doppler.

8. The noise RMS in blocks 3 and 4 was determined so that the signal + noise at $S/N = 3\text{DB}$ filled the dynamic range of 0 to 65535; after which the noise RMS was constrained to be constant while the signal was modified to yield the table in paragraph 4.

9. The following additional blocks (all of exactly the same format as described above) are to be appended, or perhaps placed on a second tape:

- a. Pure sine wave at .025 Hz
- b. Pure impulse
- c. Real world data



N. D. POS

Copy to:

→ Ampex, Scott Smader, Bob Markevitch
Carnegie-Mellon University, David Casasent, PhD
7111, David Edelblute

AMPEX

January 10, 1978

Dr. Leonard Ackler
Ensco, Inc.
8001 Forbes Place
P. O. Box 1383
Springfield, Va. 22151

Dear Dr. Ackler:

Enclosed is an outline of the points we discussed in our recent phone conversation concerning repeatability of the proposed optical processing system. Any of these topics can be explained in more detail at your discretion.

It is anticipated that the goal of having the synthetic data on film and ready for analysis by first week February will be met. A joint effort by Ampex and Carnegie-Mellon University will be made to obtain correlation data shortly thereafter.

The layout of the film-based Ampex optical system will not be considered proprietary and will be released to you when available. For the most part, the layout is based on textbook implementations. The novelty of the approach is mainly in the formatting of the data onto the film or real-time spatial modulators.

Sincerely,

AMPEX CORPORATION



L. R. Weiner, MS 3-20
Assoc. Member Research Staff
Research Department

LRW/jms

NOSC OPTICAL CORRELATOR
DOCUMENTATION FOR REPEATABILITY

- I. Ampex will maintain a catalogue which will include date of generation and the following considerations:

II. Input for Transparencies

- 1) Traceability to synthetic data tapes.
 - a) Tape date
 - b) Block/word sequence
- 2) Software processing
 - a) Latest revision date
 - b) Carrier frequency
 - c) Time/Doppler shift information
 - d) Any D/A converter Amplitude/D.C. offsets other than assumed full scale (0 - 255 bit) range

III. CRT Recorder and Film Data

- 1) CRT characteristics
 - a) Cathode D.C. voltage and analog amplitude
 - * b) Spot unblanking interval
 - * c) Special considerations (i.e., linearity correction change, sweep speed change)
- 2) Film characteristics
 - * a) Type film
 - b) Exposure
 - c) Processing (time, temperature)
 - * d) Special considerations (i.e., change of focus...)

IV. Optical Components

- * 1) Preferable to have a dedicated non-removable system with each component specifically identifiable.
- 2) Laser light levels

V. Readout and Formatting of Correlation Data

- 1) Vidicon target voltage
- 2) For digitized video data,
 - a) Shading correction procedures
 - b) Scale factors (due to partial digitization of output field)
 - c) Gamma (amplitude nonlinearity) correction procedures
 - d) Data to be recorded as 512 records x 512 bytes x 8 bits
- 3) For digitized photodiode array output should be consistent on consecutive runs. Same data format will be adhered to.

* These parameters should be assumed constant and exceptions noted where applicable.

December 30, 1977

Dr. D. Casasent
Carnegie-Mellon University
Department of Electrical Engineering
Pittsburgh, PA 15213

C/O Demetri Tsaltis

Dear Dr. Casasent:

The enclosed transparencies are a sample of our present film-making capabilities. The signals shown are patterned after your proposals in the 15 September ONR report for preliminary signal mask formats. These should be of some assistance in selecting and aligning the optics for an Image Plane Correlator. The software that has been written to drive the CRT film recorder is fairly flexible. If, after reviewing the summary of our software library you wish to propose additional formats that will serve to generate film-based ambiguity functions for the I.P.C., we will try to implement them.

Although the resolution capabilities of the CRT are not what we anticipated, I feel that system amplitude and scan linearities have been optimized.

A few notes on the CRT recorder are in order. All signal amplitudes are quantized to eight bits through the D/A converter. The full 256 level range can currently be utilized with minimal harmonic distortion (estimated 3rd harmonic at -38db with respect to fundamental). The signal blanking is designed such that the exposure time for each point is the same (currently 4 msec) regardless of the sweep rate. The camera has a f1.2 lens which is normally set in the f5.6 to f4.0 range.

The Bimat developer generates both a negative and a positive. The positive is not amplitude linear. A search for a positive process film has been made and as of yet none has been found with the sensitivity and resolution of the AHU Microfilm that we are now using.

Although the ONR program's emphasis is on recording and analyzing the synthetic data, we will be able to continually supply these preliminary masks on a short reaction time basis. Perhaps the best next step is for you to choose specific sequences of shots from the enclosed library. That way you will have the exposures organized into two sets, one for each of the liquid gates in the I.P.C. The joint transform correlator format that we discussed will eventually be implemented but we wish to first concentrate on making preliminary runs on the ONR tape data.

Dr. D. Casasent
December 30, 1977
Page 2

AMPEX

It is anticipated that we have now reached a point where transparencies can be generated on a regular basis. Your close cooperation is encouraged.

Yours very truly,



L. Weiner
Member Research Staff
Mail Stop 3-21

LW:vh

All frequencies in cycles/cm.
Amplitude and DC are given in D/A
converter units 0-255.

Roll 3A
12-28-77
AHU Microfilm
3-minute Bimat develop
Beam current bias = -62V

<u>Exposure #</u>	<u>Title</u>	<u>Aperture</u>	<u>Notes</u>
1	Raster 3	(smudged)	
2	Raster 3	f(4.0)	
3	Raster 3	f(5.6)	
4	Raster 3	f(4.0)	
5	Raster 1	f(5.6)	Start Freq. 16 } Amplitude 240
6	Raster 1	f(5.6)	Start Freq. 32 } DC offset 10
7	Raster 2	f(5.6)	Start Freq. 16 }
8	Raster 2	f(5.6)	Start Freq. 64 }
9	Raster 4	f(5.6)	Freq. 64
10	Raster 4	f(5.6)	Freq. 128
11	Raster 5	f(5.6)	LFM Freq. 2-128
12	Raster 5	f(5.6)	LFM Freq. 8-256
13	Raster 6	f(5.6)	LFM 2-128 2-256 4-400
14	Raster 7	f(5.6)	Freq. 128 } Amplitude 240
15	Raster 7	f(5.6)	Freq. 128 Phase Shifted } DC offset 10
16	Raster 7	f(5.6)	Freq. 32 Phase Shifted Amplitude 50 DC offset 20
17	Raster 7	f(5.6)	Freq. 32 Phase Shifted Amplitude 50 DC offset 0
18	--	--	--
19	--	--	--
20	Raster 8	f(5.6)	
21	Raster 8	f(5.6)	
22	Raster 9	f(5.6)	
23	Raster 9	f(5.6)	
24	IPC2	f(5.6)	Freq. 20.5 + 40.5 + 80.5 + 160.5 + 240.5 + 320.5
25	IPC1	f(5.6)	LFN 8-134 shifted } Amplitude 240
26	IPC1	f(5.6)	LFM 8-134 } DC offset 10
27	IPC1	f(5.6)	LFM 2-128 }
28	IPC1	f(5.6)	Freq. 110 } Amplitude 230
29	IPC1	f(5.6)	Freq. 100 shifted } DC offset 20
30	Raster	f(5.6)	
31	Raster	f(5.6)	
32	Raster	f(4.0)	

AMPEX

24 April 1978

Mr. J. Teeter
Code 7114
Naval Ocean Systems Center
San Diego, California 92152

Subject: Transmittal of Optical Ambiguity
Surface Digitized Data
Tape 4/21/78

Submitted by:

Ampex Corporation
401 Broadway
Redwood City, Ca. 94063

The enclosed tape contains digitized optically-formed ambiguity surfaces. It is being submitted by Ampex to ascertain the suitability of this data format for the further processing and analysis that will be done by the participants in this program. This is a preliminary step to ensure that future transfer of information can be made efficiently.

This first tape (identified as 4/21/78), consists of seven digitized surfaces. Each surface contains 128 lines of video data. The digitization was done on a line by line basis capturing 256 sequential points as eight bit interger values for each line. There is an end of file marker after each 32,768 contiguous values that compose a surface. The values are unipolar ranging from \emptyset to 255.

The surfaces were truncated to 128 lines in the vertical direction after it was determined that this format contained all the essential data. Due to the optical spatial filtering necessary to separate the correlation term from the other elements in the plane of the correlation, the most realistic aspect ratio is one in which the surface does not fill the screen vertically.

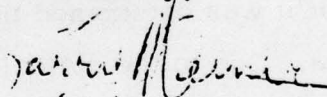
A camera using a Nuvicon imaging tube was used. This tube requires no gamma correction as would have been the case for our standard Vidicon camera. The Nuvicon camera also removes the problem of shading correction as had earlier been proposed.

It will be necessary to modify the program plan to allow for the fact that our present optical processing system is limited to working with 512 points of original synthetic data on each line of film. This corresponds to our best film making resolution of - 3 dB at 24 cycles/mm as explained in the last Ampex progress report. In this case, it will require a total of 12 epochs (instead of six) to cover the case of narrow-band signal at infinite S/N. What we propose to do is to double all the

required number of surfaces in order to achieve the same data observation times that were proposed jointly by N.O.S.C. and Ensco. Please note that in the following description of this present tape, the surfaces were all formed with 512 point segments of synthetic data modulated at a carrier frequency of 150 cycles/mm. This yields a data bandwidth on film of 10 cycles/mm (from 10 to 20 cycles/mm absolute).

Now that Ampex has fully developed the capability to record, optically process and digitize the synthetic data material, it is anticipated that the required surfaces can be produced on a short reaction basis. In particular, the surfaces suggested in the recent Ensco report should be digitized within one week of this date. It is requested that the NOSC determine the distribution of the present tape to the other program participants.

Sincerely,

A handwritten signature in dark ink, appearing to read "Larry Weiner", with a stylized flourish at the end.

Larry Weiner

LENS TAPE CONTENTS (4/21/78)

All surfaces contain 128 video lines starting at line number 150 of a T.V. frame. The autocorrelations that are included are for purposes of demonstrating the scale of the Doppler axis in the resultant surfaces and will not be included in future data sets unless requested.

Surface #	Origin	Comments
1	Block 1, point 512 → 1023	Autocorrelation shifted ± 128 points wrt itself.
2	Block 2, point 512 → 1023 Block 1, centerline of γ Shifts at point 512 → 1023	Cross correlation one epoch. $S/N = + \infty$
3	Block 2, point 550 → 1061 Block 1, centerline of γ Shifts at point 512 → 1023	Cross correlation $S/N = + \infty$ Data offset to show shift in range.
4	Block 5 point 1024 → 1535	Autocorrelation shifted ± 128 points wrt itself.
5	Block 6, point 1024 → 1535 Block 5, centerline of γ Shifts at point 1024 → 1535	Cross correlation $S/N = \emptyset$ dB one epoch
6	Baseline optical noise	Sample 1
7	Baseline optical noise	Sample 2

AMPEX

August 28, 1978

Mr. J. Teeter
Code 7114
Naval Ocean Systems Center
San Diego, Ca. 92152

Subject: Transmittal of Optical Ambiguity Surface Digitized
Data Tape

Submitted by: *L. R. Weiner*
L. R. Weiner

LRW/jms
Enclosures: cc w/enclosures to Dr. L. Ackler, Ensco
cc cover letter to Joel Trimble, ONR

This package contains material to support the results of a second iteration of LENS program optical processing. We believe that the improvements that have been made in film generation, optical layout, and digitization of the optical output will be clearly evident upon examination of the data. The material which is being transmitted represents only a collection of output data and real figures of merit will only be arrived at through a thorough analysis by the program participants. But, at first look, it appears as though a strong case for the LENS program can be built upon these results.

Accompanying this letter is an 800 bpi digital tape of the optical surfaces with a description of the recording format, a set of density plots and histograms, a partial tape dump to check validity of the data, and two pages of photographs taken from the G/ASP video displays.

The enclosed tape (identified as 8/28/78) contains 21 digitized frames. The first frame is a standard video crosshatch signal that should serve as a quick check upon reading the tape. Each correlation was done with 512 point segments of synthetic signal that were quadrature modulated by a spatial carrier with 150 cycles across the film aperture. For this iteration, a new digitizing system was made operational. The video frames were digitized using a 512 point horizontal cursor to capture a slice across the surface in the Doppler direction. This was done for 490 TV lines in each frame. This data was later truncated to the size described in the section on tape format.

Although we are currently running short on time under the present contract, an attempt will be made at a third iteration. This iteration will include surfaces of lower S/N, impulse test surfaces, range and Doppler calibration markers, and a demonstration of multiple ambiguity surfaces on a single frame. There probably will not be time to make distribution of this data to NOSC and ENSCO under this contract, but Ampex will report on results in

its final report and the material will be available for analysis during any follow-on program.

If there are any further questions, please contact Larry Weiner, Gary Newman or Bob Markevitch at (415) 367-3113.

Larry R. Weiner

AMPEX CORPORATION
RESEARCH DEPARTMENT
SURFACE DATA 8/28/78

Data points used for each correlation are referred back to the original synthetic data tape. A 512 point segment of the original 3600 data point blocks was used for each film mask with the exception of surface 0. The input mask contained the listed data point segment of a Dopplered block repeated on all 256 film lines and the 2nd or shifted mask had a centerline segment of un-Dopplered data with the same nominal time alignment (and therefore the same data point segment) as the Dopplered signal. Adjacent lines in the shifted mask are then advanced or delayed by one data point per line for a total shift of plus or minus 128 points across the film.

The entry in the table below that traces the data back to the original tape, then shows the data point segment and the two blocks from where it was extracted in the following form.

1st mask blk #/2nd mask blk #/data pts.

where data points refers to the centerline of the shifted mask and it is understood that adjacent lines in this mask are formed with time shifts in the data.

SURFACE DATA 8/28/78

SURFACE #	1st BLK/2nd BLK/DATA PTS.	S/N	REMARKS
0	--	--	TV Crosshatch
1	1/1/256-767	+INF	Autocorrelation
2	2/1/256-767	+INF	EPOCH #1
3	2/1/512-1023	+INF	EPOCH #2
4	2/1/768-1279	+INF	EPOCH #3
5	2/1/1024-1535	+INF	EPOCH #4
6	2/1/1280-1791	+INF	EPOCH #5
7	2/1/1536-2047	+INF	EPOCH #6
8	2/1/1792-2303	+INF	EPOCH #7
9	2/1/2304-2815	+INF	EPOCH #9
10	2/1/2560-3071	+INF	EPOCH #10
11	6/5/512-1023	Ø dB	EPOCH #1
12	6/5/768-1279	Ø dB	EPOCH #2
13	6/5/1024-1535	Ø dB	EPOCH #3
14	6/5/1280-1791	Ø dB	EPOCH #4
15	30/29/512-767	+INF	SINEWAVE
16	30/29/768-1279	+INF	SINEWAVE
17	--	--	BASELINE NOISE
18	--	--	BASELINE NOISE
19	--	--	BASELINE NOISE
20	--	--	UNCORRELATED SIGNAL (2 FILM MASKS AT RANDOM)

TAPE FORMAT

8/28/78

The enclosed tape contains 21 digitized optical ambiguity surfaces. Each surface contains 400 lines of video data. The digitization was done on a line by line basis with 256 sequential points as eight bit integer values for each line. Each data point is a two byte, 16 bit integer value between 0 and 255. The significant data appears in the lower (second) byte while the top byte should be all zeros. The lines form cuts through the range axis in the Doppler direction. The tape has 9 tracks, odd parity and was recorded at 800 bpi. Each of the 400 lines in a surface form a tape record with no other marks inserted. The starting word for a surface can be found from

$$W_N = (S_N * 400 \text{ lines/surface} * 256 \text{ words/line}) + 1$$

where W_N is the word number and S_N is the surface number 0 through 20. The only E.O.F. occurs after surface 20. A dump for each line of each surface is included which lists the first and last four integer values.

The black level pedestal on the increasing Doppler side of the surfaces was left in the data. This black level is caused by a spatial filter which is inserted at the 1st correlation plane to remove the signal sideband that is present there. Although it will show as a spike on the statistical data, it is thought that it might be useful in detecting any long term drifts due to ambient light changes or video clamp drifts. If preferred, it may be removed by truncating the data along the edge of the clearly defined aperture.

Care was taken to align the raster scan with the range-Doppler axis, but they may not correspond absolutely. The inclusion of range-Doppler calibration markers on the third iteration should allow us to perfectly "deskew" the output sampling.

February 1, 1979

Mr. J. Teeter

Code 7114

Naval Ocean Systems Center

San Diego, CA 92152

Subject: Additional Information Concerning Optical Ambiguity Surface
Digitized Data

Submitted by:


L.R. Weiner

LRW:js

c.c. Dr. J. Greene, ENSCO

Dr. D. Cassasent, C.M.U.

1.0 RANGE-DOPPLER SCALING OF DIGITIZED DATA

Digitized surfaces contain 490 lines with 256 doppler samples on each line. In the range dimension, the extreme points represent ± 128 seconds (or ± 128 data points). As shown in the figure, scales in both dimensions can be theoretically derived by considering only the last stage of the optical correlator and the vidicon image to electrical conversion. The output range scale was purposely compressed to balance the resolution in both axis.

1.1 Range Scaling

The scale in the range dimension is derived as follows: At the correlation plane, ± 128 seconds corresponds to .686 cm. This field size is the direct result of imaging the 16 mm input frame with L_2 . The .686 cm range axis was then imaged onto the vidicon so as to fill all 490 samples of the digitization. Each sample in range is therefore .522 seconds.

1.2 Doppler Scaling

For the doppler dimension, the equation written under the figure gives deflection (d) in the correlation plane for a given input spatial wavelength (D). This expression can be written in terms of optical spatial frequencies or in terms of original data temporal frequencies.

$$\text{spatial frequency} \quad d = .128 \times f_s \quad (\text{Eq. 1A})$$

or,

$$\text{temporal frequency} \quad d = 4.096 \times f_T \quad (\text{Eq. 1B})$$

using,

$$f_s(\text{cy/mm}) = f_T(\text{cy/sec}) \times 512(\text{sec})/16(\text{mm}) \quad (\text{Eq. 1C})$$

The effect on scaling of using a T.V. camera to detect an image is to introduce an additional scale factor between horizontal and vertical axis. This factor occurs because the early fathers of broadcasting decreed that viewing a square picture is not pleasant. Therefore, let the horizontal always be 1.333 times the vertical. In our system this factor was measured at 1.262. Remembering then that the range (vertical) dimension was .686 cm overall and was imaged onto the camera so as to completely fill the active raster, the doppler (horizontal) dimension becomes $.686/1.262 = .544$ cm. This manipulation has thus undone the vidicon scaling.

Since almost half of the doppler dimension when digitized with 512 samples was out of the range of interest, this data was cropped to lines of 256 samples before transmittal. Solving Equation 1B for f_T using a deflection of $5.44 \text{ mm}/2$ we find that the digitized doppler deflection represents .664 Hz overall or 2.59 mHz/sample.

2.0 COMPARISON OF THEORETICAL SCALING TO EXPERIMENTAL RESULTS

The following discussion is intended to be a quick check of the digitized surface peak coordinates. The exact coordinates of the peaks as located in the digital data field should be used for accurate results.

2.1 Doppler Scaling Experimental Results

As a check on experimental doppler scaling accuracy, plots of digitized optical surfaces show an approximate 33 point deflection between autocorrelation and doppler shifted peaks. Using the scale factor of 2.59 mHz point, this would indicate a doppler value of .085 Hz.

2.2 Range Scaling Experimental Results

Although all surfaces are centered on the same range value, we can apply the derived range scale factor to the peak range width as measured in the output data. Using an estimated 19 points as the output peak width and derived scale factor of .522 seconds/point gives 9.92 seconds. This roughly corresponds to the period time of the input data. This last manipulation does not take into account the band shape characteristics of the data and utilizes the 19 point peak width as reasonably representative of the output surfaces.

2.3 Comments on Range-Doppler Scaling

For this particular selection of optical elements it has been shown that points in range-doppler axis can be predicated. Through this example it should become apparent that lenses L_1 and L_2 are the only optical elements that will affect relative scaling of range and doppler. Therefore a system designed for particular specifications of min-max range-doppler values could be designed to make best use of video type output

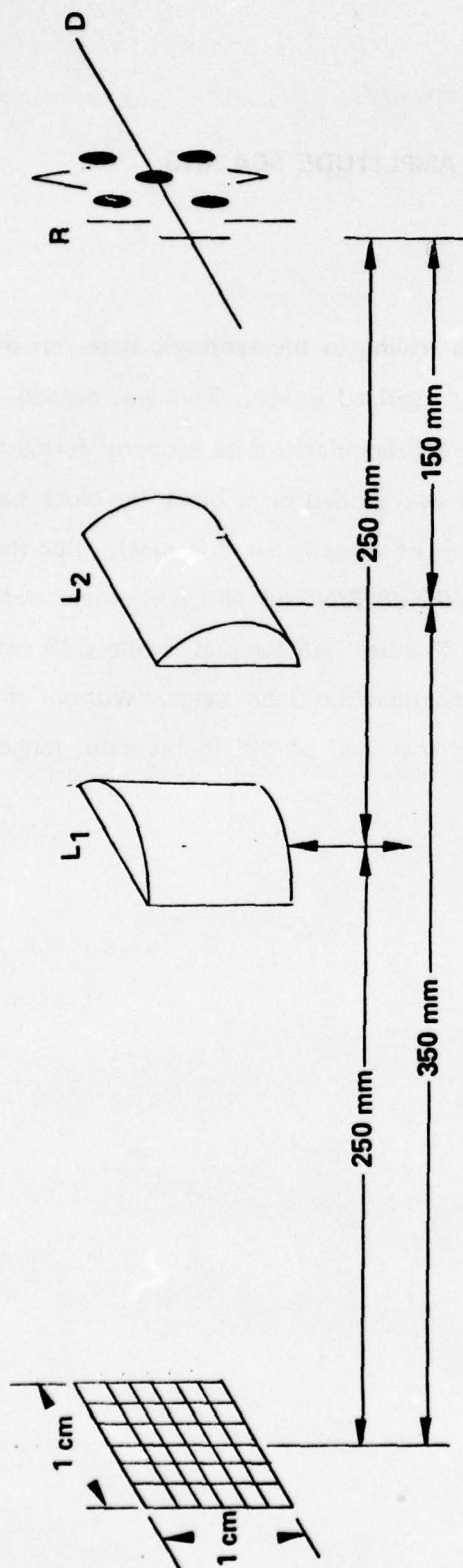
display. It must be realized that theoretically, the optical system as designed and used will preserve linearity of the scales. The main contributions to spatial nonlinearity are usually attributed to the input writing device (CRT film recorder) and output device (vidicon camera). The process of scaling therefore can be done initially by correlating data of varying doppler and range in increments of the system's resolution in order to derive both scaling and a two dimensional pattern of spatial nonlinearities. Given the relatively static nature of system scaling, the primary concern should then become the magnitude of short term - long term changes in the spatial linearity map. This recommendation is based on prior project experience at Ampex where the problem of calibrating optical spectral analysis output was emphasized. In this earlier work, the ability was gained to address points in the video output by center frequency and bandwidth rather than by simple spatial position on the screen.

The G/ASP laboratory at Ampex includes a 2 inch vidicon camera whose scan linearity is corrected through interface to a minicomputer to .4%. The process of initializing this correction can be repeated periodically, but has been found to be necessary only after several weeks of operation. This same scheme is applicable to the input writing device.

3.0 GAIN CONTROL AND AMPLITUDE SCALING

The method used in applying amplitude scaling to the synthetic data was discussed in an earlier memo accompanying the first digitized results. This was needed because of the conversion from 16 bit data to 8 bit modulated data properly formatted for input to the optical correlator. Gain control was applied on a block by block basis (a block is a pair of 3600 sample length sequences of a particular S/N case). For the two blocks of interest, $+\infty$ S/N (#1 and #2) and ϕ dB S/N (#5 and #6), there and overall amplitude scale factor of 1.244 for the ϕ dB case. All samples in the ϕ dB case were then multiplied by this factor in order to maintain the 8 bit range. Without this control, lower signal to noise cases occupying less than half of the 16 bit input range would be lost.

FINAL STAGE OF IMAGE PLANE CORRELATOR
(SCALING CONSIDERATIONS)



L₁ IS THE DOPPLER TRANSFORM LENS
L₂ IS THE RANGE IMAGING LENS

SIZE OF THE RANGE IMAGE IS $\frac{150 \text{ mm}}{350 \text{ mm}} \times 10 \text{ mm} = .429 \text{ cm}$

$$\text{DOPPLER SCALE: } d = \frac{F \lambda}{D}$$

d = DEFLECTION IN CORRELATION PLANE

F = FOCAL LENGTH OF LENS (250 mm)

λ = WAVELENGTH OF LASER LIGHT (514.5 nm)

D = SIGNAL SPATIAL WAVELENGTH AT THE INPUT

Accompanying this report are additional copies of the surface "greyplots".
The quality of reproduction on the sets that were shipped originally is questionable.
I hope these are an improvement.

February 28, 1979

Mr. J. Teeter

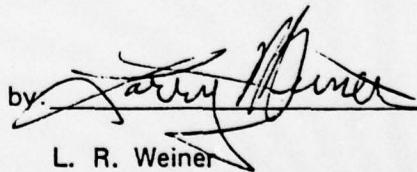
Code 7114

Naval Ocean Systems Center

San Diego, CA 92152

Subject: Transmittal of Optical Ambiguity Surface Digitized Data Tape

Submitted by:



L. R. Weiner

LRW/jms

Enclosures: cc w/enclosures to Dr. J. Greene, Ensco
cc cover letter to Joel Trimble, ONR

This package contains material to support the results of a third round of LENS program optical processing. The data in this package includes surfaces of both 512 second and 256 second integration time, surfaces composed of mixed S/N signal segments, multiple surfaces/frame with calibration markers in range and Doppler, and a pulse correlation frame. It is believed that this choice of data will aid in the thorough analysis of optical data.

Accompanying this letter is a 1600 bpi tape of the optical surfaces with a description of the recording format, a set of density plots and histograms, a partial tape dump to check validity, and isometric plots of cropped digitized data.

Several comments need to be made on new and different aspects of this data set.

1.0 DIFFERENT INTEGRATION TIMES

In the previous data set 8/28/78, the S/N ratio observed was a direct result of operating relatively close to the noise floor of the optical system. This point is also stressed in the recent Carnegie-Mellon Final Report and was attributed to the low modulation efficiency of the film-based signal.

As an experiment in S/N improvement, some surfaces have been processed at 256 second integration time instead of the previous value of 512. This has the effect of lowering the spatial frequencies on film well into the Modulation Transfer Function bandpass. For 512 second processing, the MTF was down 3 to 4 dB at the bandedge. At 256 seconds, a 6 to 8 dB advantage should be observed in optical output to optical noise.

Surfaces identified with 512 second integration were made with 512 data points, 256 second surfaces with 256 data points. In each case the tau shift is ± 1 second per line with the center line of the correlation starting at the indicated point in the data block.

2.0 MULTIPLE SURFACES/FRAME WITH RANGE-DOPPLER

Surfaces labeled MULTI or MULTIONE are composites of a crosscorrelation and the two associated autocorrelations. Each surface in the frame has ± 32 seconds in the range axis and may be identified by the centerline start point. MULTI uses 512 seconds of data, MULTIONE uses 256. The markers are correlated Barker codes that should be 8 seconds wide and occur every $64 + 16 = 80$ seconds in range. The binary codes were modulated with different frequencies to cause different Doppler values. These frequencies were 120, 135, 150, 165, and 180 spatial cycles. This composite was cross correlated with a code modulated at 150 cycles. Therefore, the center marker is at zero Doppler with corresponding percentages at the other markers. Scaling for all surfaces can be derived from the position of the markers.

3.0 IMPULSE SURFACE

In lieu of using a single point impulse function which would not work because of energy considerations (and also because the algorithm requires a band-shifting of the original data), a pulse burst was used. A 4 cycle (32 point) pulse burst was centered in the 1024 point aperture of the film recorder. On the shifted mask, the shift was ± 2 CRT points/line which gives a correlation extent of ± 16 lines.

4.0 POWER SCALING

In order to process the (lower modulation efficiency) 512 second data, the input light power was raised from 11 mw to 34 mw. No direct comparison of peak amplitudes between the two cases should be attempted. However, all data within an integration time case was recorded at the same gain settings.

It must also be reiterated that the gain for each S/N case was modified before processing to fill an 8 bit range. These normalizations are available upon request.

5.0 NOTES ON DIGITIZATION

The lower pedestal that exists on this set of data is due to solving an A/D problem that existed at the time of the last iteration which forced us to forsake the lower conversion values. (i.e. < 32). Present data therefore makes better use of the 256 values available.

There is some concern that the first 8 surfaces may have been slightly clipped by a marginal camera pedestal setting. This problem would be noticed by a sharp cutoff of the distributions at the lower end or by an abnormally constant floor in the data. Time does not allow us to investigate this or to redo these frames. They should still show dramatic improvement in the distribution characteristics.

6.0 ISOMETRIC PLOTS

Isometric plots do not show the entire 256 x 400 point image but are windowed down to 128 x 256 points.

TAPE FORMAT**2/28/79**

The enclosed tape contains 20 digitized optical ambiguity surfaces. Each surface contains 400 lines of video data. The digitization was done on a line by line basis with 256 sequential points as eight bit integer values for each line. Each data point is a two byte, 16 bit integer value between 0 and 255. The significant data appears in the lower (second) byte while the top byte should be all zeros. The lines form cuts through the range axis in the Doppler direction. The tape has 9 tracks, odd parity and was recorded at 1600 bpi. Each of the the 400 lines in a surface form a tape record with no other marks inserted. The starting word for a surface can be found from

$$W_N = (S_N * 400 \text{ lines/surface} * 256 \text{ words/line}) + 1$$

where W_N is the word number and S_N is the surface number 0 through 19. The only E.O.F. occurs after surface 19. A dump for each line of each surface is included which lists the first and last four integer values.

The sense of the Doppler deflection is increasing to the left and later range alignments are towards the top of each field.

Care was taken to align the raster scan with range-Doppler axis, but they may not correspond absolutely. The inclusion of range-Doppler calibration markers should allow us to perfectly "deskew" the output sampling.

SURFACE DATA 2/28/79

FRAME NO.	1ST BLK/2ND BLK/DATA POINTS	S/N	REMARKS
0	1/1/768-1023 2/1/768-1023 2/2/768-1023	+INF	MULTIONE 3 Surfaces/frame
1	1/1/1024-1279 1/2/1024-1279 2/2/1024-1279	+INF	MULTIONE 3 Surfaces/frame
2	5/5/768-1023 6/5/768-1023 6/6/768-1023	0dB	MULTIONE 3 Surfaces/frame
3	2/1/768-1023	+INF	256 Second
4	1/1/512-767	+INF	Autocorrelation
5	2/1/512-767	+INF	Crosscorrelation
6	2/1/1024-1279	+INF	
7	6/5/768-1023	0dB	
8	1/1/768-1279 2/1/768-1279 2/2/768-1279	+INF	MULTI 3 Surfaces/frame
9	1/1/768-1279	+INF	Autocorrelation
10	2/1/768-1279	+INF	
11	6/5/1024-1535	0dB	
12	Impulse 4 cycles, 32 points	±INF	

AMPEX

FRAME NO.	1ST BLK/2ND BLK/DATA POINTS	S/N	REMARKS
13	1/1/1024-1279	+INF	Autocorrelation
14	2/1/1024-1279	+INF	
15	6/5/1024-1279	0dB	
16	2/7/1024-1279	+INF/-3dB	Mixed S/N
17	6/7/1024-1279	0dB/-3dB	Mixed S/N
18	2/1/1024-1535	+INF	
19	8/7/1024-1535	-3dB/-3dB	Mixed S/N

SURFACE DATA 3/7/79

FRAME NO.	1ST BLK/2ND BLK/DATA POINTS	S/N	REMARKS
0	1/1/1024-1279 2/1/1024-1279 2/2/1024-1279	+INF	MULTIONE 3 Surfaces/frame
1	1/1/768-1023 2/1/768-1023 2/2/768-1023	+INF	MULTIONE 3 Surfaces/frame
2	5/5/768-1023 6/5/768-1023 6/6/768-1023	0dB	MULTIONE 3 Surfaces/frame
3	2/1/1024-1279	+INF	256 Seconds
4	2/1/768-1023	+INF	256 Seconds
5	2/1/1024-1535	+INF	512 Seconds
6	2/1/768-1279	+INF	512 Seconds
7	-	-	Camera Black (Laser Off)

June 15, 1979

Mr. Jim Teeter, Code 7111
Naval Ocean Systems Center
South Rosecrans Street
San Diego, CA 92152

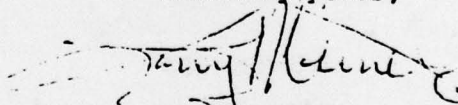
Dear Jim:

I am enclosing the results that we have discussed concerning the problems of interpreting the LENS digitized data. The items are annotated on the back of each sheet.

Because I want you to have this material ASAP, further clarifications and discussions will wait until our next meeting.

This material and the few experiments that are yet to be done will allow us to satisfactorily answer questions on the optical results.

Sincerely yours,



Larry R. Weiner
Member Research Staff
Research Department
(415) 367-4142

LRW/jms
Enclosures: 3

June 29, 1979

Mr. John Green
 Ensco, Inc.
 8001 Forbes Place
 P.O. Box 1383
 Springfield, VA 22151

Dear John:

Here are the recent results of the tests done on the camera. Please pardon the informal presentation. Annotations are on the back.

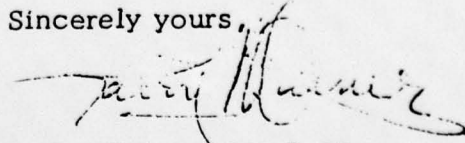
I am running some experiments to better the resolution which include:

- (4X improvement) Rescaling the optical output to fill all the active picture (and therefore all 512 digitization points).
- (2X improvement) Evaluation of a 2" vidicon camera.
- (2X improvement) Aperture correction (phaseless peaking) of vidicon electrical bandpass to bring up high frequency.

The resolution of the camera as used in our experiments was equivalent to 1.5 MHz (3 dB) or 100 cycles or 200 TV lines in the horizontal direction. This means that since the Doppler direction was contained within 25% of these points, we had only 50 spots resolved at a 3 dB point. This revelation will also affect the peak height of the correlation impulse. Implementing all of the above improvements (16X) would be just sufficient to resolve the optical output plane.

I will keep you informed.

Sincerely yours,


 L. R. Weiner, MS 3-20
 Member Research Staff
 Research Department
 (415) 367-4142

LRW/jms
 Enclosures:5

133

APPENDIX C
OPTICAL AMBIGUITY SURFACE GENERATION